APPENDIX A - CENTRAL SANDS LAKES STUDY TECHNICAL REPORT: DATA COLLECTION AND HYDROSTRATIGRAPHY

David Hart
Rachel Greve (WDNR)
Michael Parsen
J. Elmo Rawling, III
Stephen Mauel
Peter Chase

August 17, 2020

The Wisconsin Geological and Natural History Survey,
Report to the Wisconsin Department of Natural Resources

CENTRAL SANDS LAKES STUDY TECHNICAL REPORT: DATA COLLECTION AND HYDROSTRATIGRAPHY

Contents

Figures

Tables

Appendices (Electronic Files)

F. Well Summary Table
G. Geoprobe® Well Construction and Filling and Sealing Forms
H. Grain Size Analyses
I. Aquifer Tests Results: Existing Sources
J. GIS Steps for Bedrock Surface Creation
K. Geoprobe® Well Water Levels (available on WDNR web service)

CENTRAL SANDS LAKES STUDY TECHNICAL REPORT: DATA COLLECTION AND HYDROSTRATIGRAPHY

INTRODUCTION

Overview of Hydrostratigraphy Characterization Needs and Study Goals

The Central Sands Lakes Study (referred to herein as CSLS or 'the study') was developed by the Wisconsin Department of Natural Resources (WDNR) to fulfill requirements enacted in 2017 Wisconsin Act 10 ("Act 10"). The overall goal of the study is to investigate the potential for groundwater withdrawal-related impacts to Plainfield, Pleasant, and Long Lakes in Waushara County, Wisconsin. The study's primary evaluation tool is a numerical groundwater model developed for the WDNR by the U.S. Geological Survey (USGS). The model includes much of the Central Sands region, with detailed evaluation of the area near the study lakes. To improve the conceptualization of the groundwater / surface water interaction of the three study lakes and support the groundwater model, WDNR contracted with the Wisconsin Geological and Natural History Survey (WGNHS) to define the hydrostratigraphy of the Central Sands groundwater system. Hydrostratigraphy provides the basic framework for modeling flow systems by dividing the different sediments and rock units into distinct mappable domains and layers based on their hydrogeologic properties. The WGNHS project team included Rachel Greve, a WDNR Hydrogeologist, stationed at WGNHS for most of the project period.

The WGNHS reviewed existing literature and datasets relevant to regional geology and aquifer properties, refined locations for over 50,000 wells based on well construction reports (WCRs) and other sources, and conducted field investigations to better characterize the geology, groundwater levels, and fluxes in areas in and around the three lakes.

This report outlines WGNHS data collection methods, results of work completed, and work products relating to groundwater flow model dataset development and lake characterization, including hydrostratigraphic conceptualization and model layering, aquifer properties, and interpretation of lake/groundwater interactions.

Review of Previous Studies

WGNHS conducted a review of existing literature topics related to the hydrogeologic setting and water budget components of the CSLS. The review examined past studies of the water resources and geology of the Central Sands region, prior investigation carried out at the study lakes, and investigations from outside the Central Sands describing lake/groundwater interactions, tunnel channel formation, and other project-relevant topics. Items included in the review had either undergone an external academic review process (academic journal articles, Masters and PhD Theses) or were related specifically to the study lakes. The results of the literature review are accessible as an annotated bibliography (Greve and Hart, 2018), available digitally from WGNHS (https://wgnhs.wisc.edu/pubs/wofr201804/).

As part of the literature review, WGNHS also compiled the results of aquifer test results from previously published work. These data were shared with USGS to provide a range of appropriate values for aquifer hydraulic conductivity, storage properties, and anisotropy. Available data are concentrated in the northern part of the study area, and many of the aquifer data were previously compiled during the creation of the Little Plover River (LPR) groundwater model (Bradbury et al., 2017). Work conducted by Hart (2015) in central Adams County and additional aquifer test data identified using the WGNHS Hydrogeologic Data Viewer were also included in the aquifer property summary.

Hydrostratigraphic Setting of the Central Sands

The unconsolidated aquifer in the Central Sands region is connected to surface waters and is the primary aquifer used to support groundwater withdrawals from residential wells, public water supplies, and private high capacity wells. It consists mainly of sandy sediments greater than fifty feet thick. The extent of the Central Sands east of the Wisconsin River is shown in Figure 1. Sediment thicknesses in the CSLS model domain are shown in Figure 2. The sediments that make up the sand and gravel aquifer were deposited during the last ice age, between 100,000 and 20,000 years ago. The source material for these sandy glacial sediments was the sandstone bedrock that underlies most of the region. Together, the outwash sediments and sandy tills form a highly productive surficial aquifer with high hydraulic conductivity. In addition to the sandy glacial sediments, the study area includes areas of widespread fine-grained sediments. These occur in two former glacial lake basins (Glacial Lake Wisconsin and Glacial Lake Oshkosh). More localized zones of fine-grained sediments are also present; these are typically associated with collapse zones, proglacial lakes, and backwater areas. The primary glacial features in the study area are shown in Figure 3.

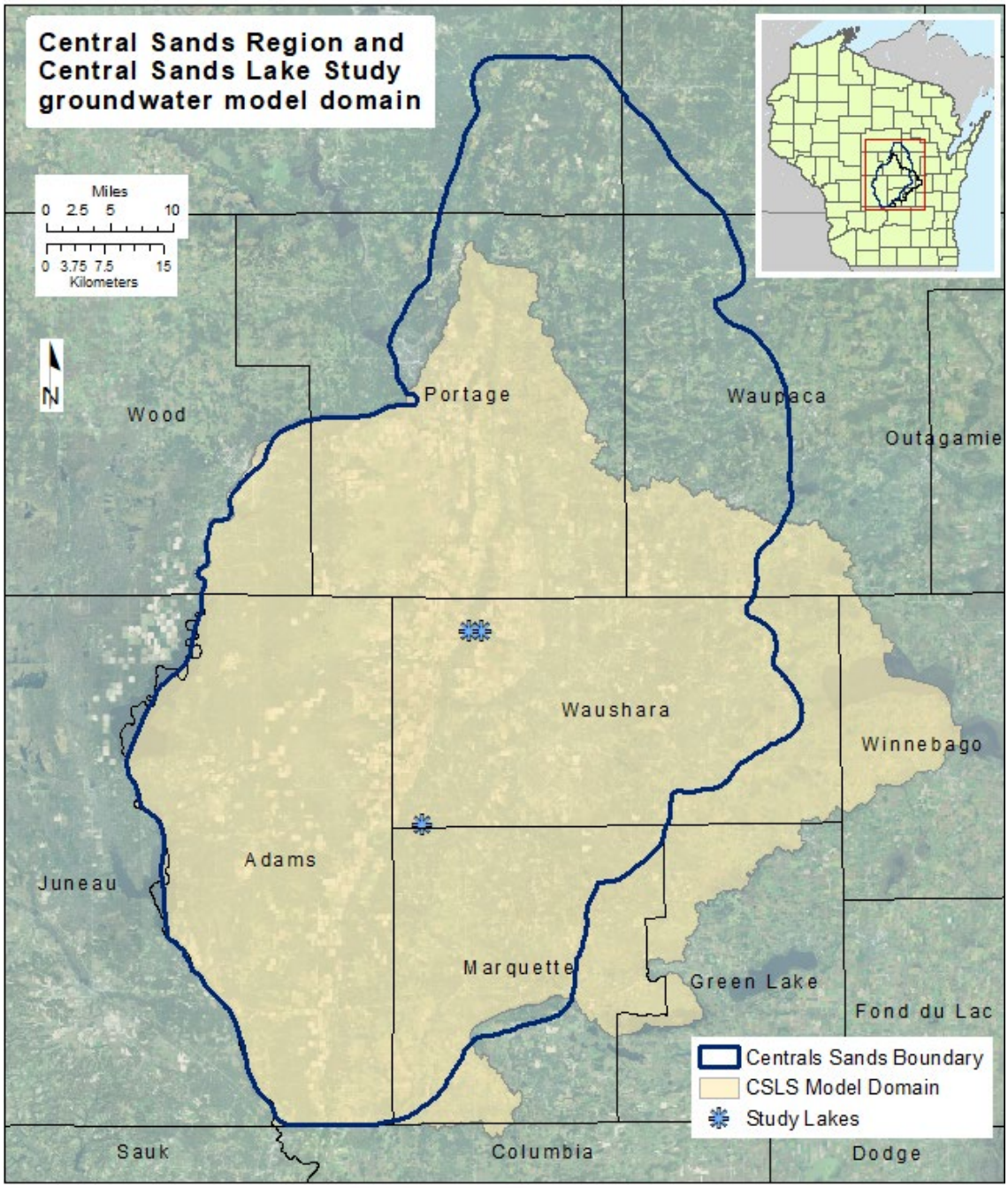

Figure 1. Extent of the Wisconsin Central Sands aquifer (sands and gravels generally greater than 50 ft thick) and the CSLS groundwater model domain. The groundwater model domain does not perfectly match the Central Sands region because the model utilizes large rivers that form natural hydraulic boundaries.

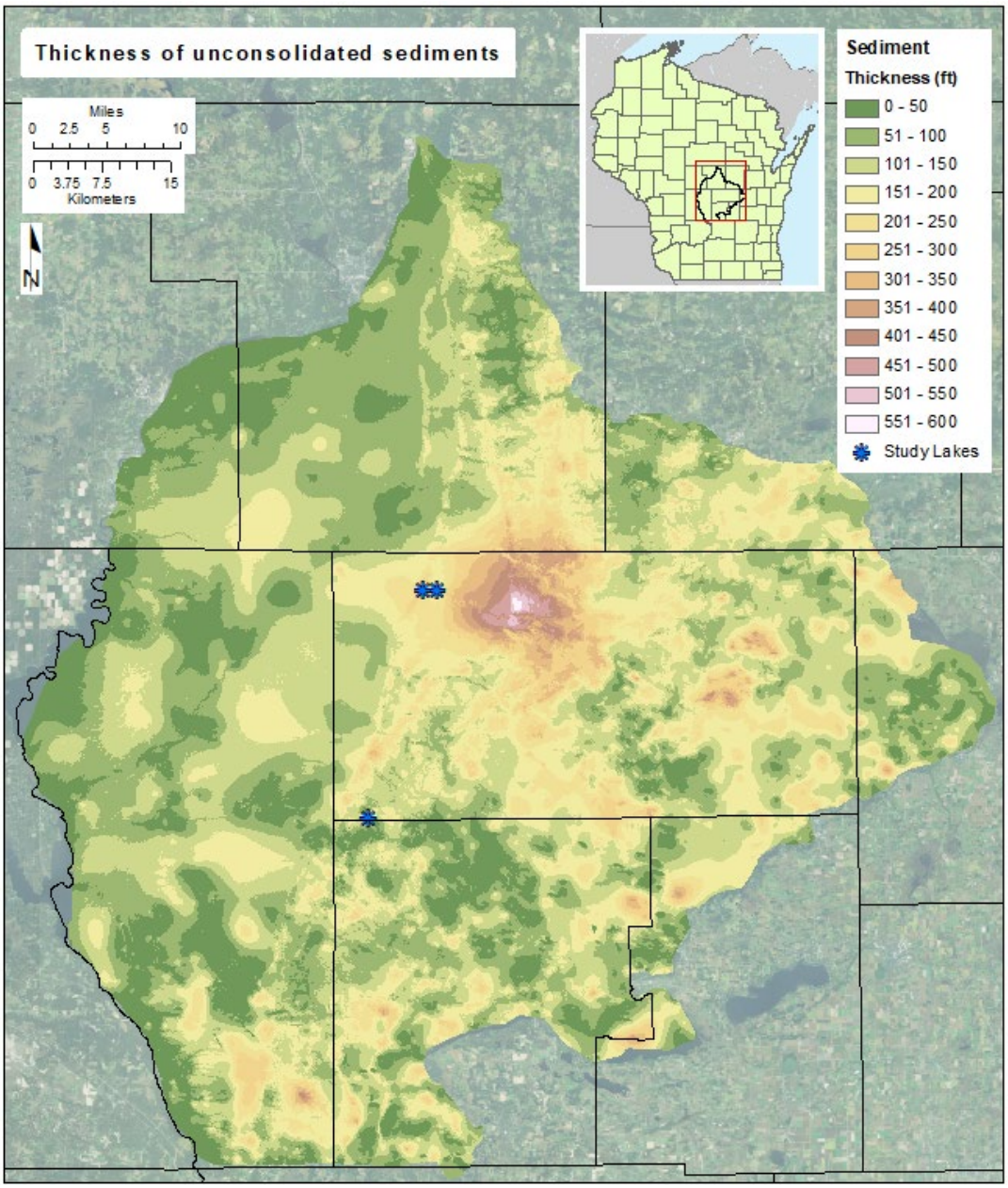

Figure 2. Thickness of unconsolidated deposits in the Central Sands model domain. Thicknesses were derived by subtracting the interpolated bedrock surface from LiDAR-derived land surface elevations. Thicknesses shown do not distinguish between sediment types

Glacial Geology

The Central Sands study area includes several prominent north-south moraines; from west to east, the Arnott, Hancock, and Almond moraines (Figures 3, 4). The Arnott Moraine is a highly weathered ridge in the northern part of the model domain. Recent work on the Arnott moraine indicates that it represents deposits from an early Late Wisconsin ice advance (around 35,000 years before present) (Ceperley et al., 2019). The Hancock Moraine represents the position of ice at the late glacial maximum (around 26,000 years ago), while the Almond moraine represents a later ice stand (26,000-19,000 years ago). The Hancock and Almond Moraines are separated by a maximum distance of about 6 miles in Waushara County and merge to form a single moraine to the north and south.

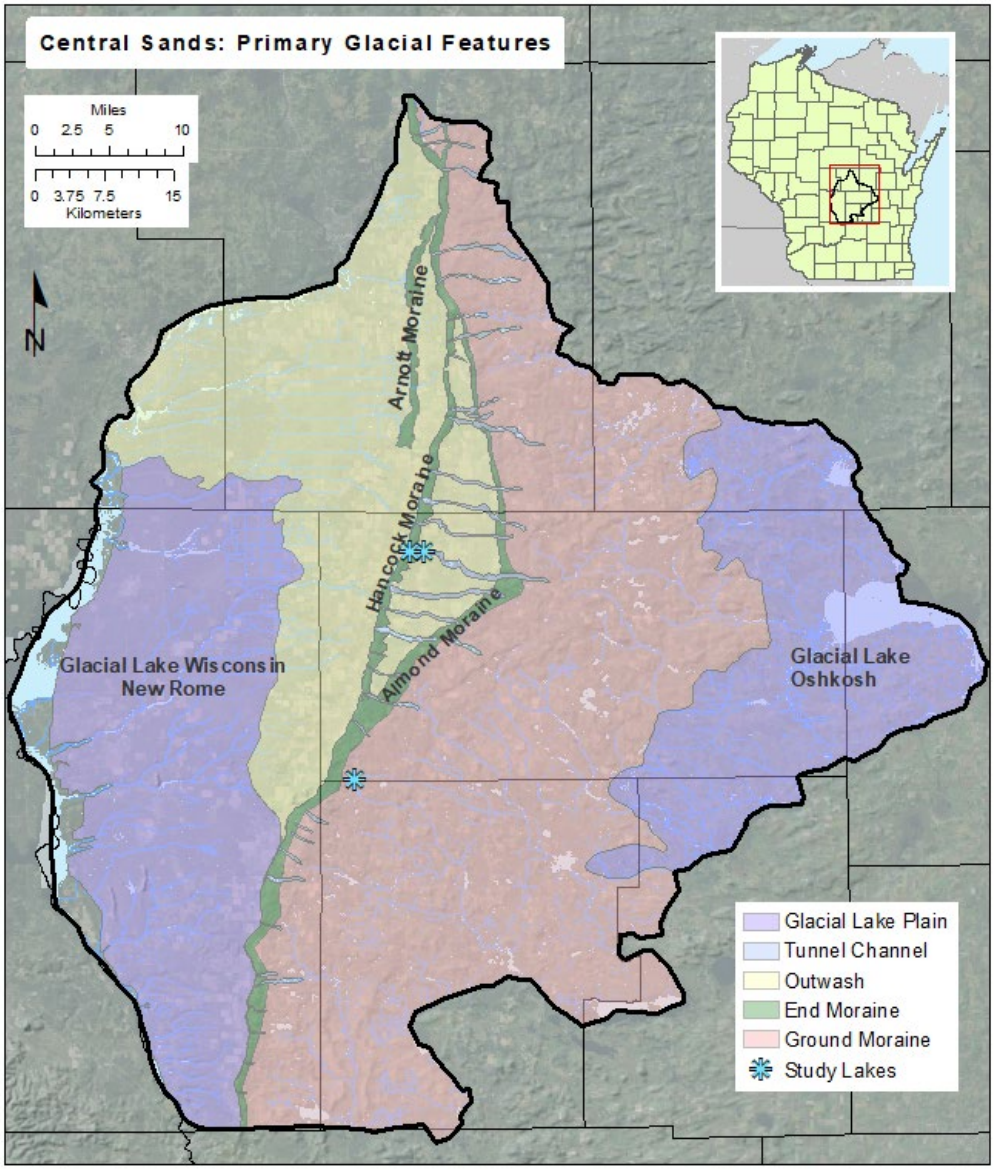

Figure 3. Primary glacial features of the Central Sands model domain.

West of the Hancock Moraine, the land surface is generally a flat outwash plain. The outwash sediments are generally high-conductivity sands and gravels, with the exception of fine sediments associated with glacial Lake Wisconsin (Syverson et al., 2011). The New Rome Member of the Big Flats Formation is a widespread silt and clay layer formed in the former glacial Lake Wisconsin basin. The New Rome Member is mainly present in Adams County, in the western part of the Central Sands (Clayton, 1987; Brownell, 1986) and consists of a mostly-continuous fine layer that ranges from less than 10 feet up to 30 feet thick. It is overlain and underlain by outwash sand and gravel and typically occurs at a depth of 15-40 feet below ground surface (Figure 5). Well construction records show that the New Rome thickens to the south and slopes downward to the south and west, away from sources of glacial sediment. The New Rome has hydraulic conductivity several orders of magnitude lower than the surrounding aquifer and forms an aquitard where it is continuous (Hart, 2015).

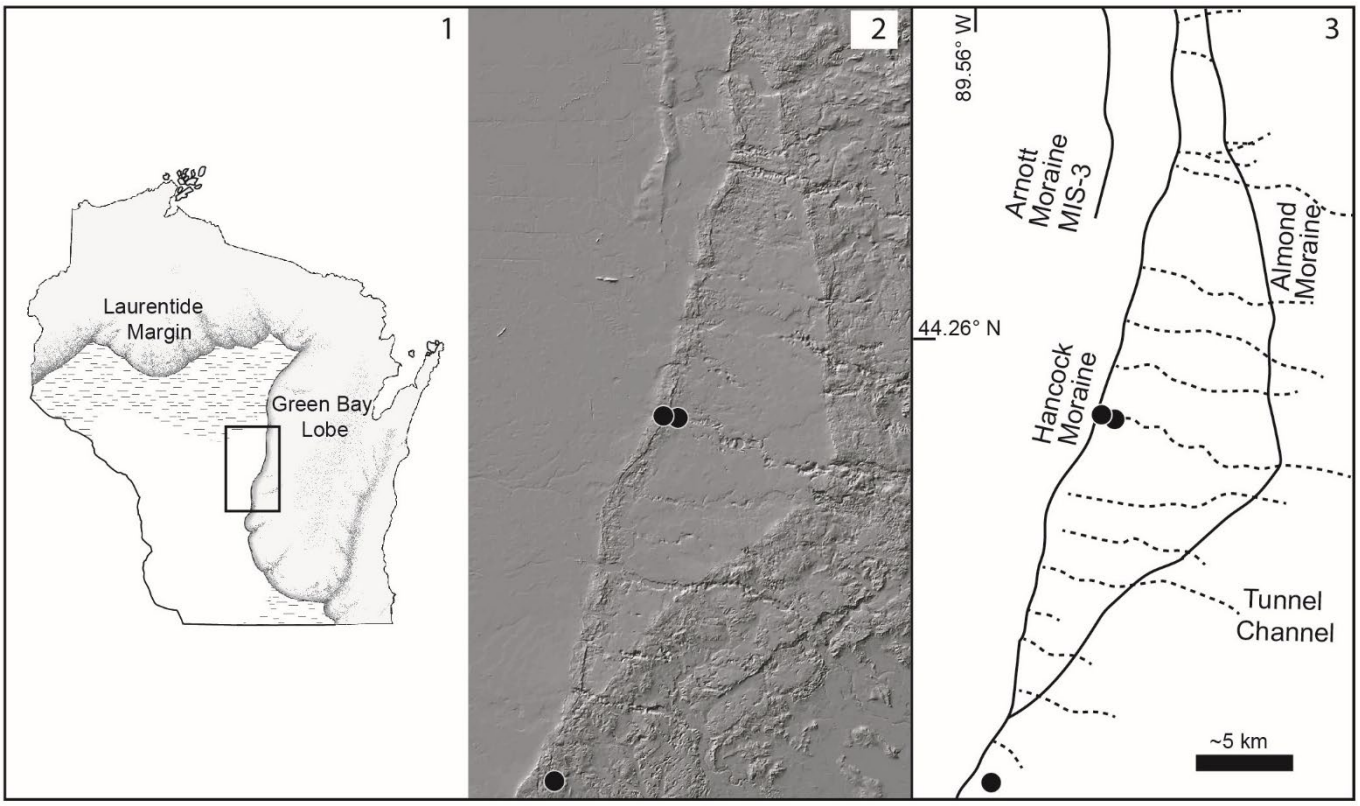

Figure 4. Location of the study lakes (black points) with respect to statewide glacial features (panel 1). Panel 2 is a hillshade image of surface topography near the study lakes. Moraines and tunnel channels are clearly visible, as is the topographic contrast between the flat-lying outwash plain to the west and the collapsed zone east of the Almond Moraine. Individual features are delineated in panel 3. Long and Plainfield Lakes are located near one another on the west end of the Plainfield Tunnel Channel (northern point). Pleasant Lake (southern point) is located in the collapsed area.

The land surface between the Almond and Hancock moraines is a flat-lying outwash plain dominated by high-conductivity sands and gravel. The stratigraphy there is complex with fine materials commonly noted in well logs. However, unlike the New Rome member west of the Hancock Moraine, these fine-grained sediment do not occur in a uniform layer, and their depth and extent varies (Figure 5). This is related to the depositional environments between the moraines, which potentially includes subglacial sediment deposited when ice was at the Arnott and Hancock positions, sediment deposited in water ponding between the two moraines, sediment deposited on stagnant ice, and sediment deposited by meltwater streams originating from ice at the Almond position to the east. All of these depositional environments can include fine-grained sediments with both lateral and vertical heterogeneity. Modern-day glacial landforms similar to those that would have been found in the Central Sands during glaciation are shown in Figure 6.

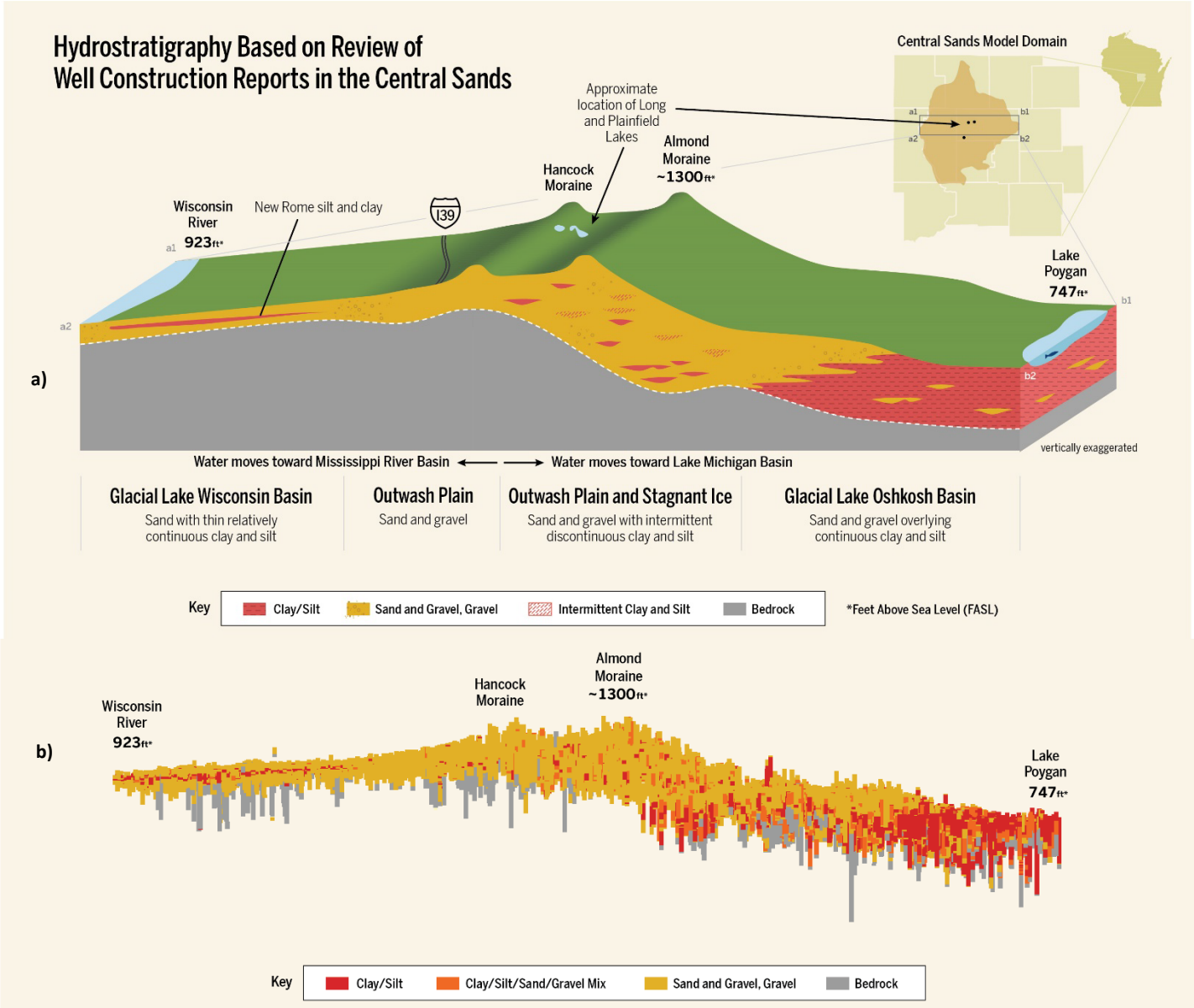

Figure 5. Schematic cross section (a) of lithologic logs (b) along a west to east profile through the center of the model domain (see inset map). Zones correspond to the primary glacial features shown in Figure 3. Vertical exaggeration is 20x.

Bruce F. Molnia, U.S. Geological Survey, Open File Report 2004-1216

NASA / Michael Studinger - http://www.nasa.gov/mission_pages/icebridge/index.html

John Bluenle, https://www.dmr.nd.gov/ndgs/ndnotes/ndn14_h.htm

Figure 6. Photographs of modern analogs of the different glacial depositional environments that gave rise to the landforms present in the Central Sands of Wisconsin.

Tunnel channels are roughly linear collapse features that generally cross-cut the Almond moraine to the east and terminate at the Hancock Moraine to the west. They form a series of linear depressions 5-30 feet below the elevation of the surrounding outwash surface. Seepage lakes are common in the low areas associated with former tunnel channels. Two of the CSLS study lakes, Plainfield Lake and Long Lake, are located within the Plainfield Tunnel Channel, one of the larger tunnel channels in the region. Plainfield Lake is located at the mouth of the tunnel channel where it crosses the Hancock Moraine. Sediments surrounding Plainfield Lake are generally coarse, especially on the west side of the lake. Fine-grained sediments are also found in the Plainfield Tunnel Channel, including the area around Long Lake and at greater depths in rotosonic boring PFD24 (Quaternary Sediment section, below). Where present, these fine sediments are overlain by 10-60 ft of coarser outwash. Tunnel channels form through catastrophic release of large volumes of supraglacial and subglacial meltwater to the ice margin during glaciation (Clayton et al., 1999; Zoet et al., 2019). These subglacial outlet channels were in-filled with collapsed ice blocks and buried under thick glacial till, outwash, and other sediments, resulting in complex stratigraphy. Sediments subsequently collapsed as buried ice melted, forming topographic lows in the modern landscape (Figure 7). Depending on the timing of ice collapse and other factors unrelated to tunnel channel formation, some parts of the tunnel channels may have been low areas during glacial recession and formed lakes or backwaters that collected finer sediments relative to the surrounding areas. For example, the Plainfield Tunnel Channel has a higher prevalence of fine-grained sediment compared to other tunnel channels in the region. This results in additional complexity when investigating tunnel channel stratigraphy.

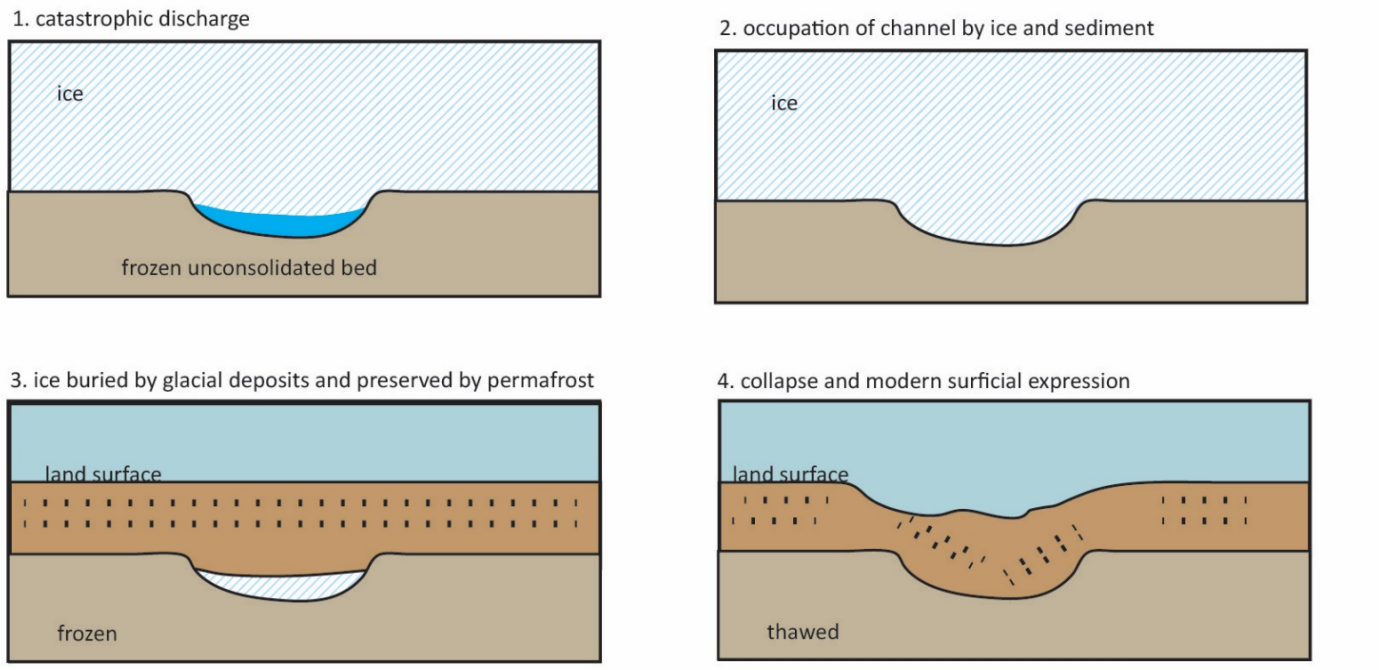

Figure 7. Time progressive illustration of tunnel channel (TC) formation from oldest to most recent (not to scale). Panel 1 represents a time of the TC excavation when water filled the base of the TC. Panel 2 represents a time after excavation when ice filled the TC. Panel 3 represents a time when ice was buried in the channel and covered with subglacial, supraglacial, and proglacial deposits. Panel 4 represents a time after the buried ice melted, the surface collapsed, and the originally horizontally deposited material dipped into the channel center. (Modified from Zoet et al., 2019)

The zone directly east of the Almond moraine is characterized by hummocky topography associated with glacial collapse; surface features include kettle lakes and ice-walled lake plains. Sediments are fairly heterogeneous, although sandy, high-conductivity materials are typically the dominant sediment type. Pleasant Lake is located within this collapsed zone. Other features of this area include several large springs and locations where artesian conditions are present. East of the collapsed zone is a hilly ground moraine with streamlined topography; drumlins are common in this zone.

After ice retreated from the Almond position, buried ice was preserved in moraines and the tunnel channels until permafrost melted sometime around 14,000 years ago (Clayton et al., 2001; Batchelor 2018). As buried ice melted the collapse of the landscape formed kettles, some of which are occupied by modern lakes, and the hummocky topography typical of the Hancock and Almond Moraines. Glacial Lake Wisconsin drained catastrophically (Clayton and Knox, 2008) as ice retreated further, likely sometime around 17,500 years ago (Carson et al., 2017), forming the Wisconsin Dells (Clayton and Attig, 1989). Eolian dunes formed on the sandy Lake Wisconsin plain until about 12,000 years ago (Rawling et al., 2008).

The eastern part of the model domain is within the glacial Lake Oshkosh basin. Sediments related to glacial Lake Oshkosh are dominated by clays and other fine-grained sediments. The clays are overlain by and interbedded with sandy outwash sediments in many places. This area is part of the CSLS model domain but it is not considered part of the Central Sands region due to the prevalence of fine-grained materials.

Bedrock Geology

The primary bedrock aquifer in the Central Sands Lakes Study area is Cambrian-age sandstone. Sandstone thickness varies considerably, from several hundred feet thick in the south to absent in the north. Sandstone outcrops as steep bluffs in the outwash plain west of the Hancock Moraine and in northern Marquette County, near Pleasant Lake. Most domestic and irrigation wells are completed in the highly productive overlying sand and gravel aquifer rather than in the sandstone aquifer.

Crystalline bedrock underlies the sandstone aquifer. The crystalline rock includes various igneous and metamorphic rock units of Precambrian age. It forms the upper bedrock unit to the northwest and to a lesser extent to the northeast part of the study area, outcropping in north central Adams County and along the Wisconsin River. In areas where crystalline bedrock is near the surface, some domestic wells draw water from fractures, but the crystalline basement rock provides only very small amounts of water and can be considered impermeable for the purposes of modeling groundwater movement.

In the eastern part of the model domain, dolomite is the upper bedrock type. Carbonate bedrock occurs mainly outside of the Central Sands region, in the Glacial Lake Oshkosh basin where numerous wells are completed in the dolomite aquifer. Within the Central Sands, dolomite bedrock caps some bluffs, such as Glover Bluff near Pleasant Lake. However, the carbonate bedrock does not occur below the water table in these areas.

WGNHS DATA COLLECTION AND ANALYSIS

The following section of this report outlines the methods and data sources WGNHS used to create a conceptual model of the geologic setting and hydraulic properties in the Central Sands groundwater model domain. Hydrostratigraphy was characterized regionally and in more detail in and around the three study lakes. Regional aquifer characteristics and geology were determined using data from well construction reports, geologic logs, the results of previously completed aquifer tests, and geophysical investigations. Near the study lakes, additional characterization work was completed using geophysics, geologic logging, aquifer tests, groundwater-level monitoring, a canoe-based survey of lake chemistry, temporary lakebed piezometers, and seepage meters. The results of these investigations were used to inform the creation of model layering, define reasonable ranges for aquifer properties, and provide nearfield head targets for the groundwater model.

Well Construction Reports

Well construction reports (WCRs) constitute a large dataset that provides information about stratigraphy, groundwater elevation, and aquifer capacity. Well drillers are required to complete and submit a WCR to the WDNR whenever a new well is constructed. Data in the WCR database cover a period of many decades, with digital records available for wells constructed post-1988. Because the reports were recorded by various well drillers over a long historical period, the quality of geologic data and accuracy of the reported well location, water level, and specific capacity measurements is variable. However, because of the large number of data points, the aggregate dataset is able to provide a reasonable picture of generalized hydrogeologic conditions.

METHODS:

Well locations of WCRs are often mapped to the quarter-quarter section, and many have locational errors. In order to make the best use of the WCR data, more accurate locations and elevations were determined to the extent possible. A combined 57,230 well records in 8 counties within the CSLS model domain were geocoded (given geographic coordinates). Of these, 30,064 wells were geolocated individually by WGNHS staff and assigned a location confidence. The location confidence gives an estimate of the accuracy of an individual point's mapped location versus the actual physical location of the well (Figure 8).

In the areas near the three study lakes (western Waushara County, southern Portage County, northwest Marquette County, and parts of eastern Adams County), nearly all well records (4099 records) were inspected and given a location confidence. In addition, 511 well records located very close to the study lakes and pre-dating 1988 were data-entered from paper records, locations were inspected and assigned a location confidence of better than the quarter-quarter section. These records were also incorporated into the WCR geodatabase.

RESULTS:

Located wells with construction information were used in the creation of geologic layering for the groundwater model, supplementing geologic log data to define depth to bedrock, depth and extent of fine-grained materials in the area between the Hancock and Almond moraines, and the extent and thickness of the New Rome layer in the Glacial Lake Wisconsin basin, in addition to model layering near the study lakes (discussed below under Conceptualization and Layer Creation).

Water levels reported at the time of well construction provide a large set of head targets for model calibration. Because the data are spread over time, these water levels represent a range of climate conditions and can provide only a generalized view of water table elevations. WGNHS compiled data from WCRs and from construction data for high capacity wells. Wells were included in the head target dataset if they had a locational precision of a quarter-quarter section or better and were located within a one-mile buffer around the model domain. Water levels from wells completed in the unconsolidated, surficial aquifer were interpolated in GIS using inverse distance weighting to help identify and remove wells with suspect data substantially in disagreement with surrounding data points. The contoured dataset provides a reasonable picture of groundwater elevation in the model domain (Figure 9). After data cleanup, water levels from a total of 9,982 unconsolidated wells and 2,368 bedrock wells were provided to USGS for potential use as head targets.

In addition to geologic layer creation and water levels for use as head target, specific capacity test information from WCRs were used to provide hydraulic conductivity estimates. Specific capacity and well construction information were entered into the TGUESS spreadsheet program to calculate hydraulic conductivities (discussed below under Aquifer Properties).

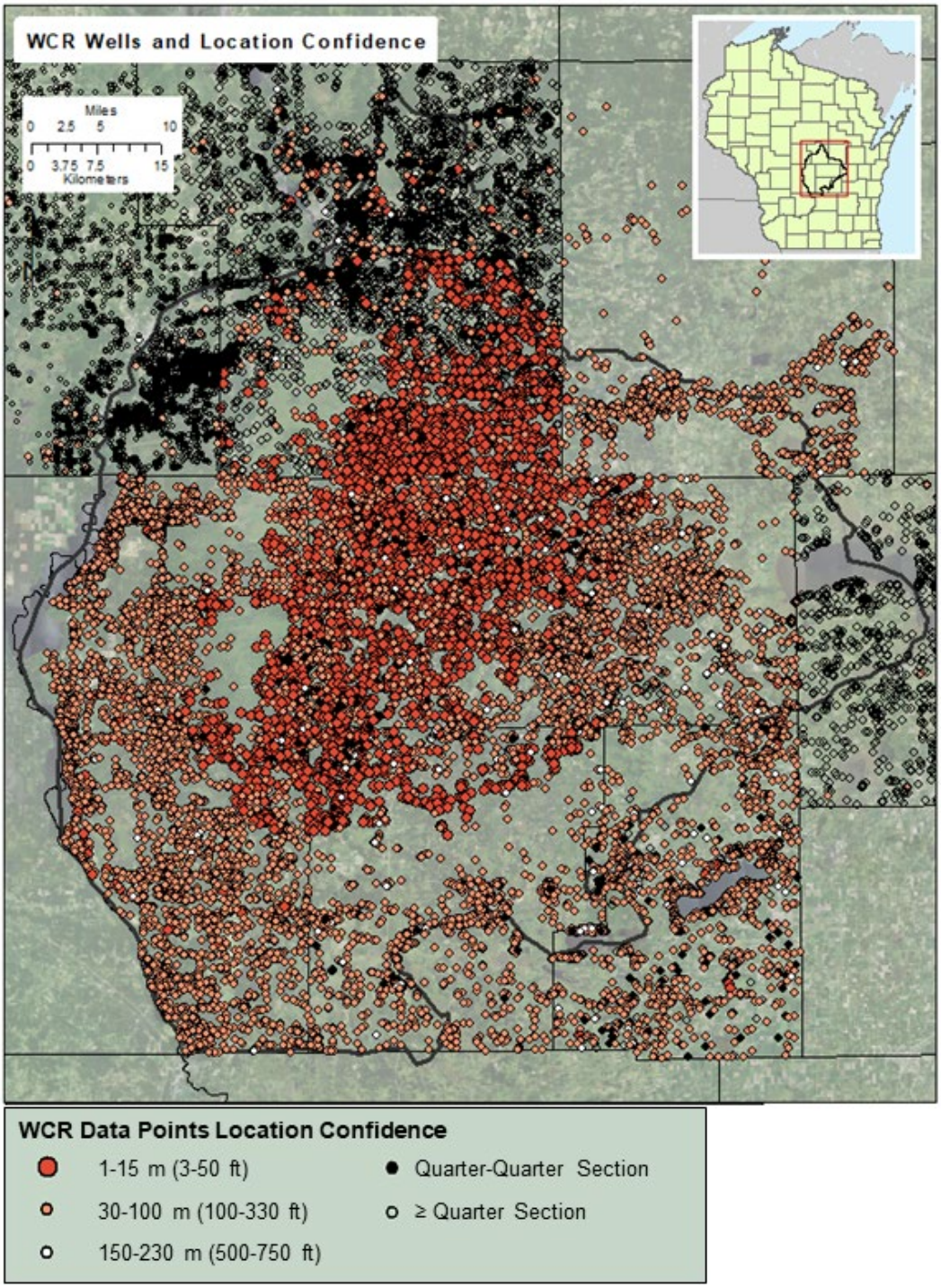

Figure 8. Locations of geocoded WCR data with assigned location confidence. Wells located near the three study lakes were examined by hand. Others were assigned locations based on address points or PLSS.

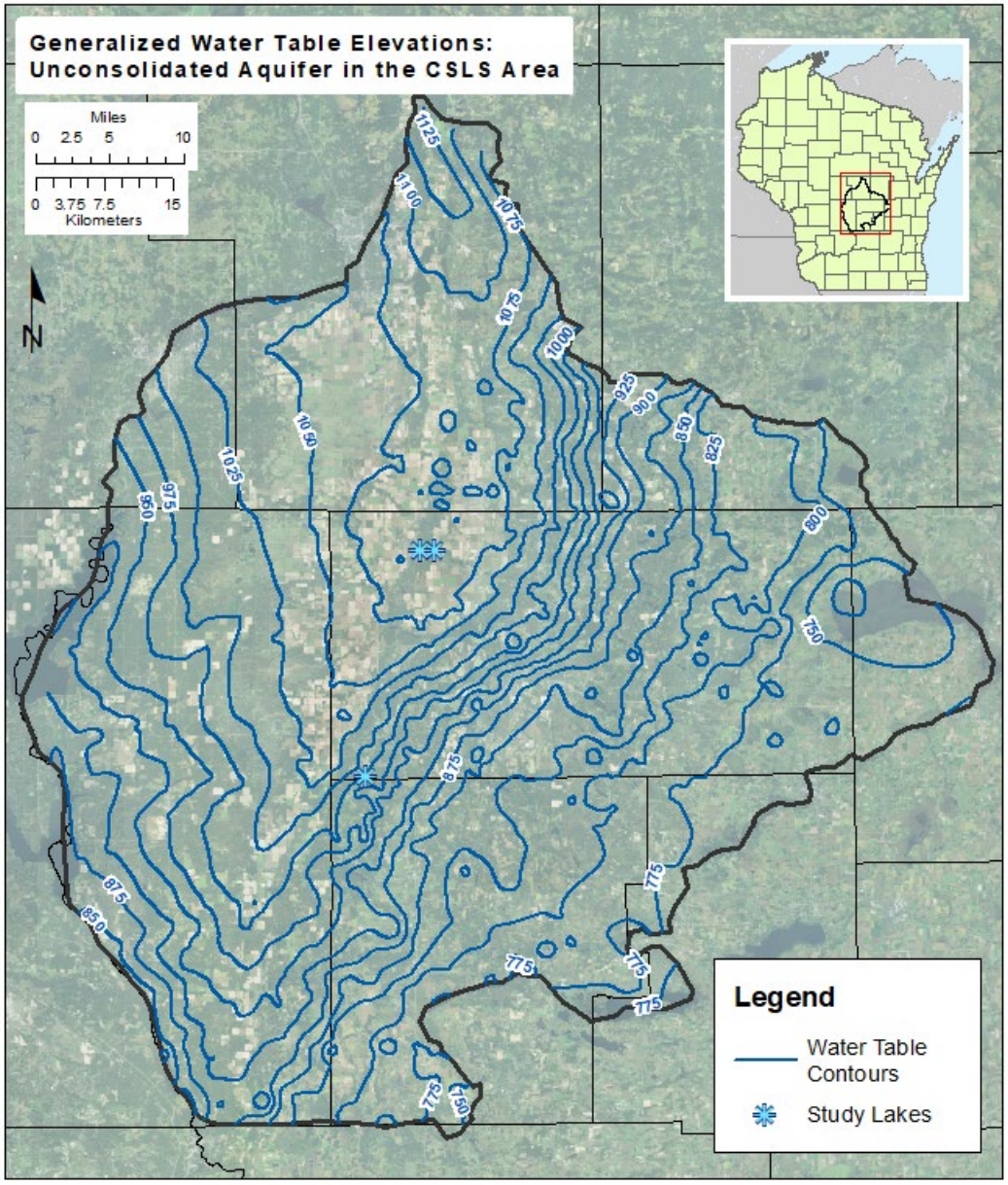

Figure 9. Regional water table contours (ft asl) created using static water-level data from wells completed in the unconsolidated aquifer (WCR data). Each WCR provides a single water-level measurement; data were collected over a period from the 1980s to present, and water table contours are an approximate representation of groundwater movement over that period.

Geophysical Investigations

Geophysical methods measure the variability in physical properties of earth materials using remote sensing techniques. Several geophysical methods were used to investigate geology and aquifer properties for the CSLS study, both regionally and in the area near the study lakes. Each method and the information derived from it is described in more detail in this section.

- A passive seismic instrument was used to estimate depth to bedrock in areas where deep well and borehole data are sparse. Passive seismic data were collected regionally, but collection efforts were primarily focused near the study lakes.

- A direct push permeameter was used to identify vertical and horizontal hydraulic conductivity variability at two Central Sands sites, a site the Glacial Lake Wisconsin lake plain west of the moraines, and a site near Plainfield Lake.
- Downhole geophysics (including gamma logging) was used to confirm zones of fine-grained sediments in boreholes at two sites in the Plainfield Tunnel channel.
- Ground penetrating radar (GPR) was used to supplement geologic boring log data at Long Lake when determining the extent and configuration of shallow fine-grained sediments.

HVSR Passive Seismic Method

Determining depth to bedrock from boring logs alone is a challenge in parts of the model domain where relatively few wells are drilled to bedrock. This includes the region around Long and Plainfield Lakes. Areas with no depth-to-bedrock data may be several miles across. WGNHS used the Horizontal-to-Vertical Spectral Ratio Passive Seismic Method (HVSR or Passive Seismic) to improve bedrock depth estimates near the study lakes and to overcome data gaps in other parts of the model domain.

Passive seismic is a fast, non-invasive geophysical method for acquiring depth-to-bedrock estimates. The instrument is a small seismometer that measures vibrations that are already present in the ground from sources such as lake waves and distant traffic. After data collection, seismic waveform processing software is used to obtain a frequency that corresponds to the sediment/bedrock contact. A short calculation is performed to determine a depth-to-bedrock estimate from this frequency.

METHODS:

Data Collection and Processing

Before data collection, the passive seismic instrument's legs are pushed into the ground to provide the necessary coupling between the ground and instrument, and the instrument is leveled. The instrument then collects three components of ambient ground motion, generally north-south, east-west, and vertical, for 10-20 minutes.

To process data, a Fourier transform is used to display the different frequencies that created the acquired ground motion waveforms. These are displayed as north-south, east-west, and vertical components. The frequency indicating the sediment/bedrock contact is the frequency where the movement of the horizontal components are the largest compared to the vertical component. This is the resonant frequency of the sediment, and is seen in the spectral output as a peak when frequency is plotted against the horizontal-to-vertical spectral ratio (HVSR). This observed HVSR peak frequency is inversely proportional to the sediment thickness or depth-to-bedrock as shown in Equation 1 below.

$$z = a\, f^{-b} \qquad \text{Equation 1}$$

where z is depth (ft), a is an empirical coefficient, f is frequency (Hz), and b is a second empirical coefficient (Ibs-von Seht and Wohlenberg, 1999). Different a and b coefficients have been determined for different landscapes, so a basic understanding of the subsurface is used to determine the proper

coefficients. Calibration of these empirical parameters was also done by collecting HVSR passive seismic data at locations where depth to bedrock is known.

Passive Seismic Calibration

WGNHS collected passive seismic data at 18 points near wells with known depths to bedrock in the study area. The known sediment thicknesses plotted with the peak frequency in Figure 10 as a log-log plot. A power law was fitted to the data giving coefficients of a=271.9 and b=1.159. WGNHS also conducted an error analysis to provide estimates of error in measurements. Confidence intervals at 68% (1 standard deviation) and 95% (1.98 standard deviations) are shown on the plot. The error scales with depth and frequency. At high frequencies and shallow depths, the absolute error is smaller than at low frequencies and greater depths. However, the relative errors scales with depth. For example, a frequency of 6 Hz corresponds to a depth of 33 feet and has a 68% confidence interval between 23 and 49 feet. A frequency of 1 Hz corresponds to a depth of 272 feet and has a 68% confidence interval between 194 and 384 feet. These errors are comparatively large (± 40% of the predicted depth) but the ease of data collection and prohibitively high cost of other methods such as drilling make this a viable alternative in those areas where depth-to-bedrock data is sparse. Figure 11 shows the locations of the calibration points (blue crosses).

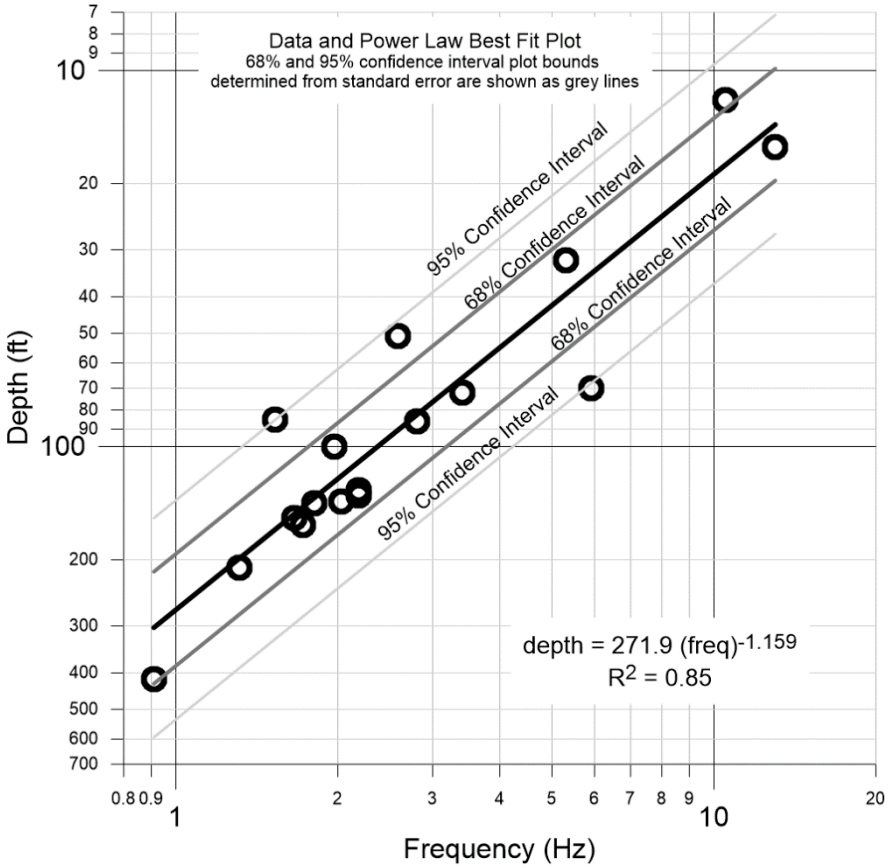

Figure 10. Calibration plot for passive seismic method in the study area.

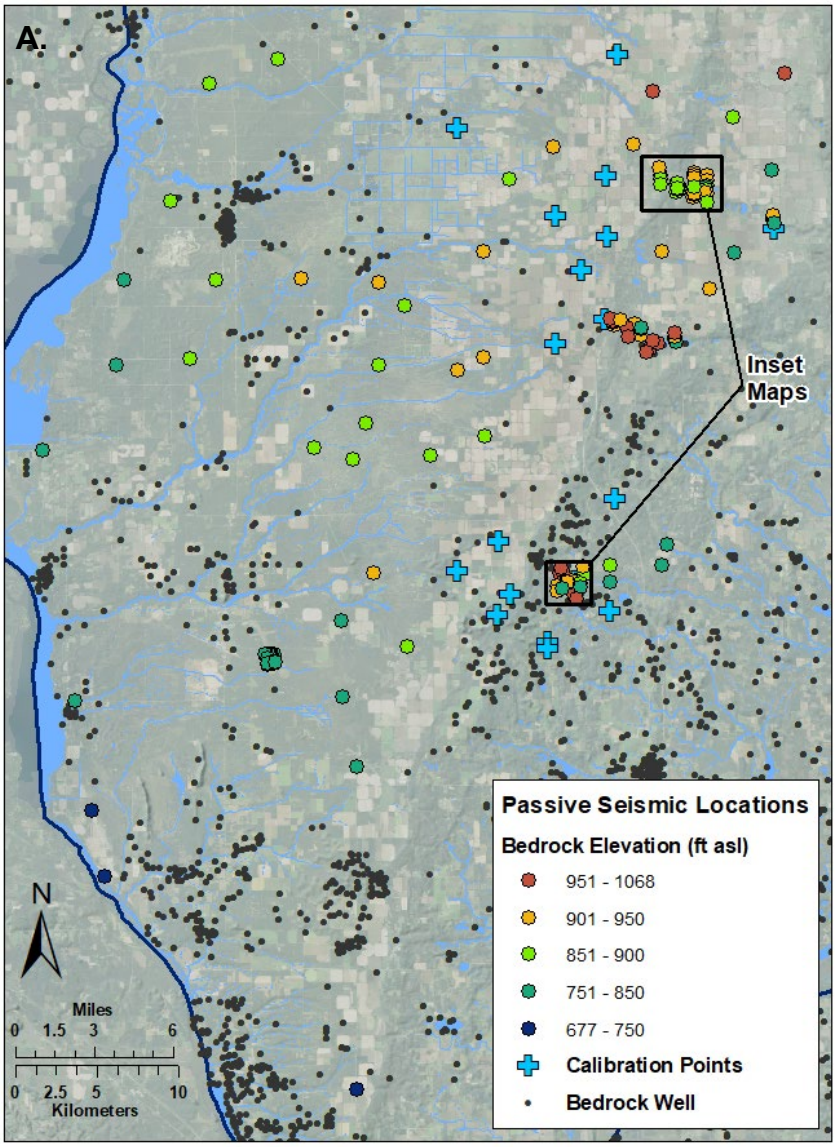

Figure 11 (a) Location of passive seismic measurements and calibration points across the CSLS area. Locations of wells with depth to bedrock information are also shown. Passive seismic data collection was concentrated in areas with little depth-to-bedrock data and (b) around the study lakes.

Bedrock elevation from passive seismic data: study lakes

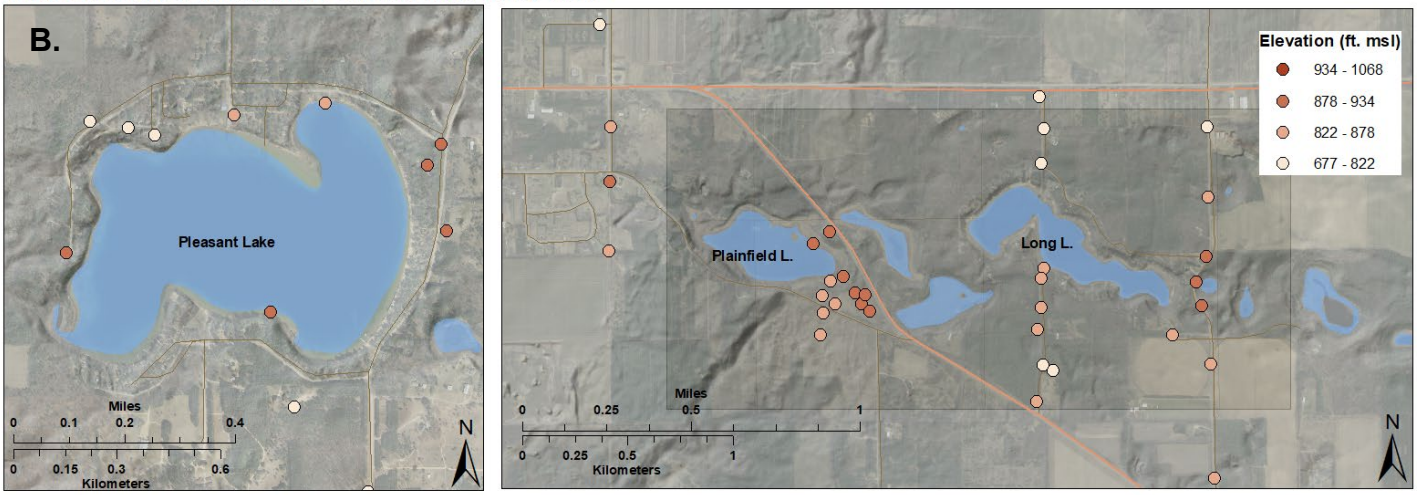

RESULTS:

WGNHS collected and processed 140 passive seismic points in the study area. These data and data points where wells were drilled to bedrock are shown in Figure 11. Passive seismic data collection efforts were focused in areas with sparse well data and in areas near the study lakes. The bedrock elevations estimated from the passive seismic data are shown as colored dots. Results show that the bedrock surface elevation within the Plainfield and Hancock tunnel channels is 20 or more feet lower than bedrock just outside the channels, indicating possible scouring of the bedrock surface during tunnel channel formation or tunnel channel formation along a preexisting bedrock channel. Passive seismic measurements around Pleasant Lake also show variability in the bedrock surface consistent with well log data, including an east-west-trending buried bedrock valley. Bedrock elevations from passive seismic points around Pleasant Lake and through the Plainfield Tunnel Channel are shown on Figure 11b. Passive seismic-derived bedrock elevations were used together with data from wells, borings, and outcrops to create the elevation map of the upper bedrock surface for groundwater model layer creation.

Direct Push Permeameter

Aquifer hydraulic conductivity varies laterally and with depth. Determining the degree of that variability aids in the creation of a hydrogeologic conceptual model and to ensure that the numeric groundwater model reflects real-world conditions. As part of a collaboration with Stanford University and the USGS, the Kansas Geological Survey collected hydraulic conductivity data using direct push permeameter (DPP) at two sites in the model domain: the Wallendal site near Friendship in Adams County and a site on the eastern edge of Plainfield Lake. These two sites are located in different depositional environments approximately 20 miles apart. The Wallendal site is located in the Glacial Lake Wisconsin basin (Figure 3 and 12A) and the Plainfield Lake site is located in the Plainfield tunnel channel, in an area of stagant ice between the Hancock and Almond moraines (Figure 3 and 12B). The DPP measurements provide a measure of horizontal and vertical hydraulic conductivity variations, in addition to bulk conductivity estimates for the sites and their two very different depositional environments. Rotosonic core was also collected at the Wallendal site; this allows comparison between hydraulic conductivity and the aquifer material.

METHODS:

Investigators used a Geoprobe® drill rig to collect direct push permeameter (DPP) measurements. The direct push permeameter data is collected by pushing a probe into the sediment, pressurizing the tip of the probe and measuring the time needed for the pressure to decay (Butler and others, 2007). This method was used to estimate hydraulic conductivity at depth intervals of 1.6 ft in two test holes at each site. Drilling more than one test hole allows investigators to determine variation in hydraulic conductivity with distance as well as depth. The locations of the test borings are shown in Figure 12A and B. The borings at Plainfield Lake are 44 feet apart and at the Wallendal site the borings are 33 feet apart.

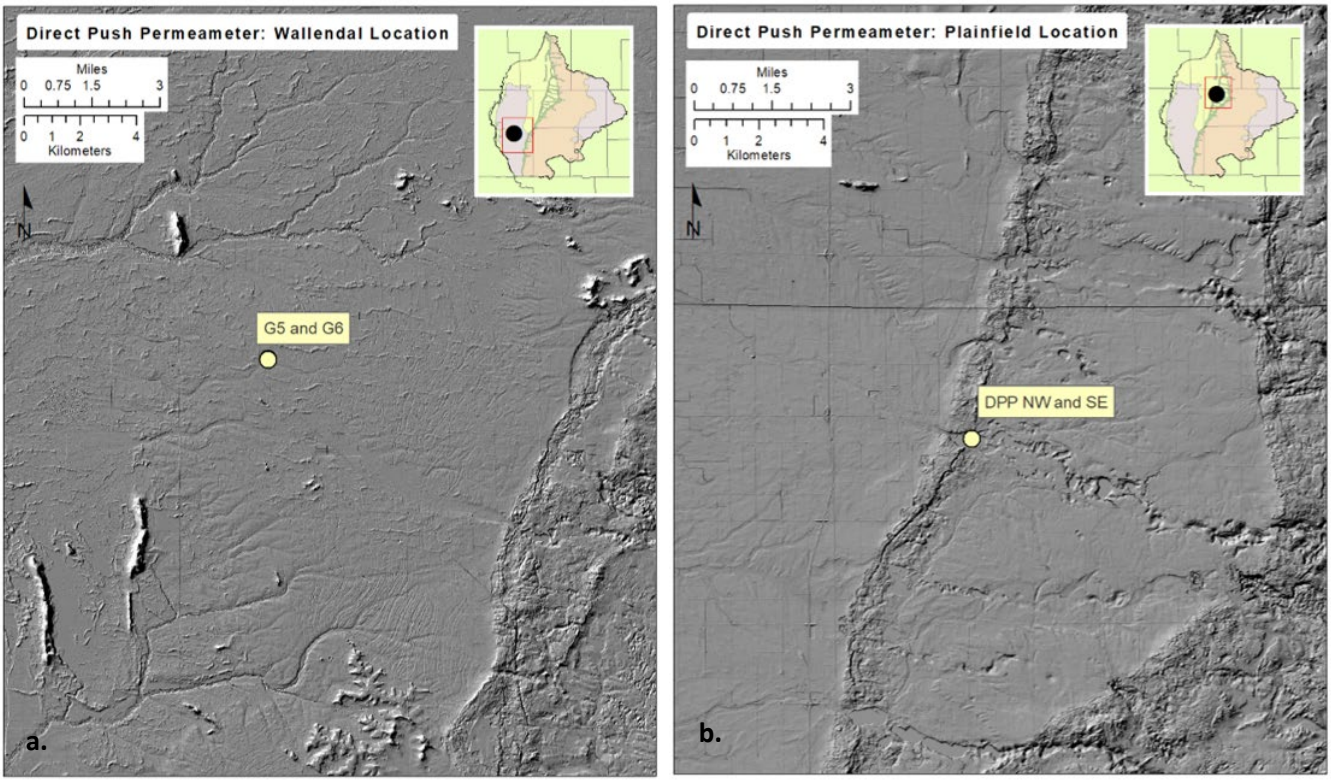

Figure 12. Locations of the DPP testing. Figure (a) shows the location where DPP was conducted in two borings at the Wallendal site, located within the basin of Glacial Lake Wisconsin. Figure (b) shows the location where DPP was conducted in two borings near Plainfield Lake, located just west of the Hancock moraine and in the Plainfield tunnel channel.

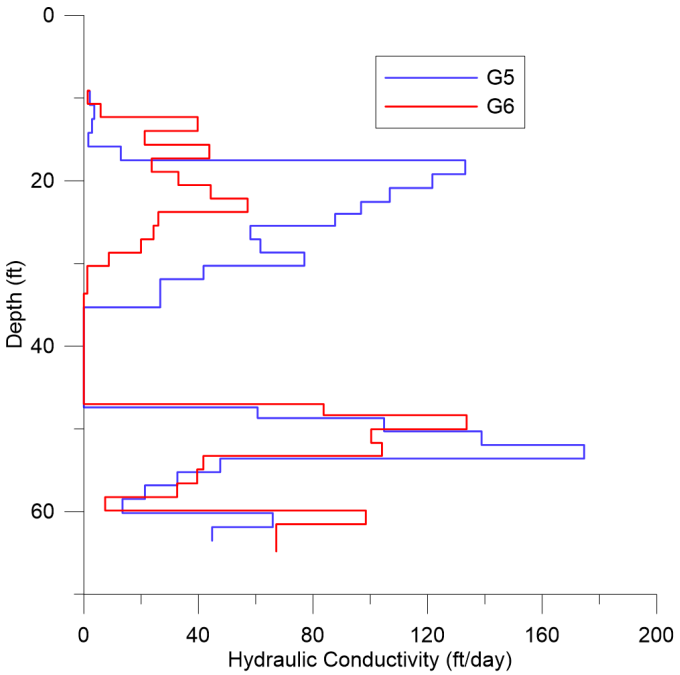

Figure 13. Direct push hydraulic conductivities at the Wallendal Site, Adams County. The low-conductivity zone from 35-48 feet depth in the Wallendal borings corresponds to the New Rome clay layer.

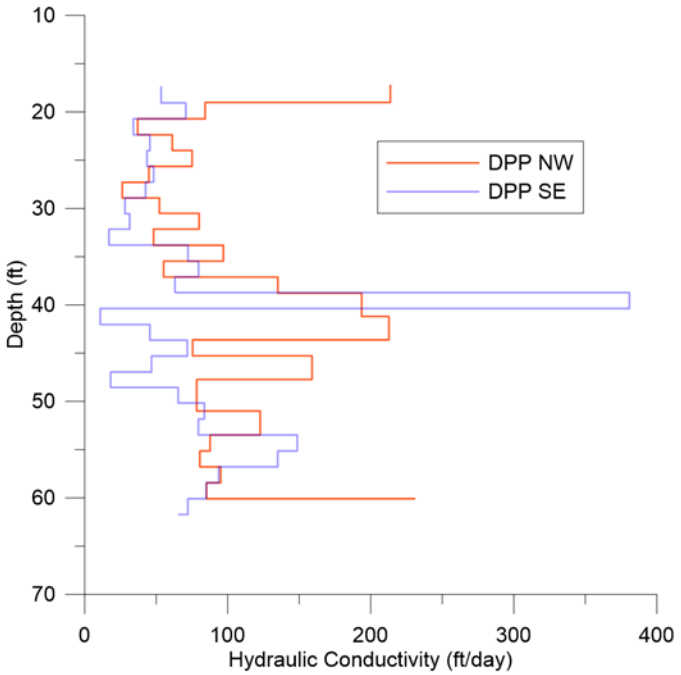

Figure 14. Direct push hydraulic conductivities at Plainfield Lake.

RESULTS:

The results for the two DPP field sites are shown as step plots of hydraulic conductivity with depth in Figures 13 and 14. The lateral correlation at the Wallendal site borings is shown by the overall similarity of the hydraulic conductivities with depth in this pair of borings and their relative variations with depth. The New Rome formation is indicated by the low conductivity zone from 35 to 48 feet. Lateral correlation at the Plainfield site in borings DPP NW and DPP SE is not as pronounced as at the Wallendal site but is present as indicated by the peaks in hydraulic conductivities around 40 ft depth and lower hydraulic conductivity values from 25 to 35 feet.

Although lateral correlation is evident between the boring pairs at both sites, the method also shows how heterogeneous these sediments are with depth. The variation of hydraulic conductivity with depth is over more than an order magnitude for all the borings, even neglecting the New Rome Formation. The differences between the hydraulic conductivites of the borings are often on the order of hundreds of feet per day or factors of two or more. This variation is expected for these sediments and would play a role in transport issues and calculations such as isotope analyses for flow paths that have length scales similar to the borings distances. However, variations on this scale are unlikely to be important on the scale of the CSLS groundwater modeling, which simulates regional groundwater movements controlled by overall aquifer conductivity (Bradbury and Muldoon, 1990).

Bulk hydraulic conductivities can be calculated for these sediments using the weighted average of the conductivities calculated for each boring. At the Wallendal site, the hydraulic conductivities of the

sediment above the New Rome for the G5 and G6 borings were 55 and 26 ft/d, respectively. The hydraulic conductivities of the sediment below the New Rome for G5 and G6 borings were similar at 71 and 69 ft/d, respectively. At the Wallendal site, pumping tests above and below the New Rome yielded hydraulic conductivities of 302 and 66 feet per day, respectively (Hart, 2015). While the pumping test value above the New Rome does not match the DPP bulk calculated values, the pumping test value below the New Rome is again similar to the DPP bulk calculated values. At the Plainfield site, the hydraulic conductivities for the DPP NW and DPP SE borings are 101 and 75 ft/d, respectively. A specific capacity test in a nearby well, PFL05, gave a similar result of 81 ft/d.

Down-hole geophysics

Down-hole geophysical gamma logs were collected from the rotosonic borings in the Plainfield tunnel channel (LL101 and PFD24, locations shown in Figure 22) and at one of the mud rotary core holes (PFL101, shown on Figure 17). Gamma logs provide information on lithostratigraphy (where rock or sediment units are differentiated based on their physical characteristics).

METHODS:

Gamma logs record variations in natural gamma radiation present with depth and can help to characterize geology and hydrostratigraphy. Gamma radiation comes primarily from potassium, uranium and thorium. Since uranium and thorium are present only at very low concentrations, most of the gamma radiation comes from potassium which is relatively abundant in silts and clays. Therefore, the gamma log can help to identify finer grained sediment intervals in a boring.

RESULTS:

The geophysical logs from the Plainfield tunnel channel rotosonic boreholes (PFD24 and LL101) and the Plainfield Lake mud rotary borehole (PFL101) are included with the boring logs in Appendix A. No elevated gamma readings were recorded in boring PFL101, and no fine-grained sediment was seen in the cores collected in the boring. Slightly elevated gamma readings correspond to finer grained sediment from 110-135 and 300-315 feet below grade in the eastern rotosonic core hole (PFD24). High gamma readings at the bottom of rotosonic hole PFD24 correspond to the granitic bedrock encountered at the bottom of the boring. Potassium is commonly abundant in granite and uranium and thorium are sometimes present at low concentrations; both of these factors lead to elevated gamma readings in granite.

Ground Penetrating Radar

Ground penetrating radar (GPR) lines near Long Lake were collected in 2015 as part of a previous study of the stratigraphy of Glacial Lake Wisconsin. They are included in this report to provide additional data on the sediments near and beneath Long Lake.

METHODS:

Ground penetrating radar uses pulses of electromagnetic waves to image the subsurface. These waves penetrate the earth and are reflected by sediment and rock with different physical properties. They are most sensitive to changes in water and clay content so changes in porosity and lithology produce strong reflections. In these surveys, the GPR unit transmits and receives signals as it is towed across the surface, creating a continuous record of reflectors when they are present. Additional information on GPR theory can be found in Reynolds, 1997. We used a Sensors and Software SIR-3000 pulse and record unit with a 80-MHz antenna to collect the data. The starts and ends of the data lines were geolocated with a Garmin Oregon 550t GPS. The data were analyzed using Sensors and Software's RADAN 7 software.

RESULTS:

The GPR lines show what is likely the tunnel channel collapse surfaces on the west and south edges of Long Lake (Figures 15 and 16). Lines 7 and 11 both show strong continuous undulating reflections from near land surface to depths of nearly 20 meters (66 feet). The depths to the top of fine-grained sediments observed in the direct-push borings and well construction reports coincide with at the of the GPR reflections. This suggests nearly continuous fine-grained sediments at these locations. However, the continuous reflectors in Line 7 do not appear to extend all the way to the north and south ends of the line, indicating, in agreement with the direct-push borings and well construction reports, that the fine-grained sediments are found near Long Lake but do not extend in a continuous layer far from the lake. Other GPR lines were either collected near the same locations and redundant or the signal was not easily interpreted. The data were collected in the spring of 2015 when the lake levels were much lower than present making it possible to image an area now underwater in Line 11.

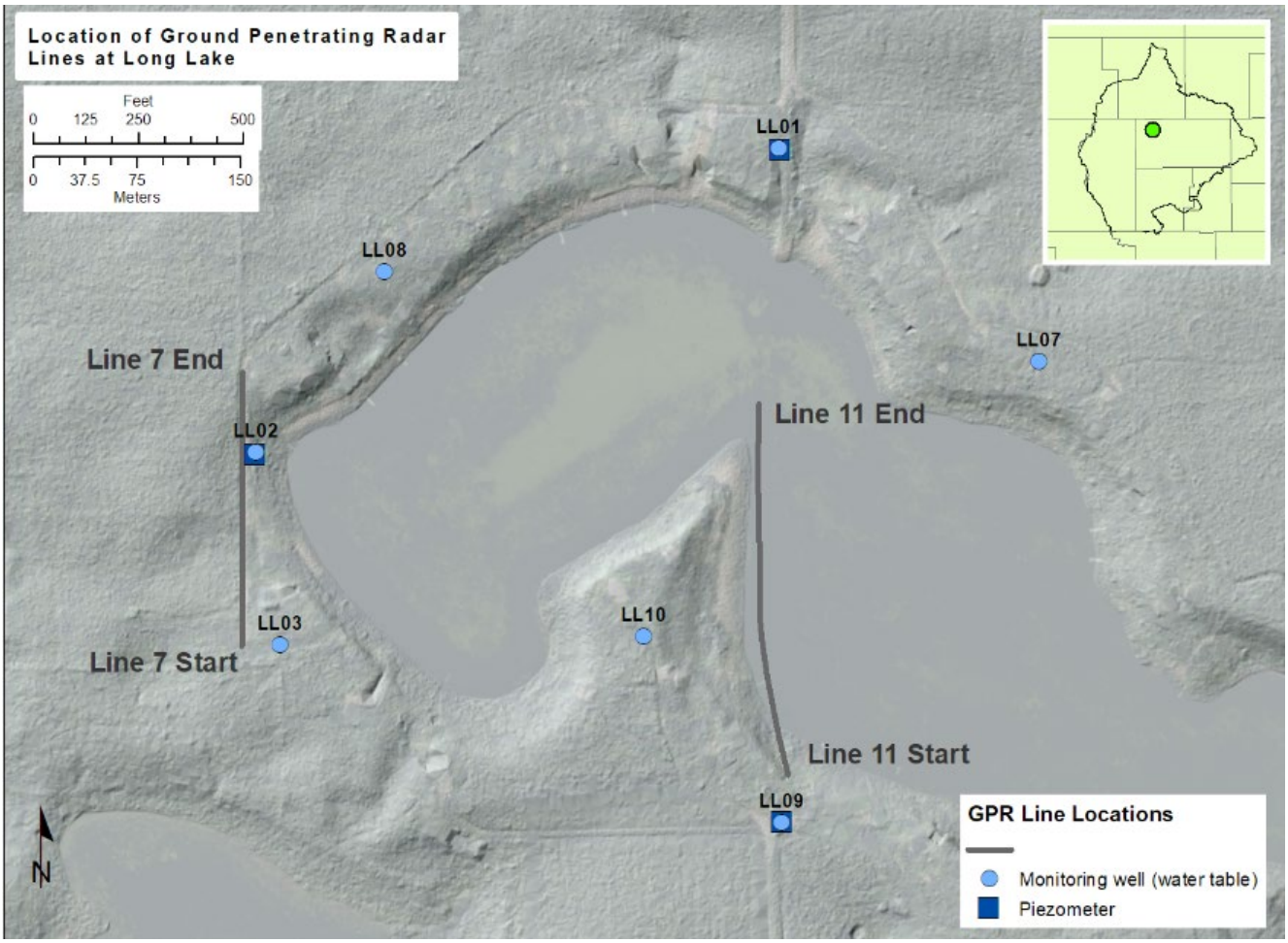

Figure 15. Locations of GPR Lines 7 and 11.

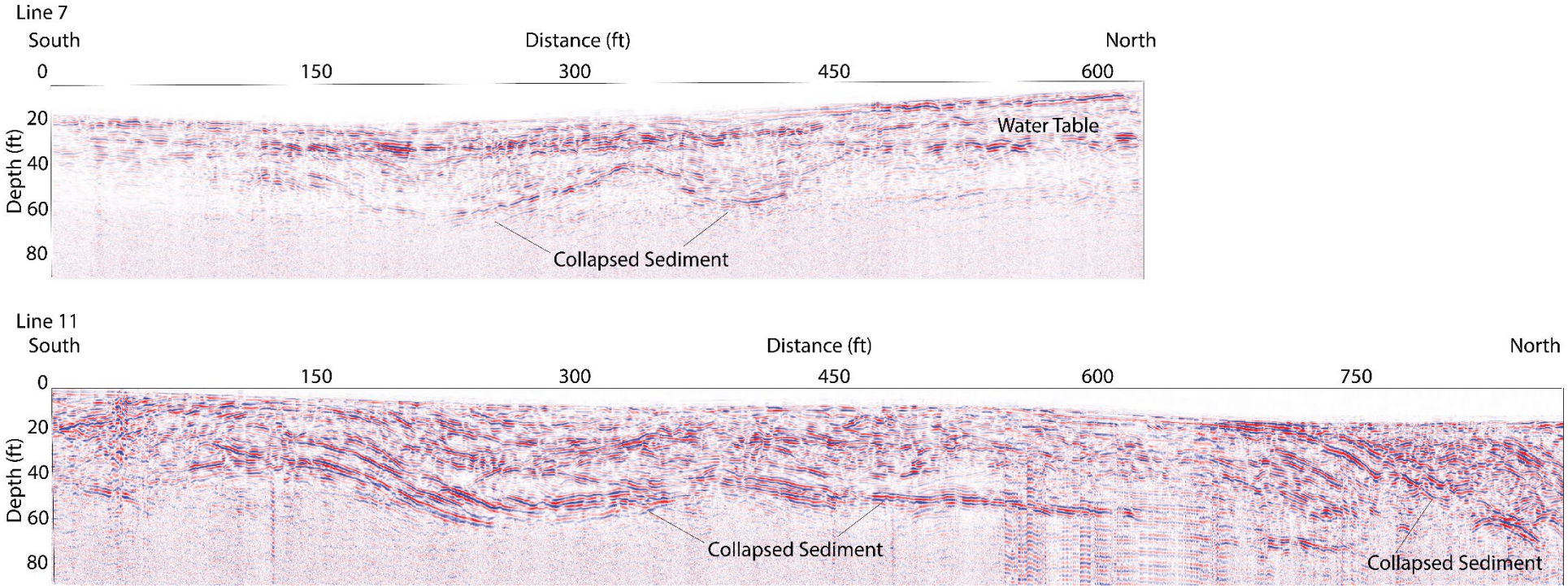

Figure 16. GPR records along Lines 7 and 11. The collapsed sediment is apparent in both lines. The water table in Line 7 is also indicated.

Quaternary Sediment Data Collection

The characteristics of aquifer materials (grain size, layering, geologic structure) determine the flow paths and velocity of groundwater movement and the details of groundwater-surface water interactions. Quaternary sediments were collected for the CSLS using several different methods. Geologic materials were sampled using a direct-push method at more than 30 locations around the study lakes, at two locations in the Plainfield Tunnel channel using rotosonic coring, and near Plainfield Lake using mud rotary coring. These borings provide better characterization of aquifer materials, contribute to the creation of conceptual models, and inform the creation of hydrostratigraphy. Grain size analysis and geologic unit descriptions from the study borings were used to supplement information found in well construction reports, existing geologic logs, and geophysical data. Data were synthesized to create conceptual cross-sections for the study lakes and Plainfield Tunnel Channel (shown below in Hydrostratigraphy – Conceptualization and layer creation).

Direct-Push Borings

Core was collected from Geoprobe® direct push cores during the installation of 32 monitoring wells surrounding the study lakes (locations shown on Figures 17, 18).

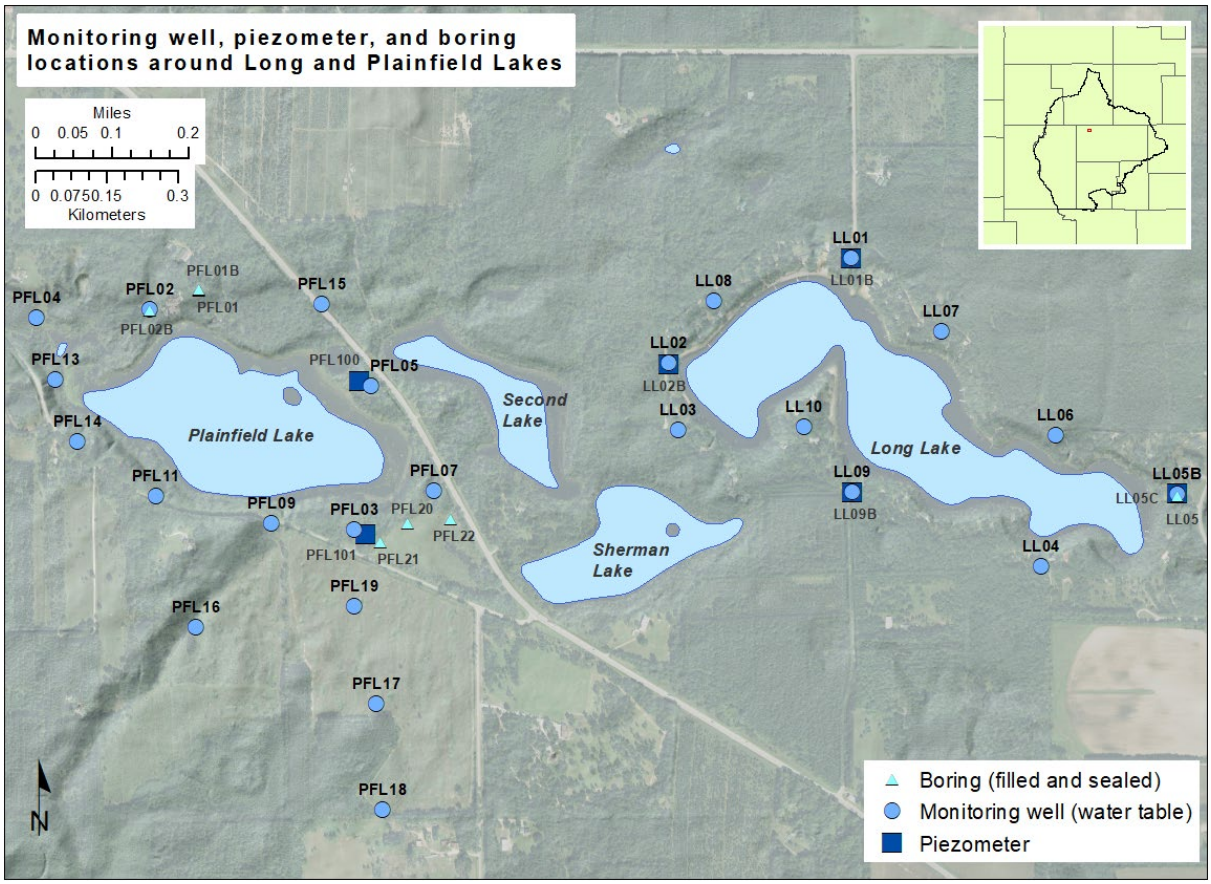

Figure 17. Monitoring points at Long and Plainfield Lakes. LL01B, LL02B, LL05C, LL09B, PFL100, and PFL101 are piezometers. Boreholes PFL01, PFL01B, PFL02B, LL05, PFL20, PFL21, and PFL22 were not converted to monitoring wells and therefore filled and sealed. PFL22 was filled and sealed without sample recovery due technical problems during drilling.

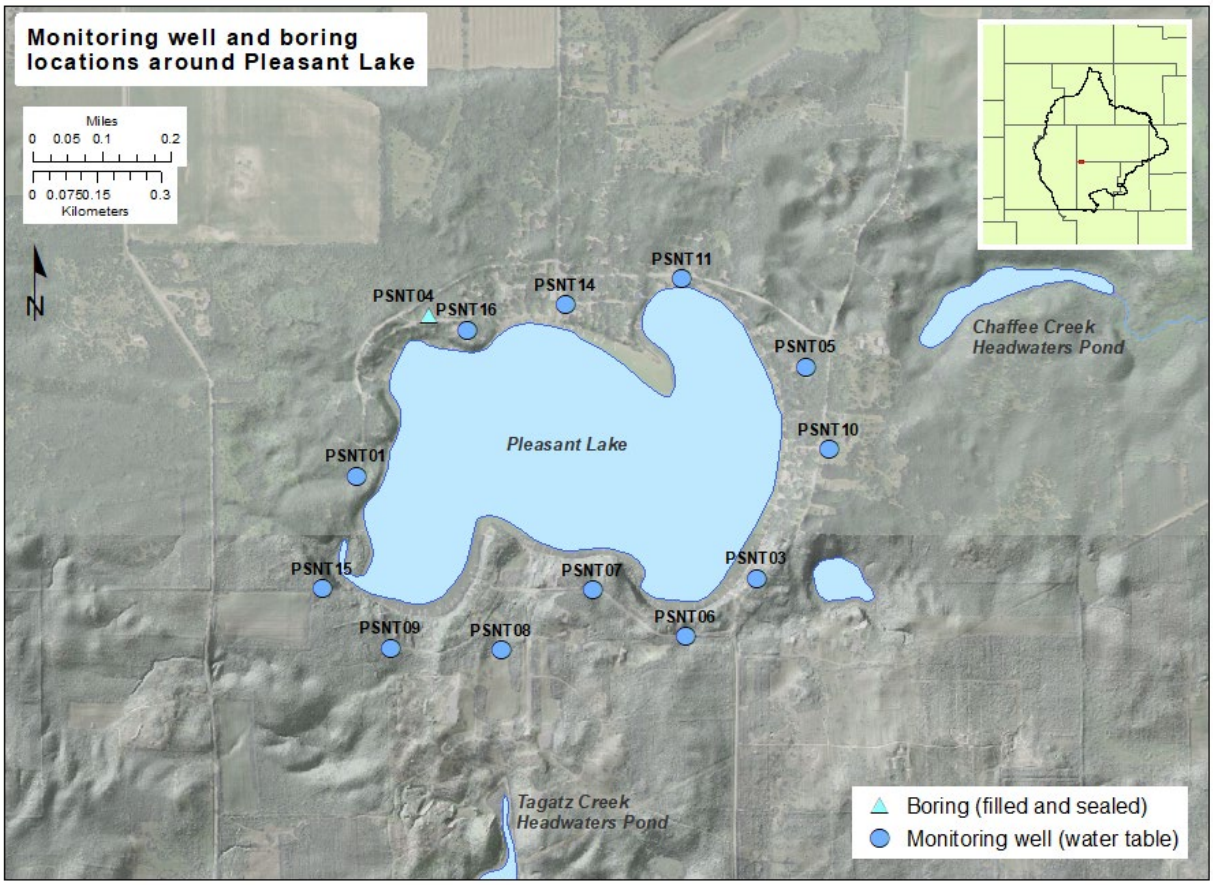

Figure 18. Monitoring well, piezometer, and boring locations around Pleasant Lake. PSNT04 was not converted to a monitoring well and was filled and sealed.

DATA COLLECTION METHODS:

Direct push coring is conducted in five-foot flights and is useful for shallow sample collection up to ~100 feet depth, but often considerably less (50-70 feet). Direct push cores collected for this study ranged from 10-101 feet deep. Continuous sample collection is possible with direct-push coring. However, incomplete recovery occurs when friction within the sample barrel is greater than friction outside of it. This results in the sample barrel pushing past sediment, rather than collecting it within the barrel. Re-coring of sediment that collapses into the hole can occur with direct push sampling when using an open sample barrel. The direct push method collects cores with a diameter of 1-2 inches. The larger, 2-inch barrel is preferred in shallow (~30 feet) borings because it allows for the largest potential sample to be collected. However, in deeper borings, the 2-inch barrel is left as casing in the ground and a 1-inch sample barrel was used to retrieve a smaller sample volume. This prevents the need for re-coring and in general was used to collect samples in borings >50 feet deep. In total, approximately 1338 feet of core was drilled in the 32 direct push borings, with 28-92% sample recovery.

Cores were stored, described, photographed, and sampled. Samples were collected for grain-size analysis from each four- or five-foot interval, at lithologic contacts, or within intervals of interest (e.g. fine-grained

intervals). Grain size was analyzed by laser diffraction (Miller and Scheatzl, 2012) using a Malvern Mastersizer 2000E on the <2mm diameter grains (sediment sand-size and smaller). Sediment greater than sand-size was removed prior to the analysis. No attempt was made to quantify the percent gravel in the sediment given the small sample size recovered in the sample tubes, however the amount of gravel present can be qualitatively assessed using the core photos (Appendix A). While clay fraction particles may be defined as having a grain size of 2 μm (ISO 14688-1:2017) or 4 μm (Wentworth Class), our analysis used a clay/silt boundary of 8 μm to avoid potential issues with underestimation of clay compared to traditional methods (Konert and Vandenberghe, 1997; Wen et al., 2002). This report also includes the silt-clay boundary at 2 μm in Appendix H.

RESULTS:

Quaternary sediments collected in Central Sands study soil borings around the three study lakes showed grain sizes that range from coarse sand and gravel (more common) to clay (less common). Given that the majority of the coring associated with this project occurred within areas of collapse it is difficult to assess if the variability here is representative of, or anomalous compared with, the regional stratigraphy outside collapsed areas. However, the majority of the samples collected were sands and gravels (Figure 19, 20). Grain-size results are located in Appendix H.

Fine-grained sediments are of particular interest for the hydrostratigraphy of the area. In general, samples surrounding Long Lake include much more fine-grained sediment than nearby Plainfield Lake (Figure 21). These samples are both located within the collapse of the Plainfield Tunnel Channel, and areas of collapse typically have more complicated, heterogeneous, lithologies than the regional stratigraphy. Where fine-grained sediment is observed at Long Lake it occurs at about 25 feet depth, is approximately 15 feet thick and laminated (Figure 21a). Sediment surrounding Pleasant Lake is generally coarse sand and gravel (Figure 19c). Fine-grained units there are similar to siltier gravel units at Plainfield Lake, or occur within the first 15 feet below the surface. This is likely due to heterogeneity within the collapsed topography of the moraine where Pleasant Lake is located. Sediment surrounding Pleasant Lake is typically siltier near the surface, a configuration also observed by Rawling et al. (2008), or in relatively silty zones within gravely sediment (Figure 21c). While these silty zones do contain a higher percentage of silt than the surrounding sand and gravel, most occur in gravelly layers and likely are not laterally continuous or barriers to groundwater flow. In addition, the percent silt (Figure 20) is overestimated relative to the entire sediment package in samples with high gravel content. This is because the percent silt is calculated relative to only the sample fraction with a grain size of 2mm (sand) or smaller, excluding gravel.

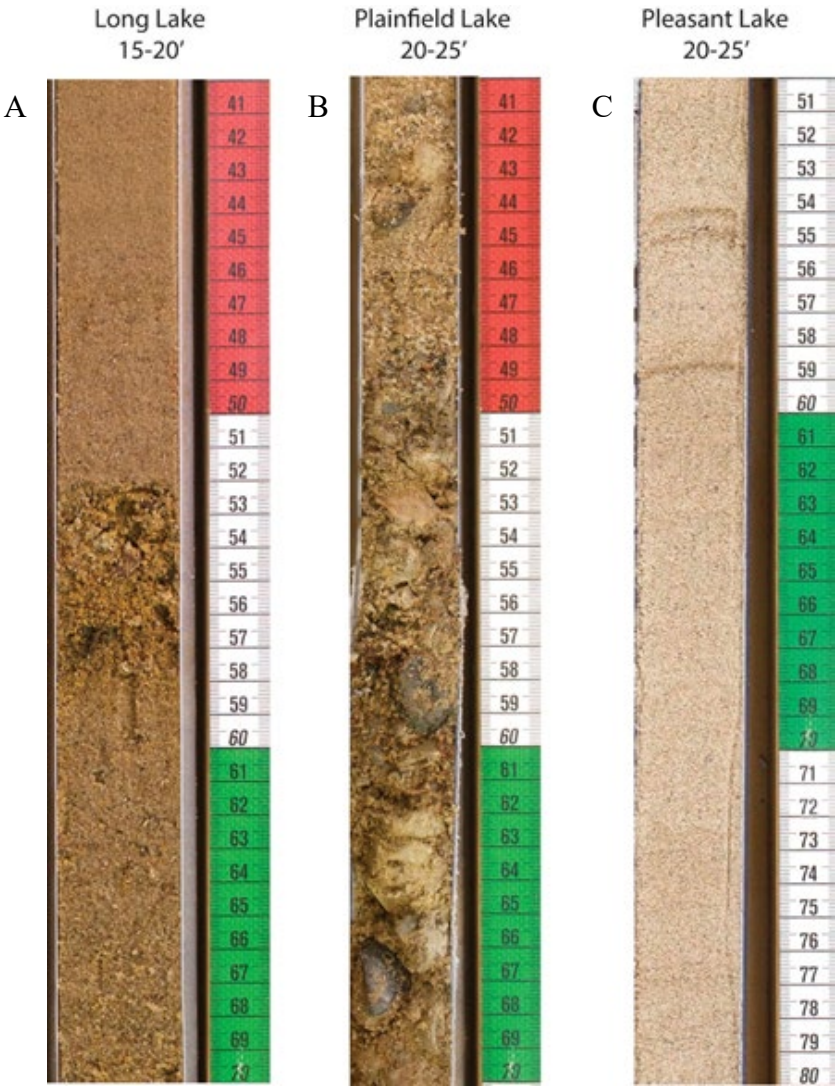

Figure 19. Examples of typical coarse-grained sediment from direct push samples (scale in cm). (a) Long Lake: interbedded sand and gravel in core LL-09 (b) Plainfield Lake: sandy gravel in core PFL-14 (c) Pleasant Lake: well-sorted sand in core PSNT-07.

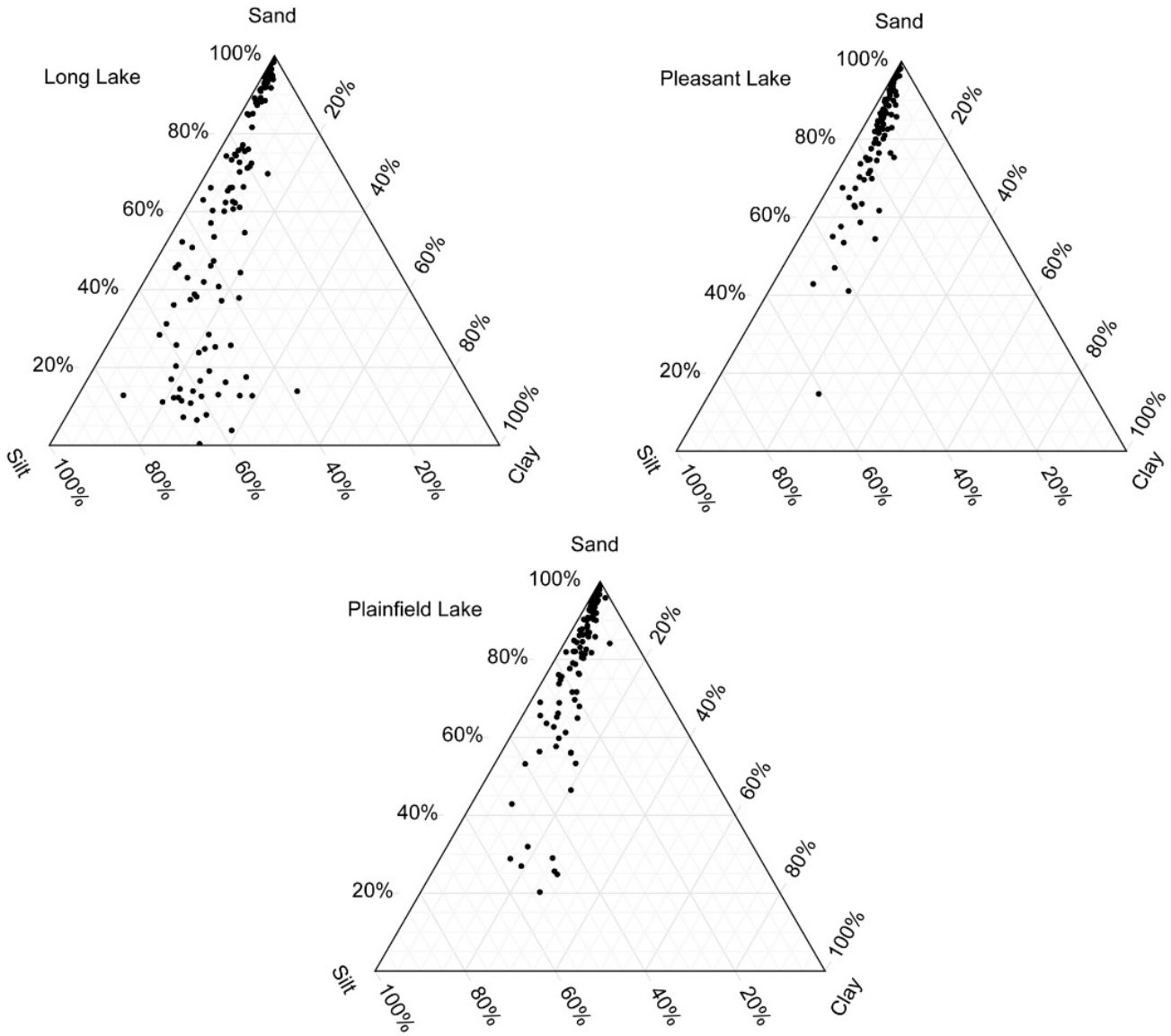

Figure 20. Distribution of <2mm fraction of sediment (sand-sized and smaller) from Long, Plainfield and Pleasant Lakes.

Figure 21. Examples of finer-grained sediment from Geoprobe® samples. (a) Long Lake: contact at 78 cm between sand overlying laminated silty-clay in core LL-08 (b) Plainfield Lake: example of silty gravel between 132-137 cm where the <2mm fraction is ~30% silt in core PFL-11 (percent of only the sand and smaller grain-size fraction, not including the gravel) (c) Pleasant Lake: example of heterogenous sediment within the collapsed moraine in core PSNT-09, sediment between 67-69 cm is ~50% silt and 30% clay.

Rotosonic Borings

Rotosonic coring was used to target deep sediments and determine bedrock depth at two locations within the Plainfield Tunnel Channel (Zoet et al., 2019). Tunnel channels contain a variety of sediment types and are an area of particular concern for hydrostratigraphy in the Central Sands, especially since Long Lake and Plainfield Lake are situated within the Plainfield Tunnel Channel. In the Central Sands, tunnel channels originally formed when water discharged beneath the Green Bay Lobe during the Hancock Phase of glaciation. Buried ice that was preserved in the channel melted after permafrost conditions ended in the area, creating the modern surface expression of linear collapse zones (Figure 7). A rotosonic boring was sited within the Plainfield Tunnel Channel three miles southeast of the study

lakes ("eastern rotosonic core" – PFD24) in a location coinciding with a previously-completed active seismic survey line (Figure 22) (Zoet et al., 2019). This allowed integration of the rotosonic boring results with the active seismic results to create a more complete picture of tunnel channel sediments and configuration. A second rotosonic boring was also located within the Plainfield Tunnel Channel, 750 feet south of Long Lake ("western rotosonic core" – LL101). Core logs and photos of the rotosonic borings can be found in Appendix A.

DATA COLLECTION METHODS:

Rotosonic coring is conducted in 20-foot flights, and the method is not restricted as to maximum boring depth. The rotosonic core diameter was 4 inches. As with direct push coring, continuous sample collection is possible with rotosonic coring, and incomplete sample recovery occurs where friction within the sample barrel exceeds friction outside the barrel. In general, coarse sediments had poorer sample recovery rates than finer sediments. Rotosonic coring is cased with a 6-inch pipe. The eastern rotosonic boring, PFD24, was 416 feet deep, with 46% sample recovery. The western rotosonic boring, LL101, was 255 feet deep, with 54% sample recovery.

The rotosonic core samples were handled and analyzed using the methods described for the direct-push cores, above. Sediments from western rotosonic boring, LL101, were described and photographed for inclusion in this report, but grain-size analysis was not conducted because of time constraints (boring was completed in late 2019). Samples from the 20-foot coring flights were divided into four-foot intervals for storage.

RESULTS:

The eastern rotosonic core, PFD24, was used to investigate deep stratigraphy in the center of the Plainfield Tunnel channel, including identification of fine-grained strata and depth to bedrock. Data were compared to stratigraphic data from the previous active seismic survey (Figures 22, 23) (Zoet et al., 2019). At this location, the active seismic results show the channel to be approximately 1500 ft wide in the subsurface; this is nearly equal to its surface expression. However, the subsurface tunnel channel depth is 210 ft, nearly six times deeper than the surface expression collapse of 35 ft below the surrounding land surface. This rotosonic boring confirmed the bright reflector noted at 1017 ft asl (310 m asl) in the active seismic profile was a lithologic change from sand and gravel to laminated lake sediment (Figure 23, 24). Two fine-grained zones including silts and laminated clays were recorded in PFD24 core from 113-132 ft bgs (999-1018 ft asl) and 275-318 ft bgs (813-855 ft asl). However, the bulk of the sample recovered was well-sorted sand or sand and gravel.

Vertical variations in hydraulic conductivity of several order of magnitude were estimated using the Hazen equation,

$$K_H = C_H D_{10}^2, \qquad \text{(Equation 3)}$$

where K_H is the hydraulic conductivity, in cm/s, C_H is an empirical coefficient ($mm^{-1}s^{-1}$) with a range of values from 0.01 to 10, most commonly given as 1, and D_{10} is the 10^{th} percentile grain size of a sample's distribution, in mm. The K_H calculated here used a C_H value of 1. The Hazen equation was derived for saturated sands, and assumes that the D_{10} grain size is between 0.1 mm and 3 mm. Because only half the samples from the eastern rotosonic boring, PFD24, had D_{10} in that range and because the equation does not account for aquifer properties such as compaction, the hydraulic conductivity distribution shown in Figure 25 should be taken to be qualitative rather than quantitative.

Bedrock was deeper than expected at 416.5 ft bgs and consisted of weathered Precambrian crystalline rock. The rotosonic boring samples are representative of the collapsed zone within the tunnel channel; future sample collection in uncollapsed areas will aid in determine if the stratigraphy observed here is representative of areas outside of collapsed zone or is unique to the tunnel channels.

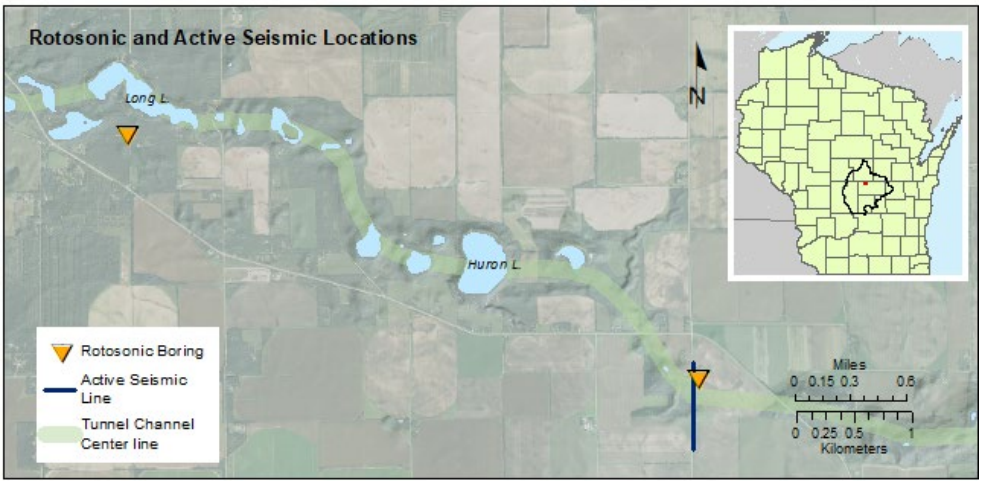

Figure 22. Locations of rotosonic borings drilled in the Plainfield Tunnel Channel. The eastern boring, PFD24, was completed adjacent to a previously-completed active seismic line. The western boring, LL101, was completed near the edge of the tunnel channel, 750 ft south of Long Lake.

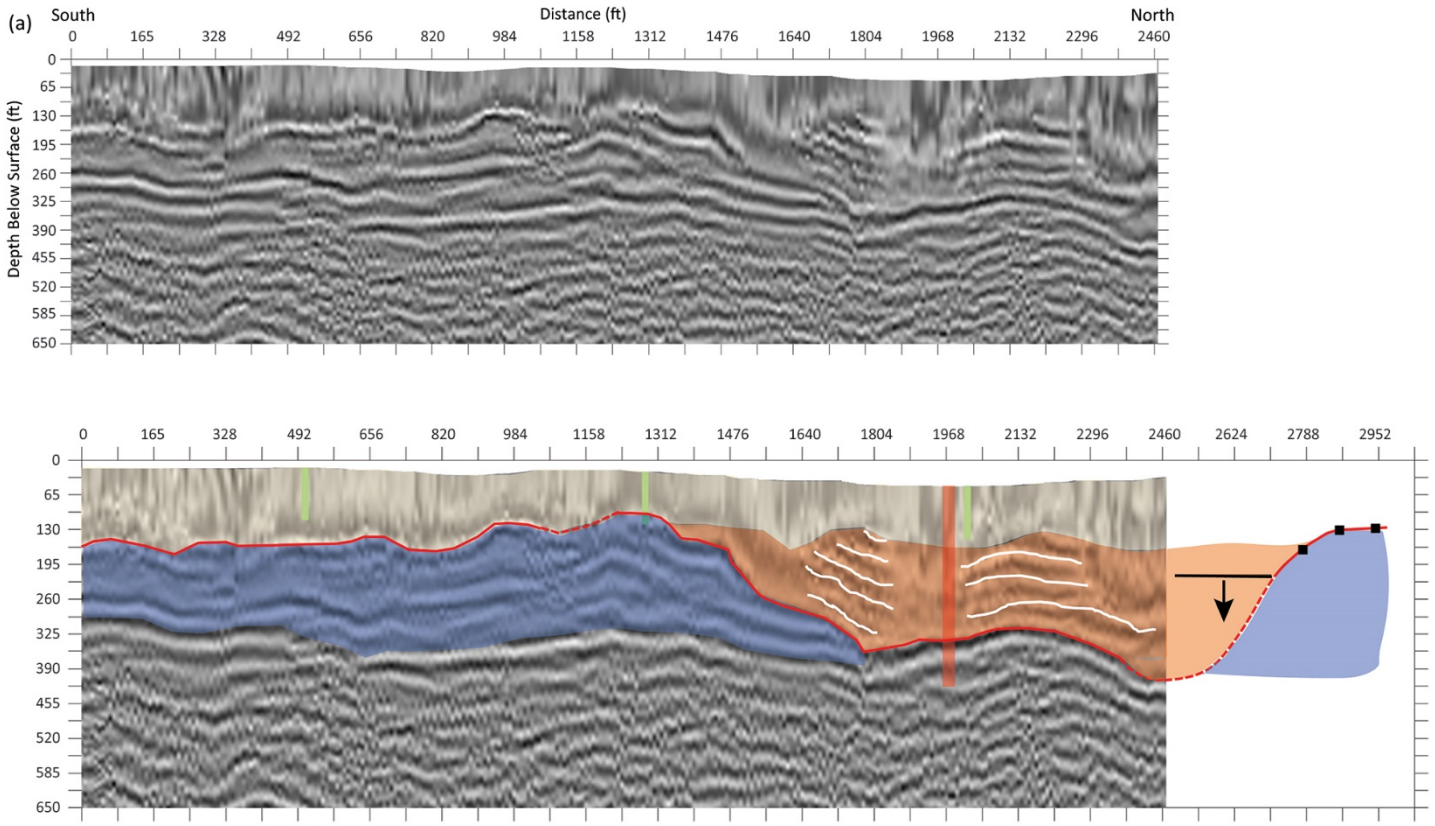

Figure 23. A 0.6-mi (1-km) seismic profile was collected across a tunnel channel with 8.2 ft (2.5 m) common midpoint spacing at nominally 12 folds. Hammer blow and assisted weight drop sources were used and impacts were stacked ca. 5-fold to improve the signal to noise ratio. Upper panel has final elevation corrected stacked image with no interpretation while the lower panel has interpretations of seismic reflectors. Lower Panel is passive and active seismic data. These data indicate a channel depth of about 210 ft (65m) with an approximate width of 1475 ft (450m). The solid red line indicates a contact that was observed with the geophysical data, while the dashed line indicates an inferred contact. In the region of the dashed line, the contact must exist below the vertical bar that signifies a depth of 195 ft below land surface. Green rectangles represent the depth of sampling with Geoprobe®, the red rectangle is the location of rotosonic boring PFD24.

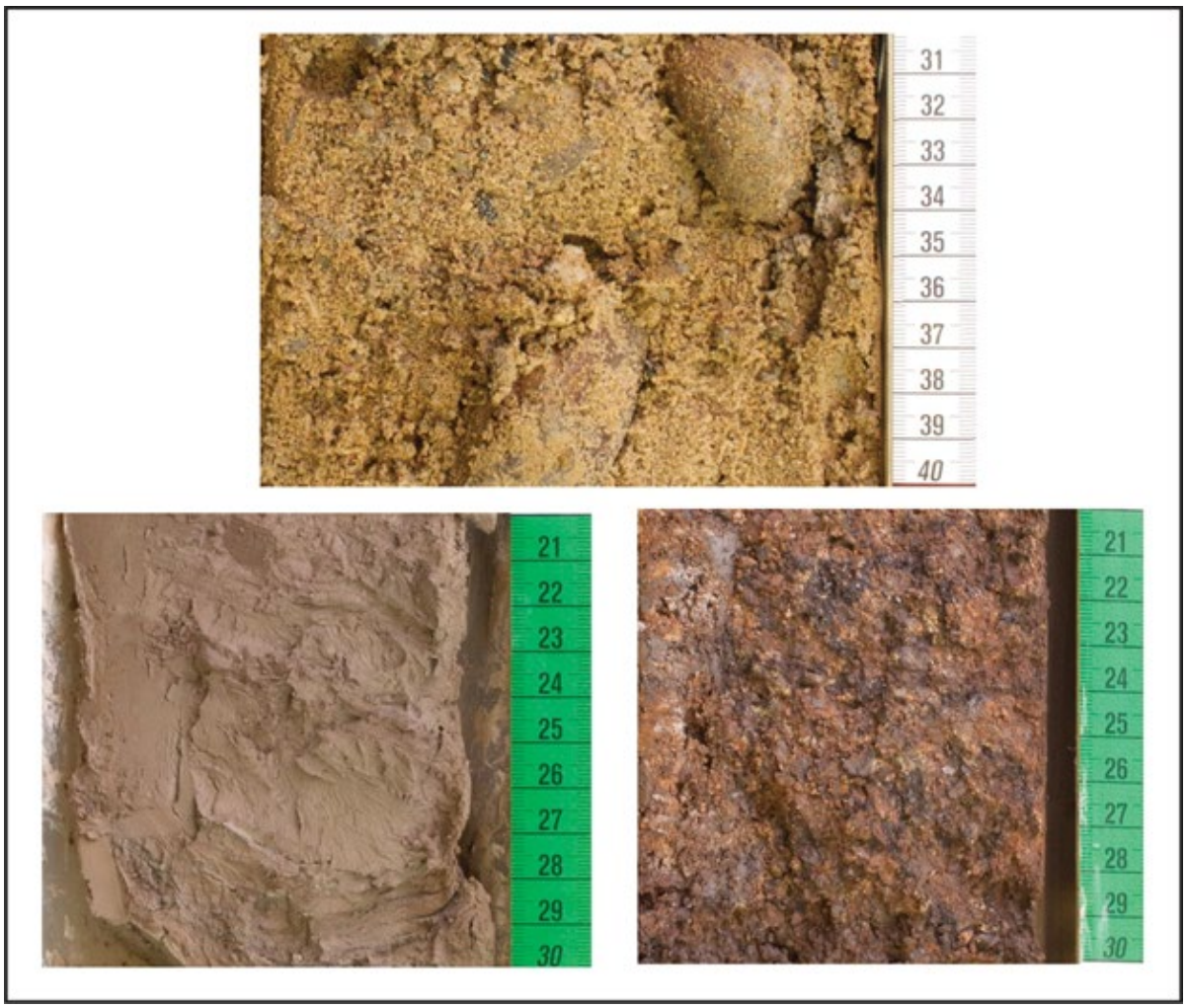

Figure 24. Examples of lithologies in eastern rotosonic boring PFD24, collected through the center of the Plainfield Tunnel Channel. Upper panel is sand and gravel 40-45 ft below ground surface (bgs), lower left is laminated fine-grained sediment 119-132 ft bgs, and the lower right is the bedrock 411-416.5 ft bgs.

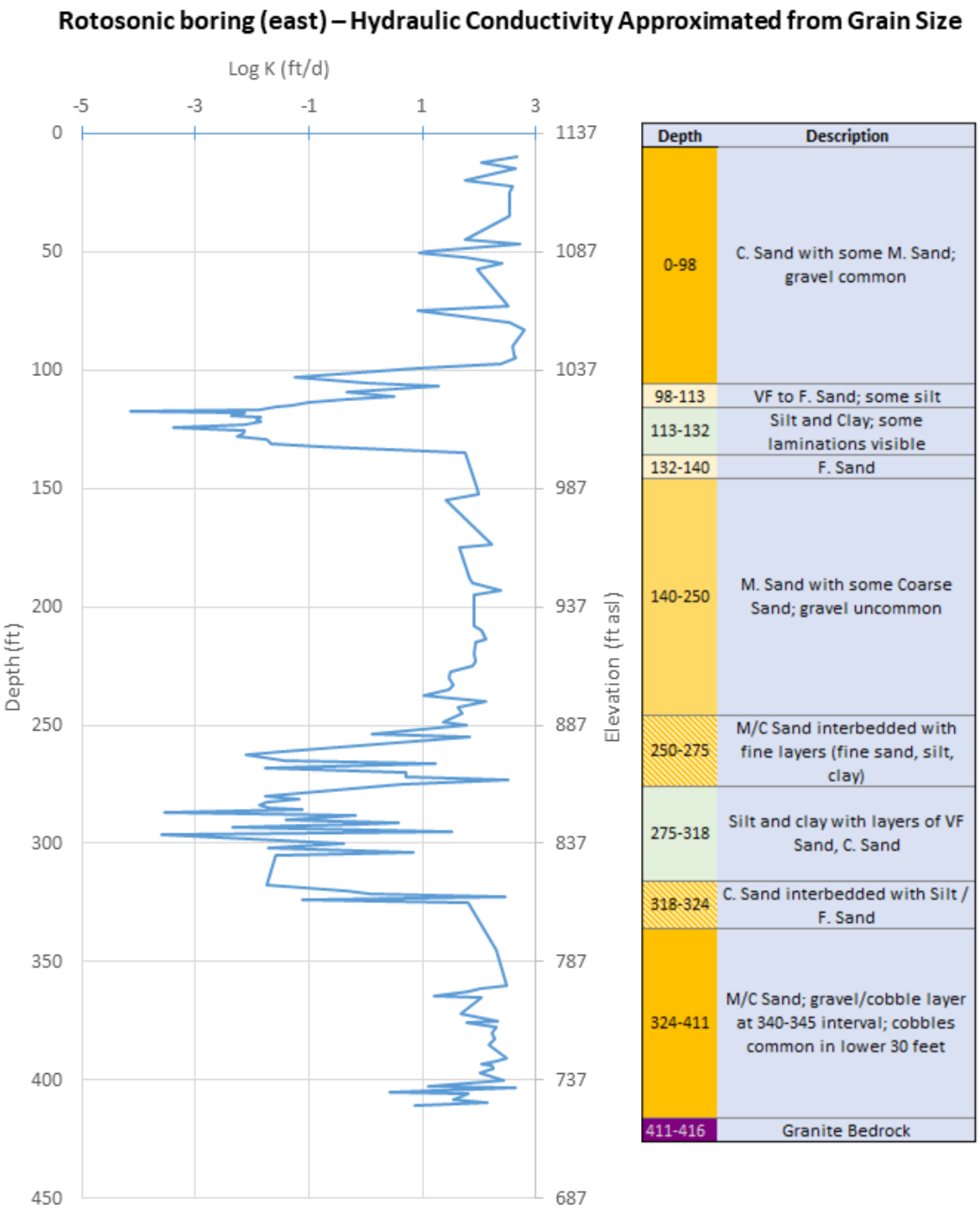

Figure 25. East rotosonic core, PFD24: generalized stratigraphy and hydraulic conductivity estimates from grain-size analysis. Hydraulic conductivity estimates were derived using the Hazen equation and should be considered qualitative as some formula assumptions are not met for all samples. (VF = very fine, F = fine, M = medium, C = coarse)

The western rotosonic core, LL101, was collected to investigate deep stratigraphy near Long Lake, including the extent of fine-grained sediments and depth to bedrock. Well construction reports and direct-push sample collection at Long Lake indicate that fine-grained sediments are common near the lake. The core was collected near the edge of the surface collapse that indicates the location of the Plainfield Tunnel, 750 feet south of Long Lake. Based on the relationship between the collapsed area and

the edge of the tunnel channel observed in the seismic survey at the eastern boring, it is likely the western core is located near the edge of the tunnel channel. However, without a nearby seismic survey the core location relative to the tunnel channel is uncertain. The Long Lake rotosonic core was collected in December 2019, and the geologic description of the core sediment available at the time of this report does not include laboratory grain-size analysis. The majority of the sediment collected in the core was well-sorted sand or sand and gravel that was likely deposited as outwash. Fine-grained sediment was collected in the LL101 at a similar depth to fine-grained sediments observed in the direct-push cores near Long Lake. In the rotosonic core, this consisted of ~1cm silty laminated beds in dominantly medium sand at 35-40 ft bgs (Figure 26). Geophysical work on the west end of the lake indicated lateral continuity of the upper surface of fine-grained sediments, so the fine-grained sediment noted in the rotosonic core may represent a single unit within the outwash that is thicker near the lake and thins to the south. The only other fine-grained sediment encountered was a massive silty very fine sand from 200-235 ft bgs. The fine-grained units may be distal outwash or possibly lake sediment. Sandstone bedrock was encountered at 245 ft bgs. A generalized geologic description of the boring is shown in Figure 27. More detailed description is provided in Appendix A.

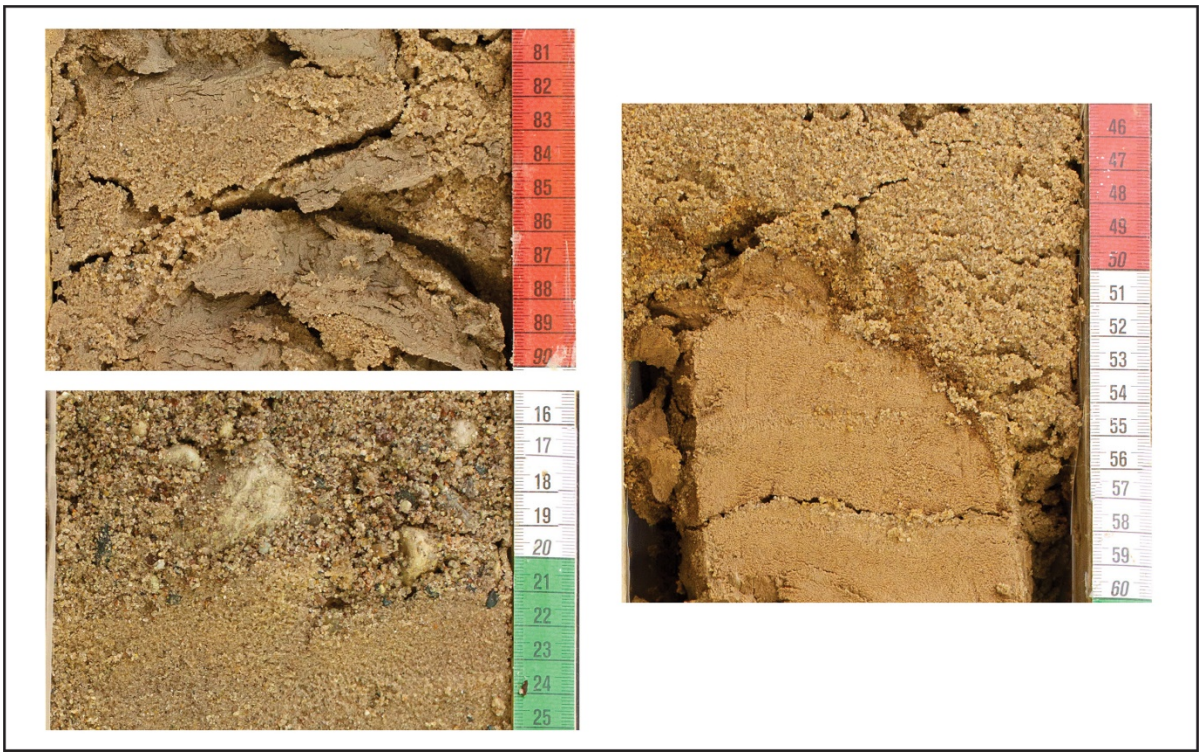

Figure 26. Examples of lithologies in the western rotosonic boring, LL101, collected south of Long Lake in the Plainfield Tunnel Channel. Upper left panel is broken laminated silty clay beds interbedded with sand 35-40 ft below ground surface (bgs), lower left is interbedded sand and gravel, 160-165 ft bgs. The photo at the right shows the contact between sand and massive very fine sand and silt 215-220 ft bgs.

Depth	Description
0-25	sand and gravel
25-30	fine to medium sand
35-40	medium sand with silty laminated beds
40-100	sand and gravel
100-140	sand coarser at top/fine at bottom
140-175	sand and gravel
175-200	medium sand
200-235	massive silty very fine sand
235-244	sand and gravel
245	sandstone

Figure 27. West (Long Lake) rotosonic core, LL101, generalized stratigraphy.

Rotosonic boring – Wallendal Site (Adams County)

A rotosonic core was collected at the Wallendal site in Adams County in addition to the Direct-Push Permeameter testing described above. The boring location is shown in Figure 12a. This work was conducted as part of a separate study prior to the CSLS. The core was photographed and logged according to the methods described for the Plainfield Tunnel Channel rotosonic core. This core, NMR-G7, has a prepared log shown in Appendix A. A range of sediment types were observed in the Wallendal rotosonic core, including both coarse outwash sands and the fine-grained New Rome Member. The observed changes in sediment type were well-correlated with the DPP results.

Mud Rotary Coring

A mud rotary core was collected near Plainfield Lake. Mud rotary coring used a 10-foot sample barrel and extended to a depth of 100 feet. The core had poor recovery due to the prevalence of coarse-grained sediments, with generally less than a foot of recovery per 10 feet sampled. In general, sample recovery was somewhat better in finer-grained sediments, while well-sorted sand and gravel below the water table had the lowest percent sample recovery.

Aquifer Properties

The hydraulic conductivity and storage properties of the sand and gravel aquifer and the bedrock aquifer are used to estimate flow through the groundwater system. Aquifer properties estimated from well data are used in the groundwater flow model to provide a reasonable range of values for calibrated modeling parameters. WGNHS compiled past aquifer testing results reported in published sources, estimated hydraulic conductivity from specific capacity tests reported in well construction logs. Pumping tests were performed to determine hydraulic conductivity at 36 water table monitoring wells and piezometers installed around the three study lakes.

Aquifer Test Data - Literature Review

Aquifer test data for the sand and gravel aquifer in the Central Sands region are available in several published reports. The results of 22 multi-well pumping tests and 46 slug tests are available. As shown in Figure 28, the majority of these tests were conducted in the northwestern part of the model domain (outwash plain). Test results are summarized in Table 1 and listed in Appendix I. The arithmetic mean hydraulic conductivity derived from slug tests is 106 ft/d. The mean hydraulic conductivity from pumping tests is 234 ft/d. Due to aquifer heterogeneity, it is typical for aquifer tests that assess a larger portion of the aquifer, such as multi-well pump tests, to produce higher conductivity values than those assessing smaller volumes (Bradbury and Muldoon, 1990). Multi-well tests are also used to determine aquifer storage properties including specific yield. Specific yields derived from multi-well pumping tests in the unconfined sand and gravel aquifer had a mean value of 0.17. These reported conductivity and specific yield values are within the range that would be expected for a sand and gravel aquifer.

Hart (2015) also conducted aquifer tests on the properties of the sand and gravel aquifer and New Rome confining unit in central Adams County. The New Rome was estimated to have a vertical conductivity of 2.6×10^{-5} ft/d (Falling Head analysis, laboratory core) to 0.56 ft/d (aquifer loading, Terzaghi Analysis).

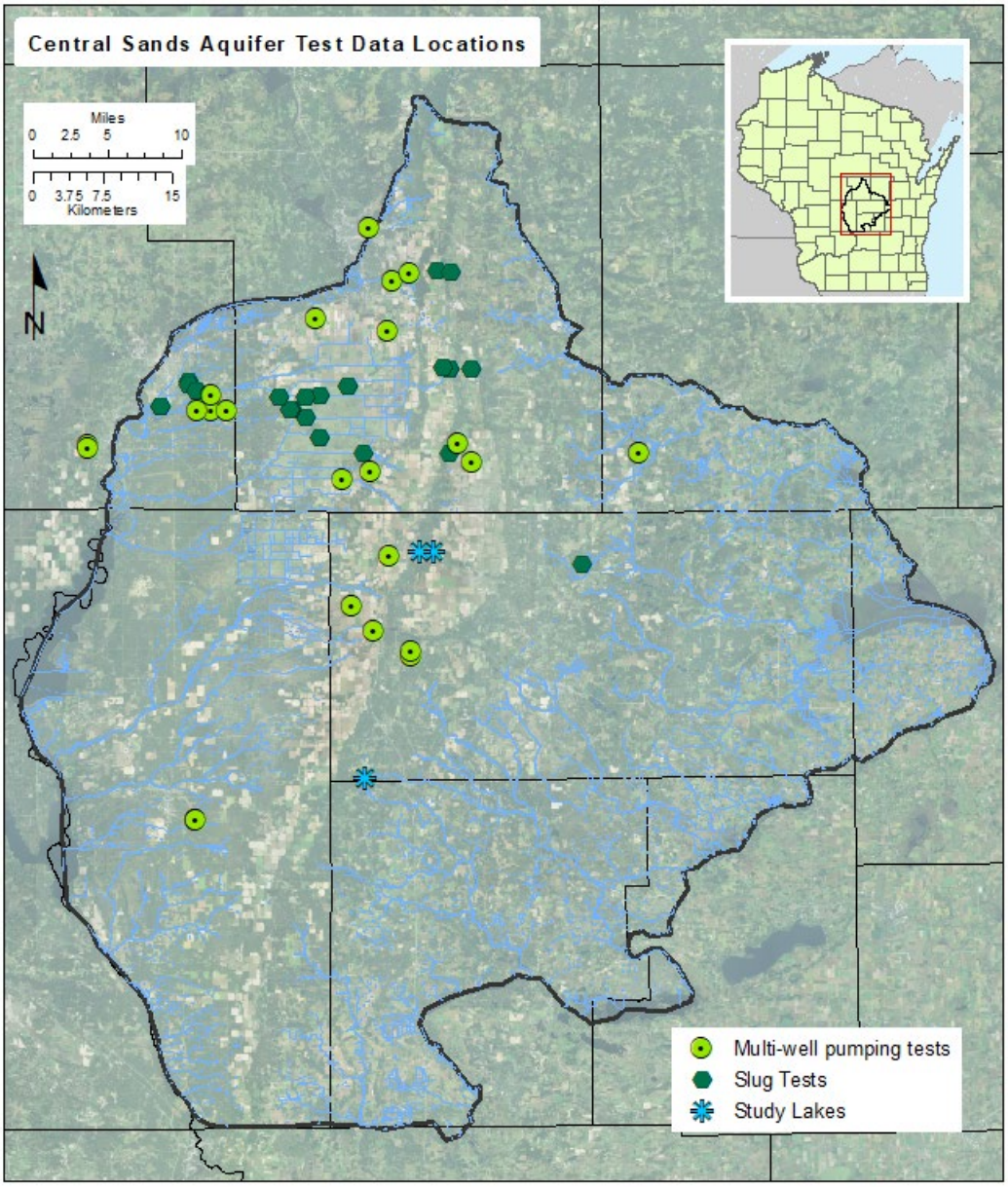

Figure 28. Locations of existing aquifer test data (prior to CSLS)

Table 1. Summary of previously published aquifer property values, CSLS model domain

	Horizontal Hydraulic Conductivity (ft/d)			
	Piezometer-slug tests	*Multi-well pumping tests*	*Anisotropy Kh:Kv*	*Specific Yield*
n	*46*	*24*	*5*	*20*
Min	0.7	66	1:1	0.026
Max	270	500	20:1	0.33
Mean	106	234	7:1	0.17

Aquifer Data from Specific Capacity Tests

Specific capacity test results are reported in most well construction reports. Specific capacity tests are typically short-term pump tests that measure the drawdown that occurs in a well at a specified pumping rate. The test is usually conducted at the time of well construction. As with WCR data, specific capacity test data are collected under a variety of conditions by many different individuals, and single test results may be more or less reliable depending on factors such as the degree of well development, length of test, or accuracy in measuring and reporting flow rates and water levels. However, the results of these tests constitute a large dataset that WGNHS used in aggregate to assess typical hydraulic conductivity values in the unconsolidated and bedrock aquifers in the CSLS model domain. Mean hydraulic conductivity for the entire model domain, areal variations in hydraulic conductivity, and variation with depth were examined.

METHODS:

Specific-capacity test data and well construction information were extracted from over 30,000 wells located in the model domain and a ten-mile buffer surrounding it. Roughly 23,000 of these wells were completed in the unconsolidated aquifer, typically in sand and gravel, while 9,500 were completed in bedrock. Aquifer tests for wells completed in the unconsolidated aquifer were examined for the entire model domain were also grouped by geographic region to evaluate the range of hydraulic conductivity values over different depositional settings (outwash plain, glacial Lake Wisconsin, end moraine, etc. – see Figure 3). All bedrock wells were considered a single category for the purposes of this analysis. The TGUESS code (Bradbury and Rothschild, 1985) was used to convert specific capacity test data to hydraulic conductivity values. TGUESS treats specific capacity tests as short-term single-well pumping tests.

RESULTS:

For the entire area evaluated (model domain plus a 10-mile buffer), the mean hydraulic conductivity for unconsolidated wells was 137.2 ft/d, while the mean hydraulic conductivity for bedrock wells was 18.8 ft/d.

Hydraulic conductivity distributions and mean values are shown by geographic region in Figure 29, 30 and Table 2. Hydraulic conductivity values are mapped for the entire study area in Figure 31. In general, the mean hydraulic conductivity of the unconsolidated aquifer has an order of magnitude of 10^2 ft/d in all parts of the model domain except Glacial Lake Oshkosh. The outwash plain hydraulic conductivities appear to most closely match a log normal hydraulic conductivity distribution. In the outwash plain, the mean conductivity derived from TGUESS analysis is 158 ft/d; this agrees well with the mean conductivity value derived from multi-well pumping tests, 234 ft/d.

Where the fine-grained New Rome unit is present in the glacial Lake Wisconsin basin, well construction reports show a broader conductivity distribution (trimodal, with peaks between 30 ft/d and 250 ft/d).

The upper conductivity values are similar to those found in the outwash plain. Lower conductivity values are more common in wells completed below the New Rome than in those completed above it.

The end moraines in the study area (Arnott, Hancock, and Almond) are composed of sandy tills which investigators note have similar hydraulic properties to outwash but are generally more poorly sorted (Clayton, 1987; Weeks and Stangland, 1971; Holt, 1965). The hydraulic conductivity distribution of wells completed in the end moraine areas has similar conductivity to the outwash plain but has a broader range of values. The hydraulic conductivity distribution for the subset of wells located within tunnel channels has a hydraulic conductivity distribution very similar to the end moraines.

The lowest average hydraulic conductivity in unconsolidated wells is in the glacial Lake Oshkosh basin (78 ft/d). This area is outside the Central Sands, and sediments typically include thick clays. Hydraulic conductivity estimates based on well construction reports are biased high in this area because water supply wells are preferentially completed in materials with greater water-bearing capacity rather than the low-conductivity clays and silts. Results in sandier areas to the west are likely also biased somewhat high for the same reason, but because the aquifer is on average composed of more transmissive materials, this effect is less pronounced.

Table 2. Hydraulic conductivity by geographic region. Data source is WCR specific capacity tests. Hydraulic conductivity was calculated using TGUESS. Because the hydraulic conductivities have log-normal distribution, standard deviation of log K is reported.

		Mean K (ft/d)	*Range (ft/d)*	*Standard Deviation of log K*	*n*
Bedrock		15	*0.001-1925*	*1.00*	*16,726*
Unconsolidated	Outwash Plain	158	*0.008-19,049*	*0.42*	*4255*
	Intermoraine	172	*0.85-812*	*0.41*	*582*
	Glacial Lake Wisconsin / New Rome	120	*0.04-1965*	*0.49*	*3285*
	End Moraines	156	*0.5-2149*	*0.52*	*590*
	Tunnel Channels	156	*0.78-1325*	*0.49*	*323*
	Ground Moraine	112	*0.03-3961*	*0.47*	*9392*
	Glacial Lake Oshkosh	78	*0.66-1985*	*0.46*	*1067*

Figure 29. Hydraulic conductivity distribution of unconsolidated sediments grouped by geographic area. Conductivities are calculated from specific capacity tests reported on WCRs. In addition to geographic distribution, graphs for the Glacial Lake Wisconsin/New Rome and Intermorainal areas also depict the hydraulic conductivity distributions for shallow and deep wells. In all areas except for glacial Lake Oshkosh, average conductivity is on the order of 10^2 ft/d.

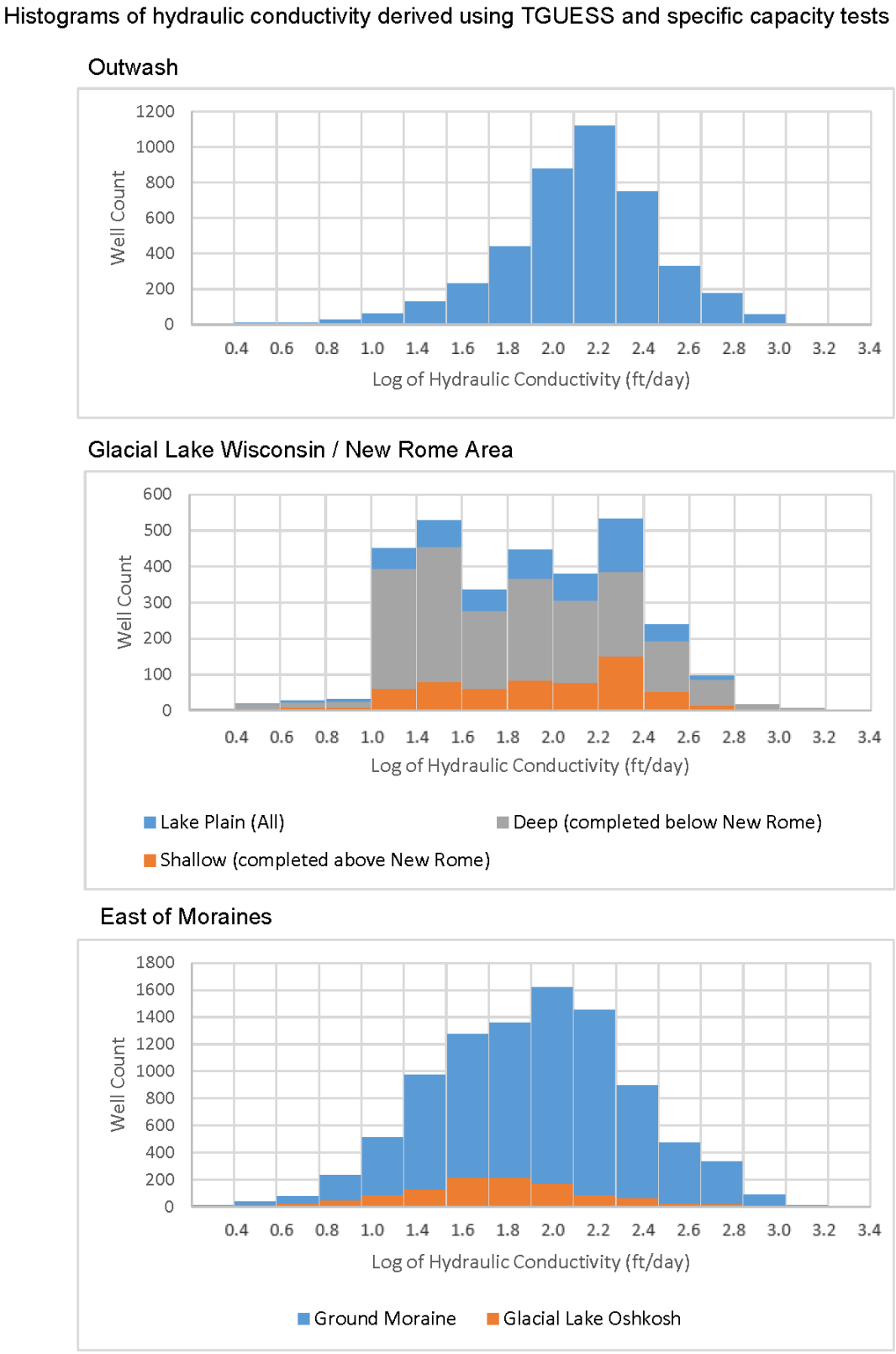

Histograms of Hydraulic Conductivity derived using TGUESS and well construction report (cont.)

End Moraines

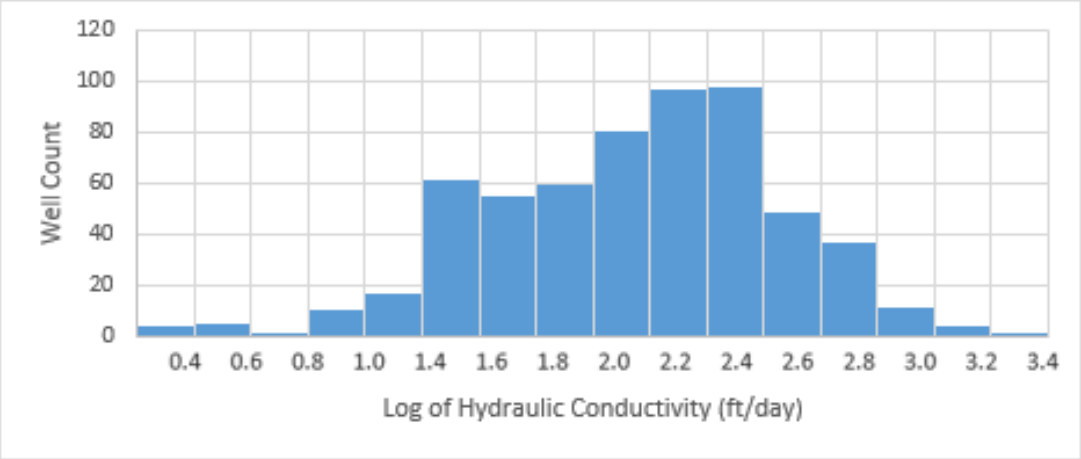

Tunnel Channels

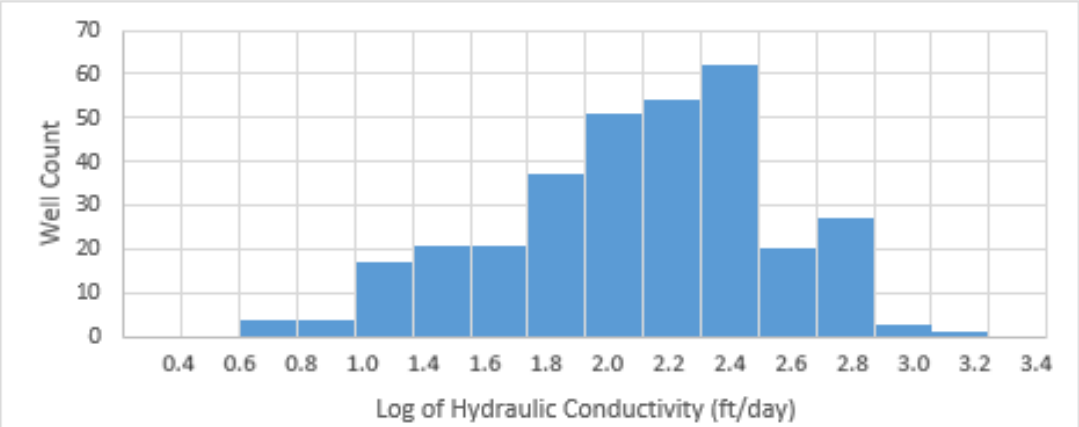

Intermoraine (including Tunnel Channels)

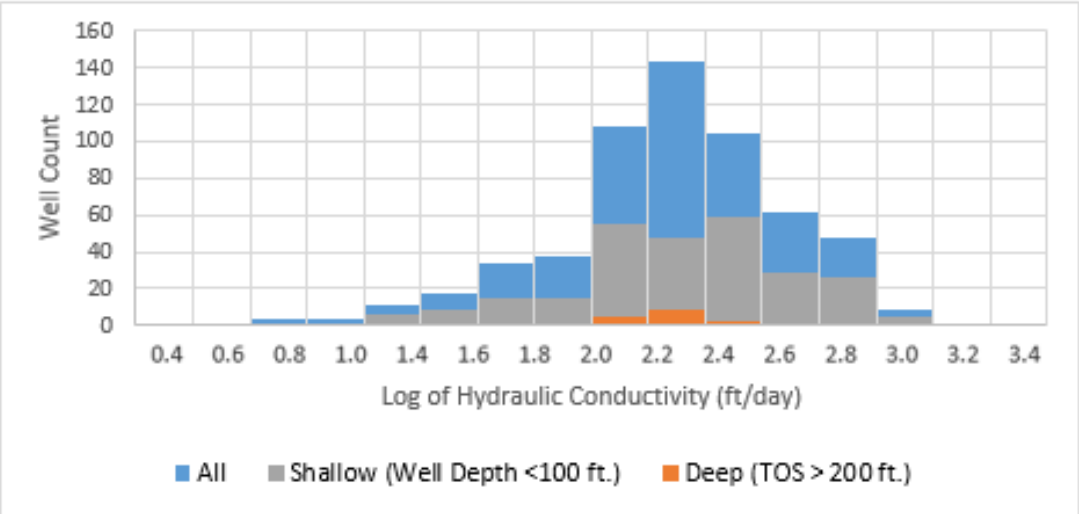

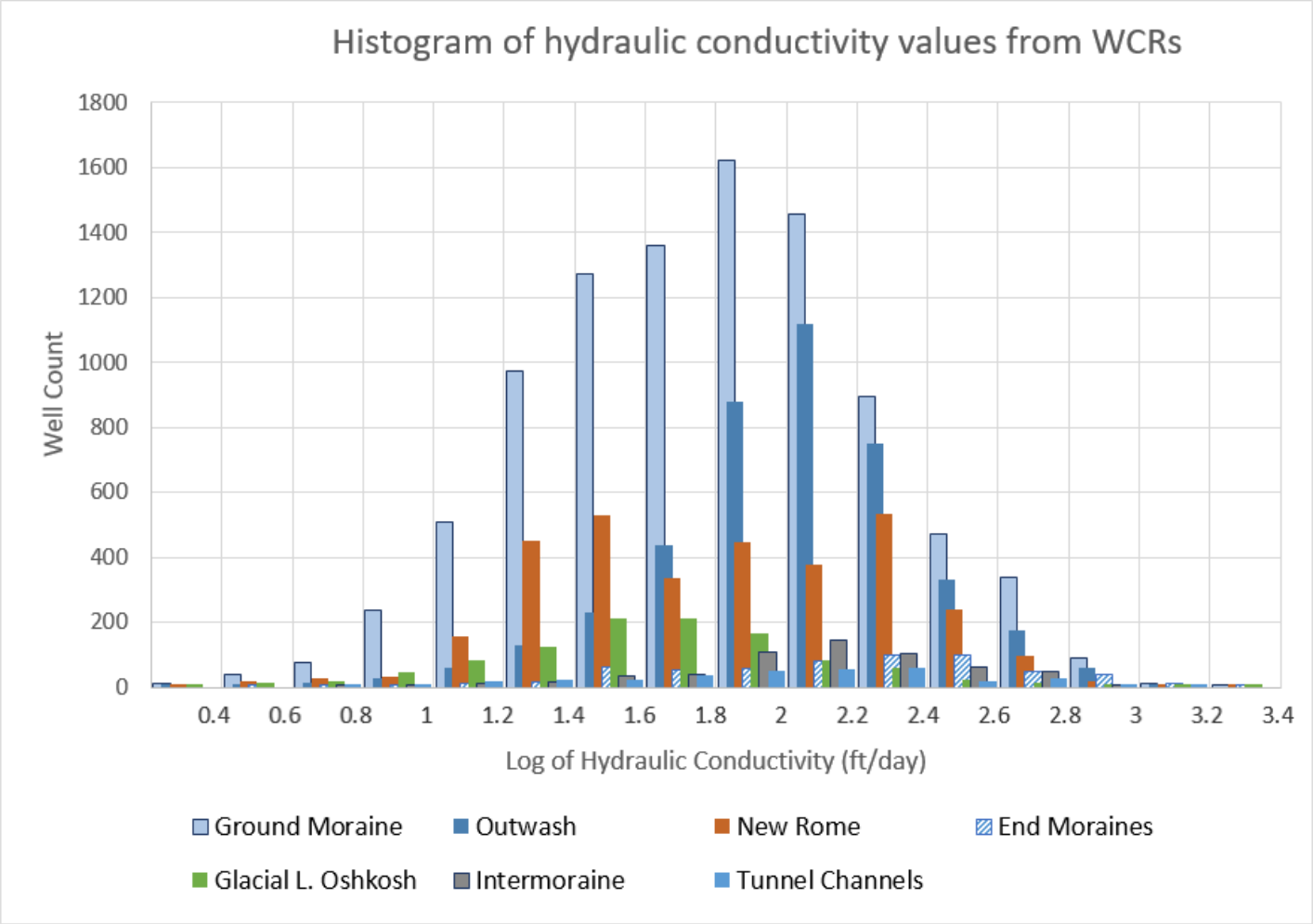

Figure 30. Summary of hydraulic conductivity distribution from specific capacity tests in unconsolidated sediments.

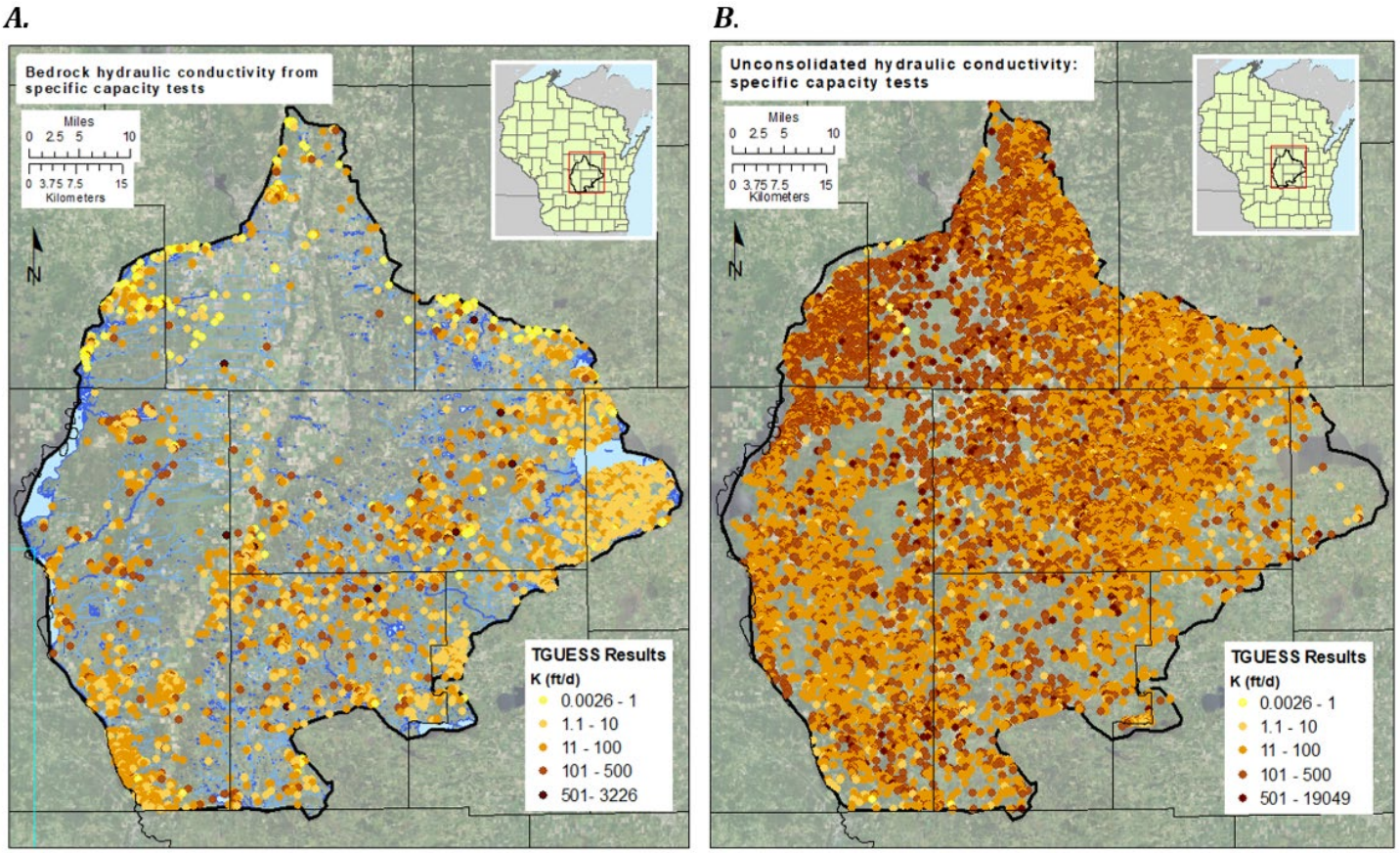

Figure 31. Hydraulic conductivity values from specific capacity tests (via TGUESS) (a) Bedrock points (b) Unconsolidated points. Bedrock conductivities are typically an order of magnitude lower than conductivity in the sand and gravel aquifer. The highest conductivities are in the outwash plain west of the Almond Moraine.

Aquifer property testing – CSLS monitoring wells

Detailed knowledge of the aquifer properties in the immediate vicinity of the three study lakes allows creation of a realistic numeric groundwater model. WGNHS tested aquifer properties at the lakes by conducting small-scale pumping or injection tests in each of the monitoring wells and piezometers installed around the study lakes.

METHODS:

Step-drawdown and step-injection tests were performed to estimate transmissivity and hydraulic conductivity of the aquifer for each monitoring well and piezometer. Because of the small well diameters (1-in PVC), a peristaltic pump, outfitted with tubing, was used to perform step pump tests when the groundwater level was less than 25 ft below land surface. At greater depths, water of a known-potable source, was injected into the well to perform step injection tests. A Solinst 3001 Levelogger Edge Series pressure transducer was deployed in the well/piezometer prior to pumping/injection and manual tape-down measurements were performed to confirm the groundwater levels during each test. The TGUESS spreadsheet was used to estimate transmissivity and hydraulic conductivity following the method of

Bradbury and Rothschild (1985). The method applies the Cooper-Jacob approximation for the Theis equation, with corrections for partial penetration and well loss.

RESULTS:

The results of aquifer testing at study wells around the lakes are shown in Figure 32 and 33 and summarized in Table 3. Aquifer test results are also shown by well in Appendix F. In general, results confirmed geological observations from exploratory coring around the lakes. The coarser-grained sediments around Plainfield Lake were associated with higher estimated hydraulic conductivity values (average of 168 ft/d), while the finer-grained sediments around Long Lake were associated with generally lower hydraulic conductivity values (average of 39 ft/d). Around Pleasant Lake, the coarser-grained sediments along the northeastern and western portion of the lake were associated with generally higher hydraulic conductivity values on the order of 100 ft/d, while finer-grained sediments observed along the southern portion of the lake were associated with lower hydraulic conductivity values of about 25-50 ft/d.

Table 3. Summary of hydraulic conductivities from aquifer tests in CSLS monitoring wells. Long Lake has the highest percent fine grained sediments in boring logs and also the lowest hydraulic conductivity values, while Plainfield Lake has few fine-grained sediments and high hydraulic conductivity.

	Hydraulic Conductivity (ft/d)			
	Range	*Mean*	*Median*	*n*
Long L.	7.3-69	39	39	14
Plainfield L.	72.6-637	168	105	10
Pleasant L.	24-130	73	60	12

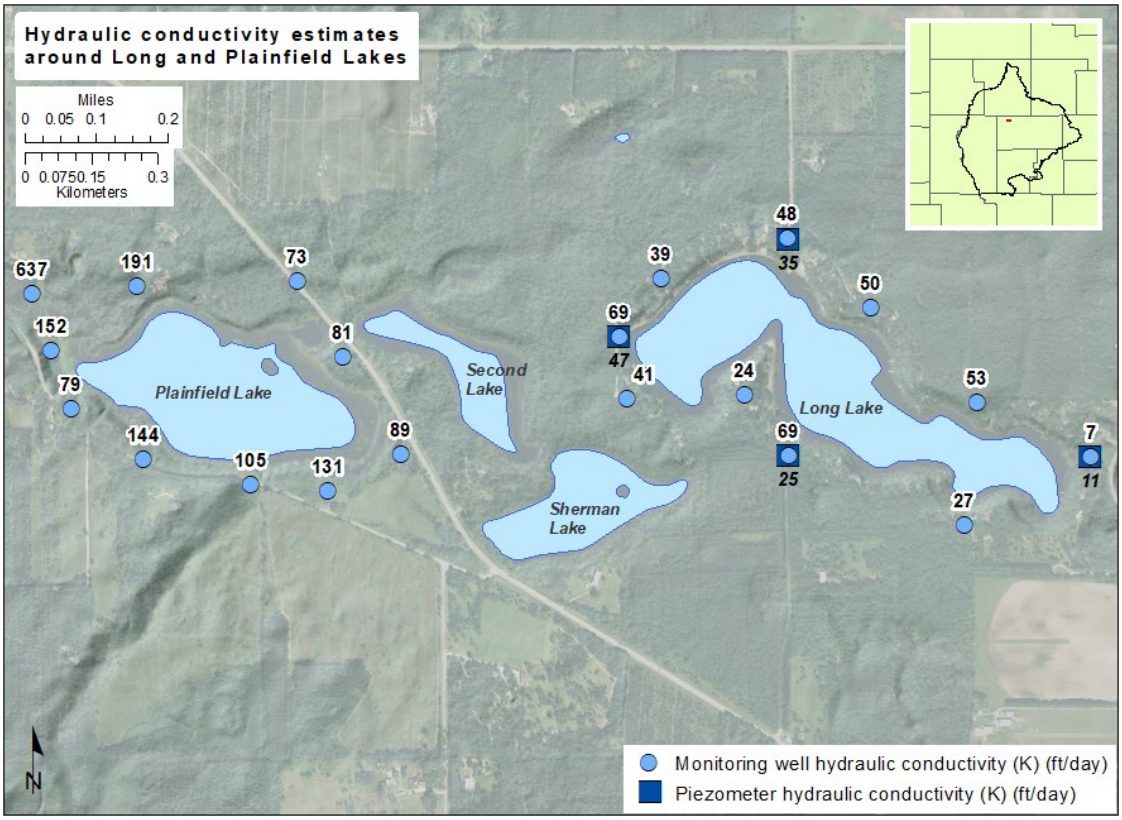

Figure 32. Hydraulic conductivity estimates for monitoring wells and piezometers around Long and Plainfield Lakes. Values for piezometers are in italics below the corresponding symbol. All values are in ft/d.

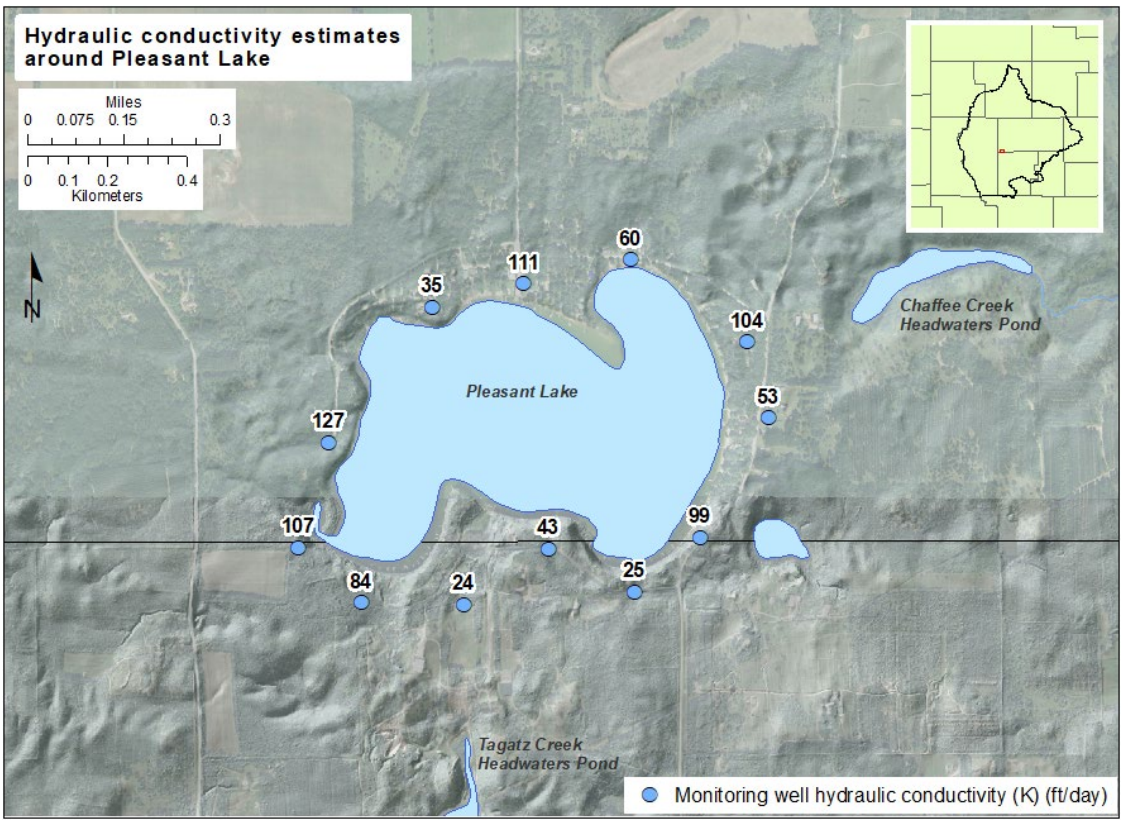

Figure 33. Hydraulic conductivity estimates for monitoring wells around Pleasant Lake. All values are in ft/d.

Hydrology Near the Study Lakes: Groundwater-level Monitoring

Geological and hydrogeological characterization is important for simulating the physical attributes of an aquifer system and understanding site-specific groundwater-surface water interactions and groundwater flow directions. This phase of the project involved the completion of several borings around Long, Plainfield, and Pleasant lakes, installation of shallow water-table monitoring wells and piezometers, hydraulic development of monitoring wells and piezometers, deployment of water-level monitoring equipment, collection and processing of groundwater-level data, and aquifer property testing. This section outlines the methods and results of this effort.

METHODS:

Boring, monitoring well and piezometer installation
WGNHS drilled exploratory borings and installed monitoring wells and piezometers around the three study lakes in July and November 2018, and in May and June 2019. In total, 50 boreholes were drilled, with 32 converted to monitoring wells and six converted to piezometers. The location of all monitoring wells, borings, and piezometers completed around Plainfield and Long lakes (Figure 17) and Pleasant Lake (Figure 18) are included below. A table summarizing boring and well attributes is included as Appendix F. Of the 50 boreholes, 48 were drilled using direct-push coring and two were drilled with mud rotary coring. Onsite Environmental performed the direct push coring and installed 32 monitoring wells and four piezometers using a track-mounted Geoprobe® 7822DT. The direct push-installed monitoring wells and piezometers were constructed with 1-in diameter schedule-40 polyvinyl chloride (PVC) casing. The Illinois Geological Survey used mud rotary drilling and installed two piezometers using 2-in diameter schedule-80 PVC casing. Direct push and mud rotary drilling methods and sample processing are discussed at greater depth in the Quaternary Sediment section.

Boreholes that hit refusal or were drilled expressly for exploratory purposes and were not converted to wells (or piezometers) were properly filled and sealed; this was documented using WDNR Borehole Filling and Sealing Report 3300-05. Well construction dimensions and methods were documented using WDNR form 4400-113A. Copies of all well construction and borehole abandonment forms are included in Appendix G. Geologic logs for all borings and drill cutting sets (PFL100, PFL101) are included in Appendix A.

Following installation, each monitoring well and piezometer was developed using a Waterra inertial pump equipped with a foot valve. In shallow wells (< 25’ to groundwater), a peristaltic pump was often connected to the Waterra inertial pump tube to more rapidly develop the monitoring well and remove more fine sediment. For deeper wells (> 25’ to groundwater), the Waterra inertial pump was activated by hand. Well and piezometer development was documented using WDNR form 4400-113B. Copies of all well development forms are included in Appendix G.

Monitoring well and piezometer development

Monitoring well and piezometer locating
WDNR and WGNHS surveyed elevations of the top of PVC well/piezometer, steel protective casing, and land surface using Real-Time Kinematic (RTK) GPS. A total station was used to establish elevation datum in locations where the GPS was unable to receive signal due to dense tree canopy. Well/piezometer and borehole locations, elevations, and construction details are listed in Appendix F. The elevations have also been integrated into the well construction and borehole filling and sealing forms included in Appendix G.

Deployment of groundwater-level monitoring equipment and data downloads
Continuous water-level measurements were collected in each study well and piezometer using Solinst 3001 Levelogger Edge Series pressure transducers with a 15-minute sampling interval. Solinst 3001 Barologger Edge Series pressure transducers deployed near Plainfield and Pleasant lakes, provided data needed to perform barometric compensations for loggers deployed around the three study lakes. Pressure transducers were deployed as wells and piezometers were constructed in July and August 2018, November 2018, and June 2019. Wells and piezometers were subsequently visited semi-annually, beginning in fall 2018, to download groundwater-level readings. At each well/piezometer visit, a manual groundwater-level reading was collected to confirm the accuracy of pressure transducer readings.

Groundwater-level data processing
Once downloaded, water-level data was corrected to compensate for barometric pressure, processed to remove erroneous data, and corrected to account for instrument drift over the course of each deployment period. Manual tape-down measurements were used to confirm groundwater levels, to process the data, and to correct for instrument drift. WGNHS provided the processed groundwater-level datasets to the WDNR for use by study collaborators.

RESULTS:

Groundwater-level monitoring

Groundwater elevations from July/August 2018 through October 2019 have risen considerably on each of the three (3) lakes. Generally speaking, the groundwater flow through Long and Plainfield lakes is from the north to south. Flow through Pleasant Lake is from northwest to southeast. Long and Plainfield Lakes are situated along a regional groundwater divide within a low-gradient system, while Pleasant Lake is in proximity to two perennial stream systems in a high-gradient groundwater discharge area. Record precipitation levels from fall 2018 into summer 2019 led to the near-continual rise in surface water and groundwater levels around all three lakes. Groundwater levels in wells/piezometers and lake levels for Long, Plainfield, and Pleasant Lakes are shown in Figures 34, 35, and 36, respectively.

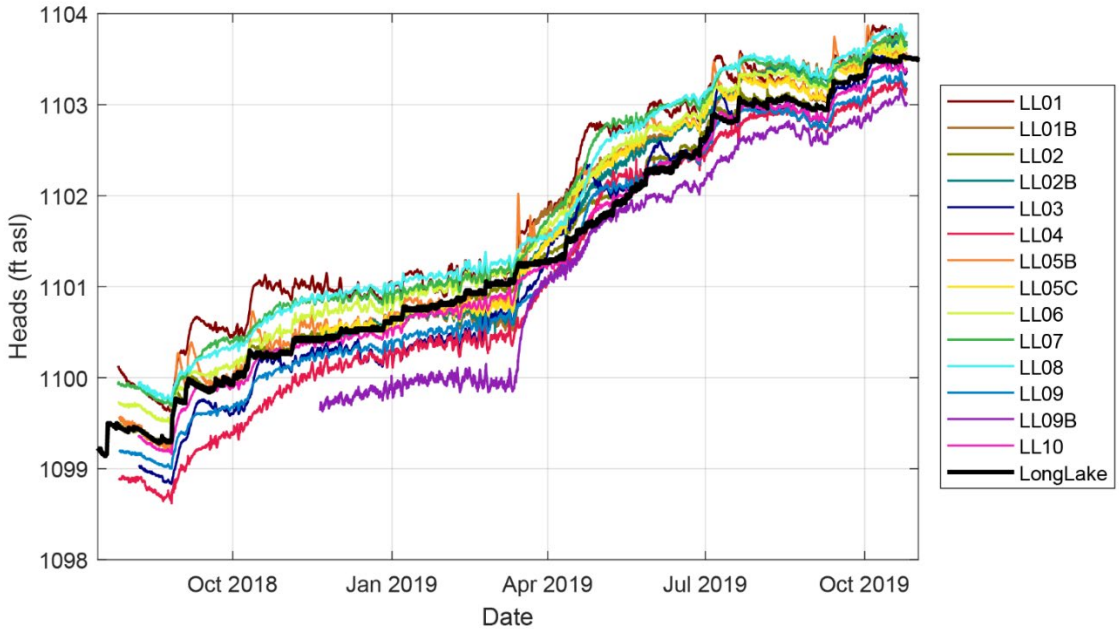

Figure 34. Groundwater levels in monitoring wells and piezometers around Long Lake from summer 2018 to fall 2019. Lake-level elevation is shown in black. Overall increase in water levels is approximately 4.5 ft over this 15-month period.

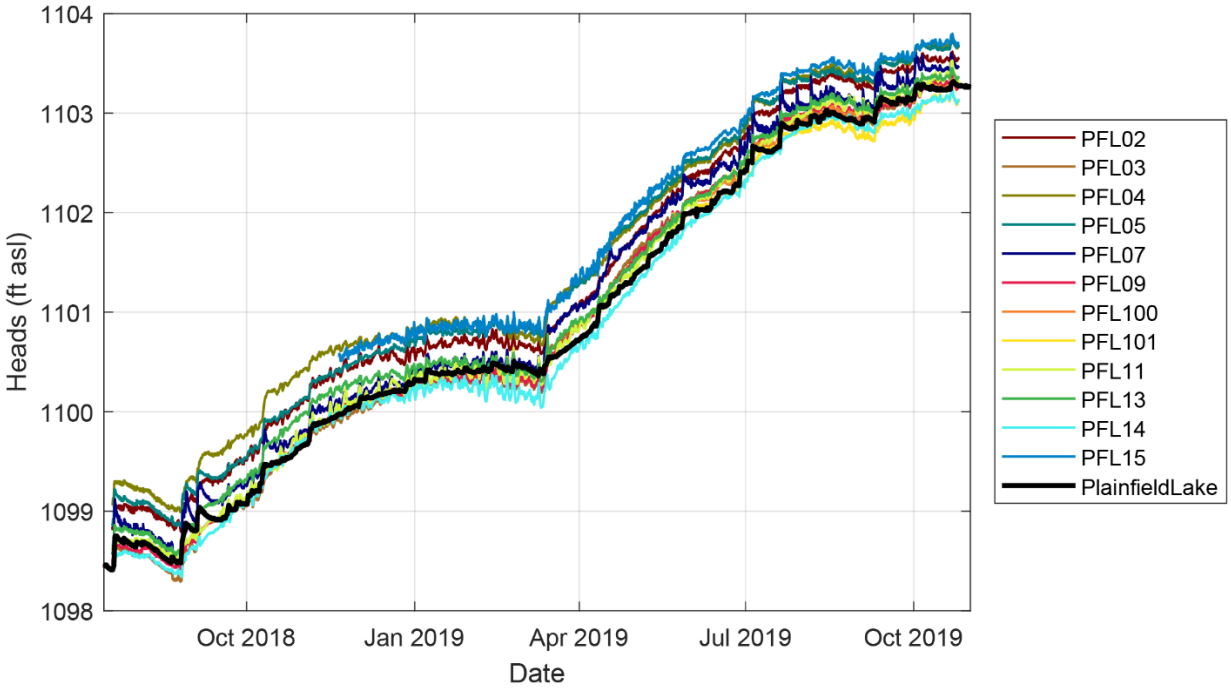

Figure 35. Groundwater levels in monitoring wells around Plainfield Lake from summer 2018 to fall 2019. Lake-level elevation is shown in black. Overall increase in water levels is approximately 4.5 ft over this 15-month period.

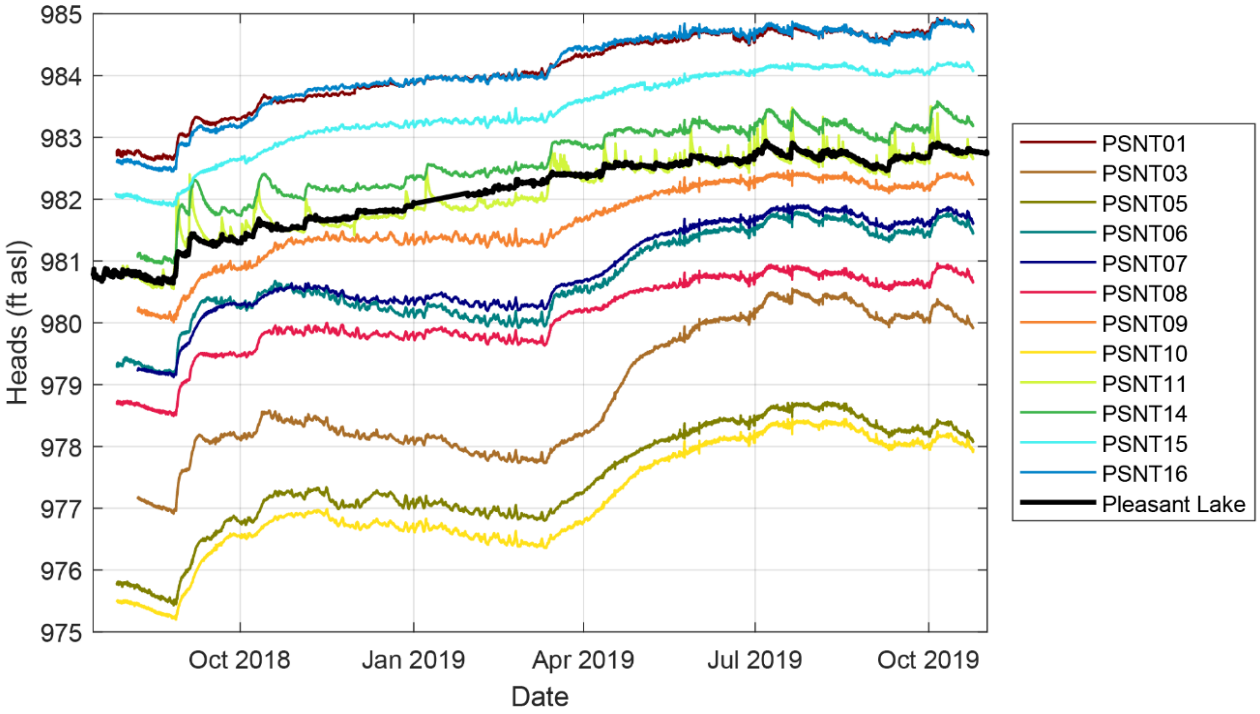

Figure 36. Groundwater levels in monitoring wells around Pleasant Lake from summer 2018 to fall 2019. Lake-level elevation is shown in black. Overall increase in water levels is approximately 2 ft over this 15-month period.

On Long and Plainfield lakes, the difference in water levels between wells and lake levels show the effects of above-average precipitation on flow patterns. Beginning in March 2019, multiple water table wells that initially had water levels below the lake level (flow out of the lake toward the well location) began to have water levels higher than lake level (flow into the lake from the well location). This change from a "flow-through" system to an almost exclusively "flow-in" system can be seen in Figure 34 and Figure 35. By May 2019, groundwater around both lakes was flowing almost entirely into the lakes. This trend continued into mid- to late summer 2019 before water levels in downgradient wells began to drop back below lake levels and the lake returned to a flow-through system. By contrast, gradients around Pleasant Lake remain steady throughout the same 15-month period, with nearby Tagatz and Chaffee Creeks constraining the local groundwater-flow regime and maintaining a distinct flow-through system. These general trends, illustrated in map view, are presented in Figures 37 and 38 for Long and Plainfield Lakes and Figures 39 and 40 for Pleasant Lake.

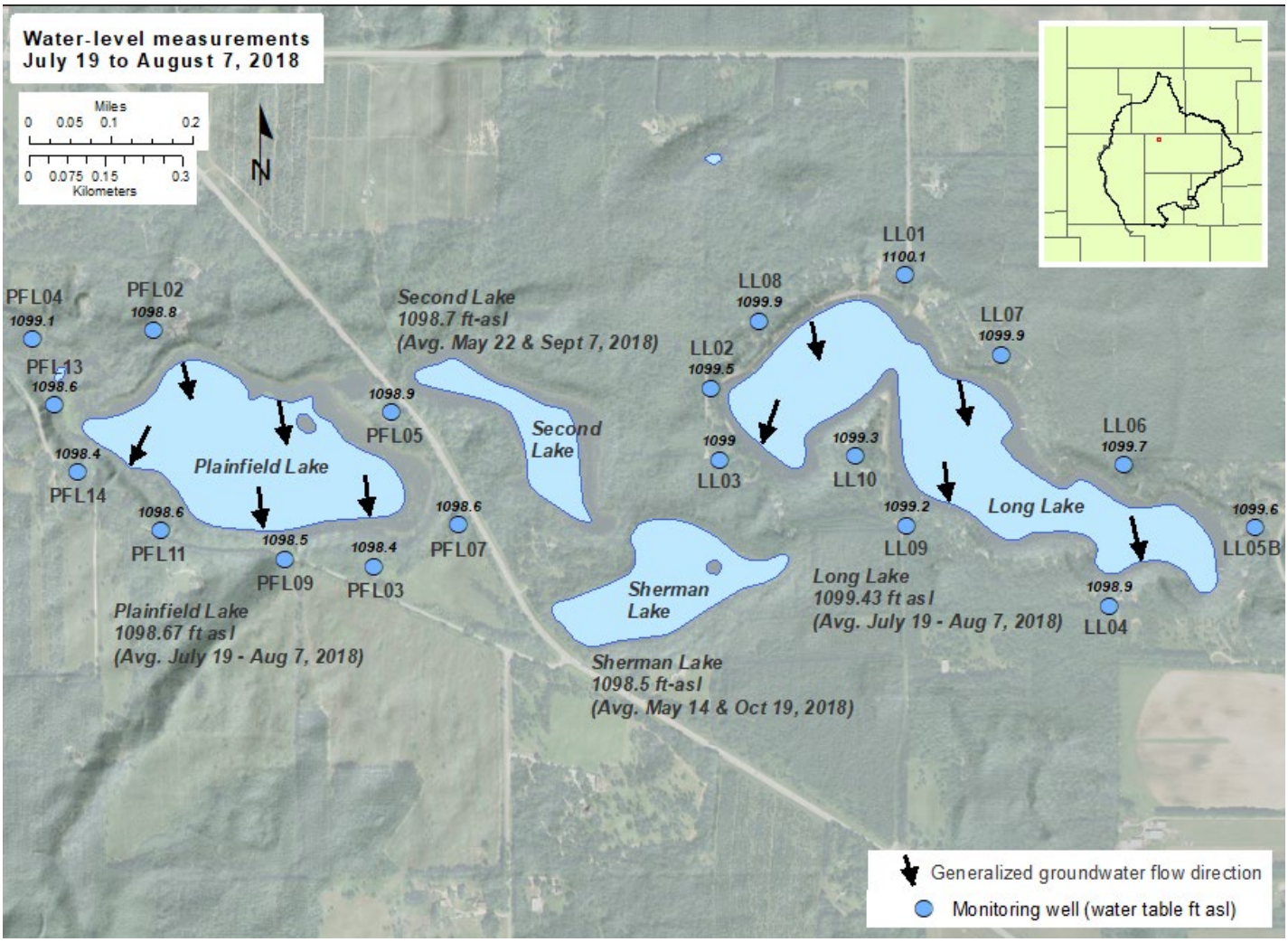

Figure 37. Groundwater levels in monitoring wells around Long and Plainfield Lakes following well installation and development in July and August 2018. Levels shown for Long and Plainfield Lakes are averages of continuous 15-minute USGS gaging station data published on their National Water Information System (NWIS) web interface. Levels reported for Second and Sherman Lakes are averages of two periodic WDNR measurements published on their Surface Water Data Viewer and represent more generalized water levels.

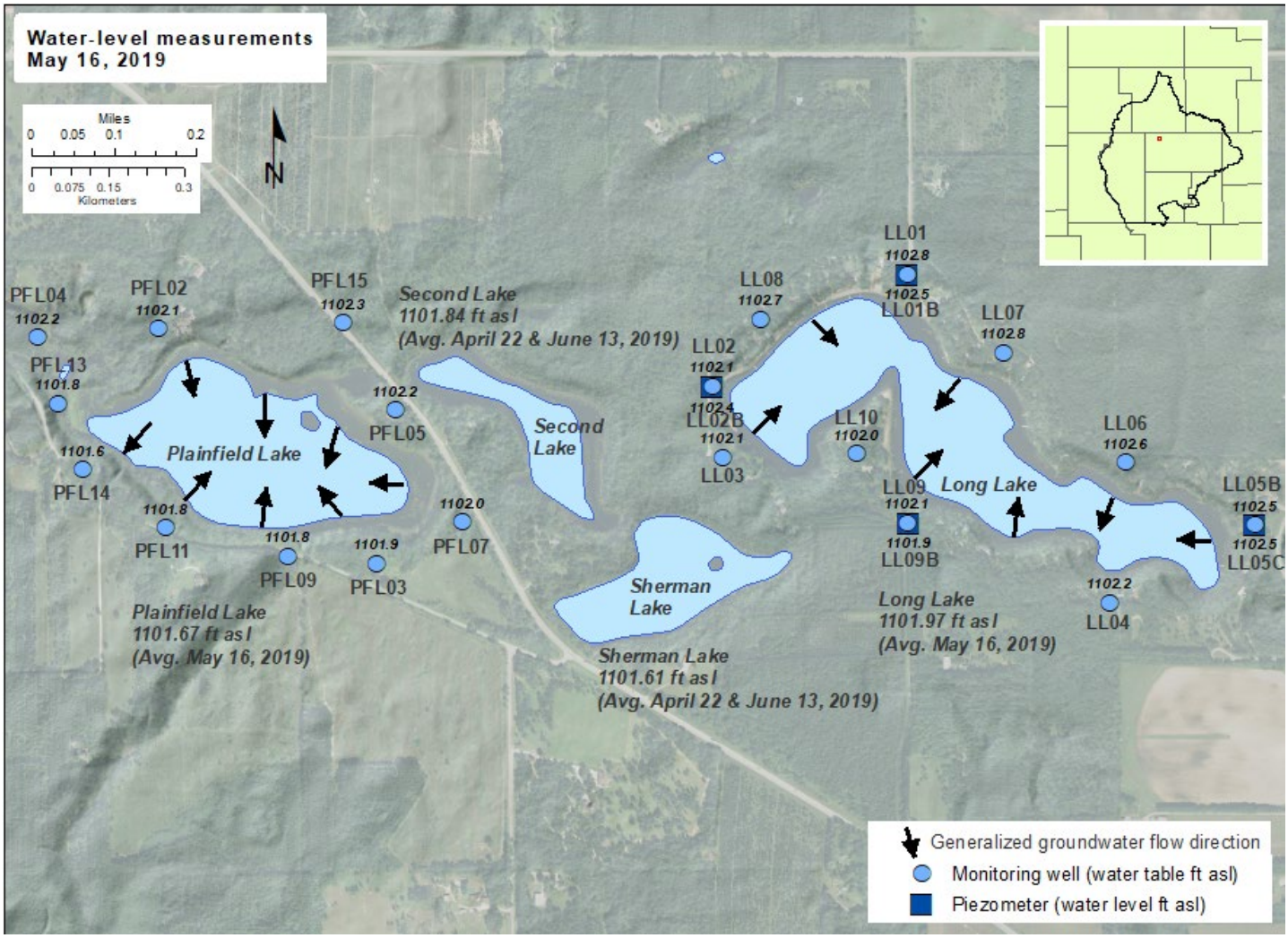

Figure 38. Groundwater levels in monitoring wells and piezometers around Long and Plainfield Lakes during pressure transducer data retrieval on May 16, 2019. Levels shown for Long and Plainfield Lakes are averages of continuous 15-minute USGS gaging station data published on their National Water Information System (NWIS) web interface. Levels reported for Second and Sherman Lakes are averages of two periodic WDNR measurements published on their Surface Water Data Viewer and represent more generalized water levels. Groundwater levels for the four piezometers around Long Lake, installed in November 2018, are in italics below the corresponding symbol.

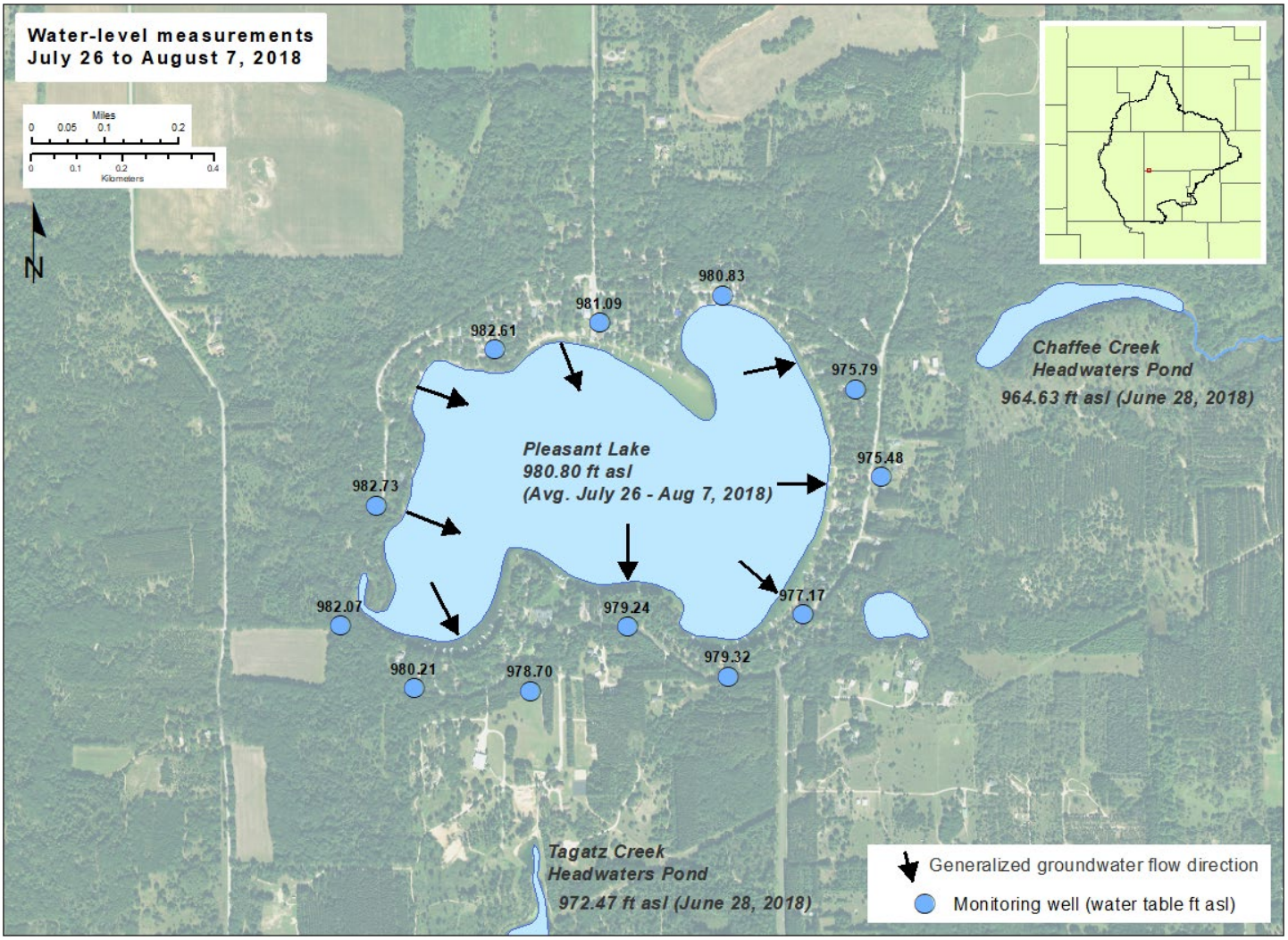

Figure 39. Groundwater levels in monitoring wells around Pleasant Lake following well installation and development in July and August 2018. Levels shown for Pleasant Lake are an average of continuous 15-minute USGS gaging station data published on their National Water Information System (NWIS) web interface. Levels reported for the Chaffee and Tagatz Creek headwater ponds are one-time WDNR measurements from late June 2018, published on their Surface Water Data Viewer, and represent more generalized water levels.

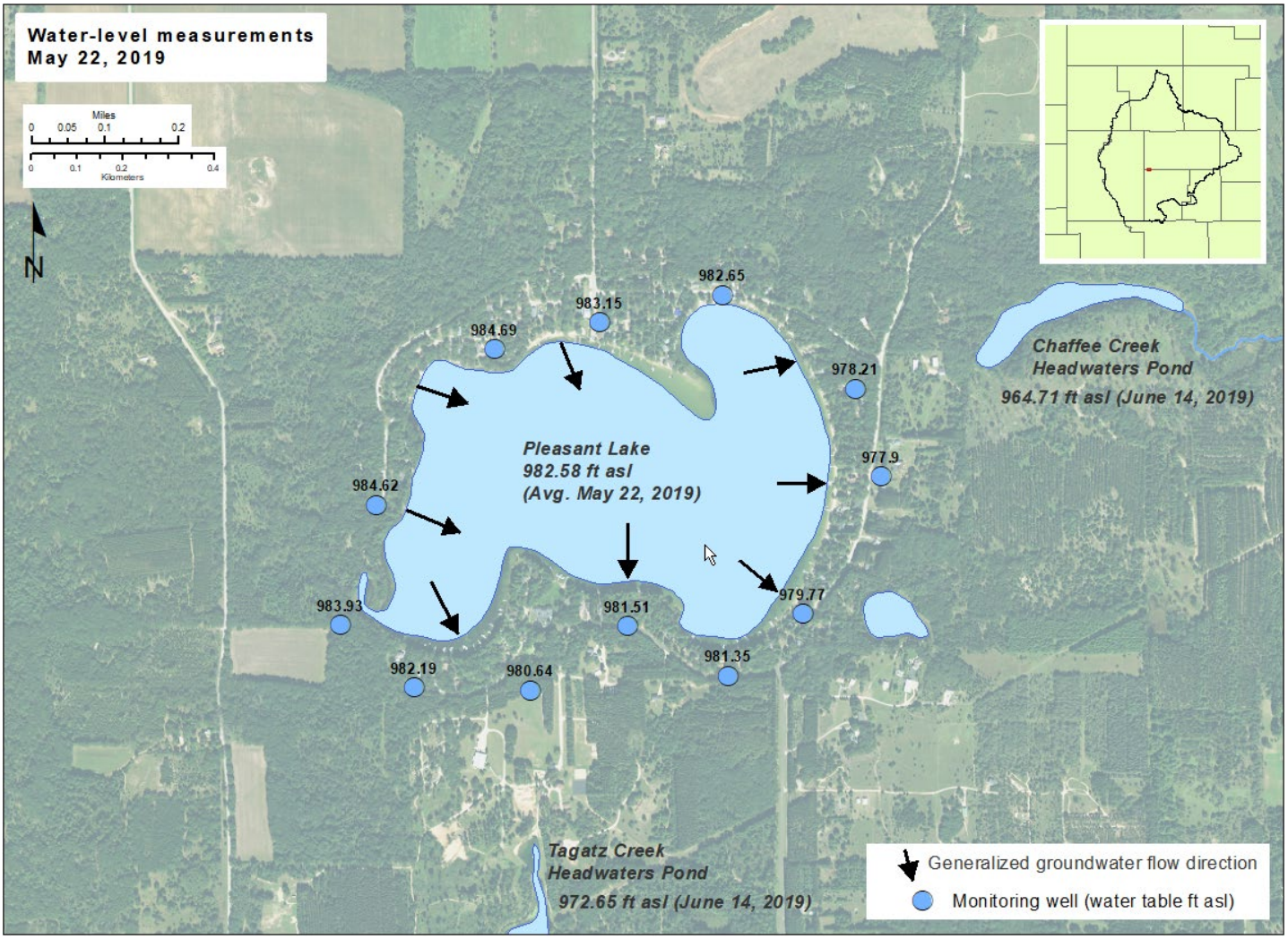

Figure 40. Groundwater levels in monitoring wells around Pleasant Lake during pressure transducer data retrieval on May 22, 2019. Levels shown for Pleasant Lake are an average of continuous 15-minute USGS gaging station data published on their National Water Information System (NWIS) web interface. Levels reported for Chaffee and Tagatz Creek headwater ponds are one-time WDNR measurements from late mid-June 2019, published on their Surface Water Data Viewer, and represent more generalized water levels.

Vertical hydraulic gradients around Long Lake

The four well/piezometer nests around Long Lake provide insight into the vertical flow regime around the lake. The exploratory borings performed around Long Lake in July and August 2018, indicated that finer-grained sand, silt, and clay-sized sediments were present at depth and influence vertical hydraulic gradients. Previous research by Kniffin (2018) also reported fine-grained sediments at depth below and adjacent to Long Lake. To evaluate the role of these fine-grained sediments in the flow system, WGNHS used nested piezometers to measure the existence, timing, and magnitude of vertical gradients around Long Lake. Piezometers were installed in November 2018 next to monitoring wells LL01, LL02, LL05B, and LL09 (Figure 17). Piezometer depths were 23-50 feet below the adjacent water table monitoring well. Each piezometer was installed within a fine- to medium-grained sand, beneath overlying deposits of finer-grained sand, silt, and clay. Noticeable hydraulic gradients were observed between the water table

monitoring wells and piezometers. Water-level trends suggest that the response of Long Lake and shallow groundwater (above the fine-grained sediments) are delayed and attenuated when compared to deeper groundwater (below the fine-grained sediments). This deeper groundwater appears to more closely track the response observed at nearby Plainfield Lake and the Plainfield Lake well/piezometer installations, where no fine-grained sediments are present. Observed water-level trends imply that Long Lake is well-connected to groundwater in both shallow wells and piezometers; however, the underlying fine-grained sediments distribute hydraulic stresses spatially and temporally, leading to the delay and attenuation of water-level trends. The hydraulic heads observed in the Long Lake piezometer nests (LL01/B, LL02/B, LL05B/C, LL09/B) are shown in Figures 41 to 44. The following paragraphs present the observations and interpretations made for Long Lake during over the 15-month data collection period.

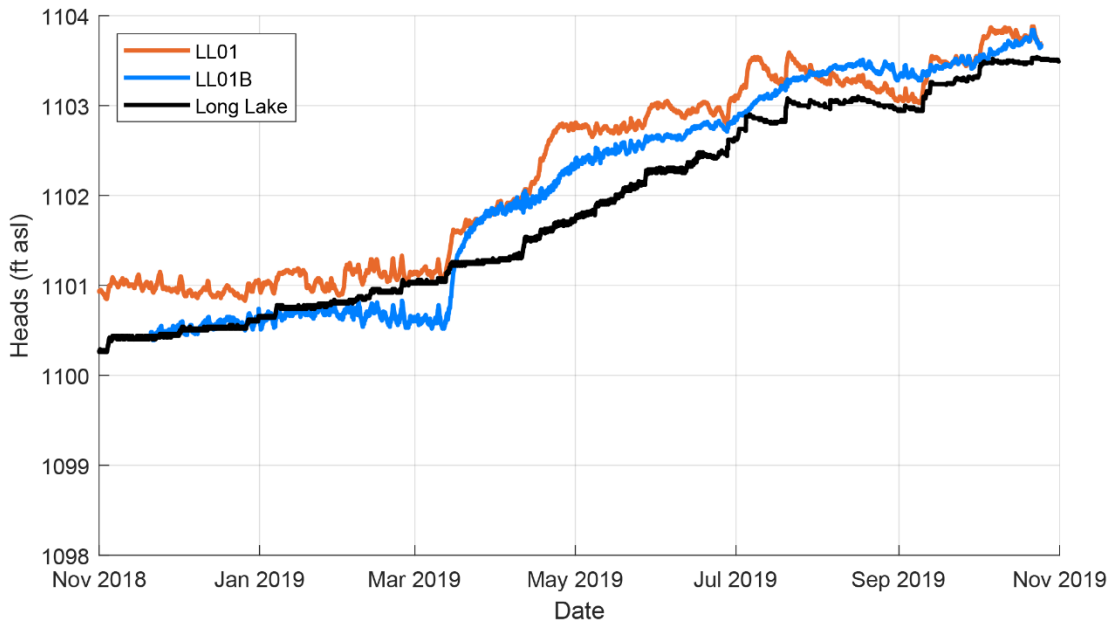

Figure 41. Hydraulic heads in monitoring well LL01 and piezometer LL01B as measured from fall 2018 to fall 2019. Lake-level elevation is shown in black, water table monitoring well is shown in orange, and deep piezometer is shown in blue.

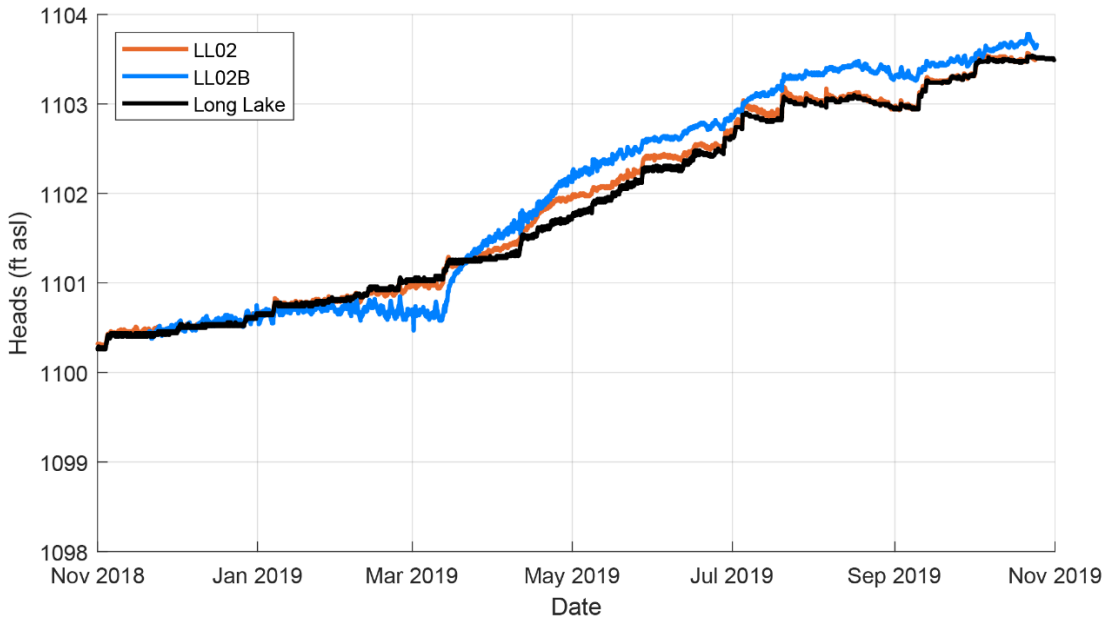

Figure 42. Hydraulic heads in monitoring well LL02 and piezometer LL02B as measured from fall 2018 to fall 2019. Lake-level elevation is shown in black, water table monitoring well is shown in orange, and deep piezometer is shown in blue.

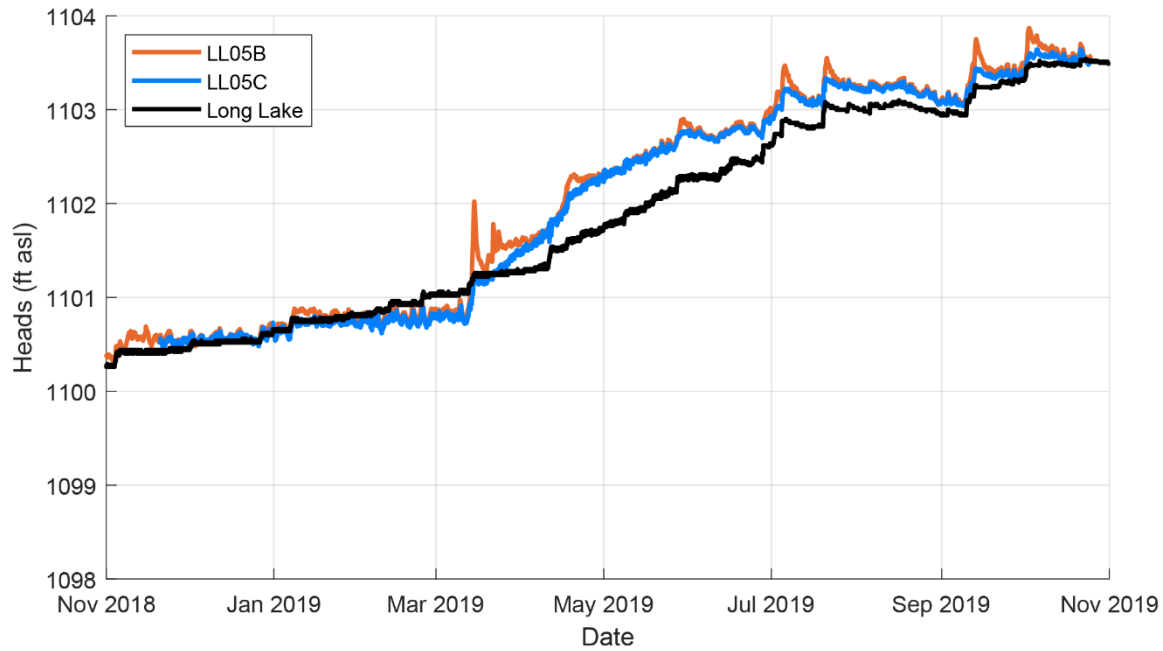

Figure 43. Hydraulic heads in monitoring well LL05B and piezometer LL05C as measured from fall 2018 to fall 2019. Lake-level elevation is shown in black, water table monitoring well is shown in orange, and deep piezometer is shown in blue.

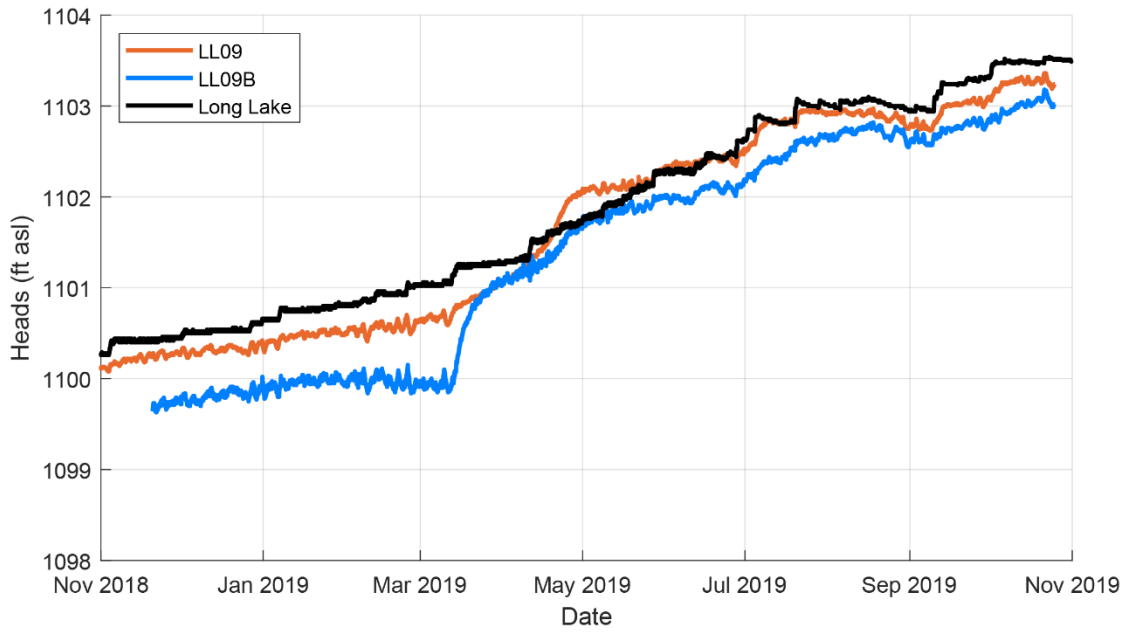

Figure 44. Hydraulic heads in monitoring well LL09 and piezometer LL09B as measured from fall 2018 to fall 2019. Lake-level elevation is shown in black, water table monitoring well is shown in orange, and deep piezometer is shown in blue.

Immediately following installation of the piezometer nests in November 2018, the general groundwater flow direction in the area was from north to south, with Long Lake behaving as a flow-through system. During this period, water-table and piezometer levels for nests LL02/B and LL05B/C (each side-gradient) overlap and closely tracked lake levels. Heads in LL01B, on the north side of the lake, also tracked lake levels, but the well nest exhibited a pronounced downward vertical gradient, with LL01 heads consistently 0.5-ft higher than LL01B. The water level in shallow monitoring well LL01 remained higher than the lake level, indicating flow toward the lake. On the south side of the lake, LLO9/B also showed a distinct downward vertical gradient of approximately 0.5 feet. Water levels in both the water table well and piezometer at LL09/B are lower than the lake level, indicating flow from the lake toward the well and piezometer.

During the winter period from January to mid-March 2019, when recharge was assumed to be significantly reduced or negligible, groundwater levels in Long Lake piezometers LL01B, LL02B, and LL09C dropped relative to lake levels. During this time period, the trend of dropping water levels is not observed for Long Lake or the surrounding shallow groundwater wells. The one exception to this trend amongst the Long Lake piezometers is LL05C, which largely tracks the trends for shallow well LL05B[1]. This suggests additional flow from shallow groundwater and a lowering of water levels in the deeper groundwater below the interval of fine-grained sediments. The increase in downward vertical gradients

[1] Review of core photos, lithologic descriptions, and water-level trends for piezometer LL05C suggest that this monitoring point may not penetrate below the base of the fine-grained sediment layer observed in piezometers LL01B, LL02B, and LL09B. The response of LL05C is therefore difficult to interpret compared to other Long Lake monitoring points. Similarly, shallow well LL05B is completed primarily within an organic silt and its hydraulic response is difficult to interpret.

at three of the four well nests appears to be attributable to shallow water levels (above the fine-grained sediments) rising and deeper water levels (in piezometers below the fine-grained sediments)dropping. This delayed response observed for Long Lake and the shallow groundwater (above the fine-grained sediments) is likely to hold true for both high-water and low-water periods.

In mid-March 2019, a series of precipitation events that coincided with spring thaw delivered significant amounts of water to Long Lake and recharge to the groundwater system. The general groundwater flow direction within the area shifted during this period as groundwater levels in LL01/LL01B and LL05B/LL05C sharply rose above lake level, indicating flow from these well nests to Long Lake. The level in piezometer LL02B also rose sharply above lake level but the response in shallow well LL02 was more subdued, rising only slightly above lake level. By mid-April 2019, water levels in LL09 also rose above lake level and Long Lake shifted to a flow-in system with no apparent groundwater outlets. While the level in LL09B remained below lake level, the flow-in conditions persisted until late June 2019, when the levels in LL09 and neighboring wells LL10 and LL04 dropped below lake level, and flow-through conditions resumed for Long Lake (Figure 34).

The gradient reversals/divergences between Long Lake, shallow monitoring wells, and piezometers, as well as the rapid water-level increases in the deeper piezometers, provide evidence that the fine-grained sediment layer delays and attenuates groundwater flow and can lead to the development of appreciable hydraulic gradients between the shallower and deeper groundwater. The shallow and deep parts of the system are hydraulically connected, as evidenced by the fact that they exhibit similar overall water-level trends; however, three of the four deep piezometers (below the fine-grained sediment layer) appear to respond more markedly to the spring thaw period. By contrast, the shallow groundwater and Long Lake exhibit a more subdued response compared to regional trends. As presented in the following section, these trends for Long Lake are distinctly different from trends observed at nearby Plainfield Lake, where no extensive fine-grained sediments were encountered at depth.

Vertical gradients around Plainfield Lake

Two piezometers were also installed upgradient and downgradient of Plainfield Lake to provide insight into the vertical flow regime. Unlike Long Lake, previous exploratory borings around Plainfield Lake did not provide evidence of finer-grained sediments at depth; however, additional investigations were performed to better characterize the groundwater system. To evaluate the existence and magnitude of vertical gradients below and near Plainfield Lake, nested piezometers PFL100 and PFL101 were installed in May 2019 next to monitoring wells PFL05 and PFL03, respectively (Figure 17). Piezometer depths were 80-85 feet below the adjacent water table monitoring well. Each piezometer was installed within a fine- to coarse-grained sand but, unlike at Long Lake, no extensive fine-grained sediments were observed between the shallow water table well and the deeper piezometer. PFL05/PFL100 and PFL03/PFL101, north and south of Plainfield Lake, maintained consistent head drops of 0.4 and 0.2 feet, respectively, from May to October 2019. The head drop between the water table monitoring wells and nested piezometers are similar to those seen at Long Lake, but because the vertical separation between the monitoring points is larger, they represent smaller vertical gradients. The hydraulic heads observed in

the Plainfield Lake piezometer nests are presented in Figures 45 and 46. The following paragraphs present the observations and interpretations made for Plainfield Lake over the 15-month data collection period.

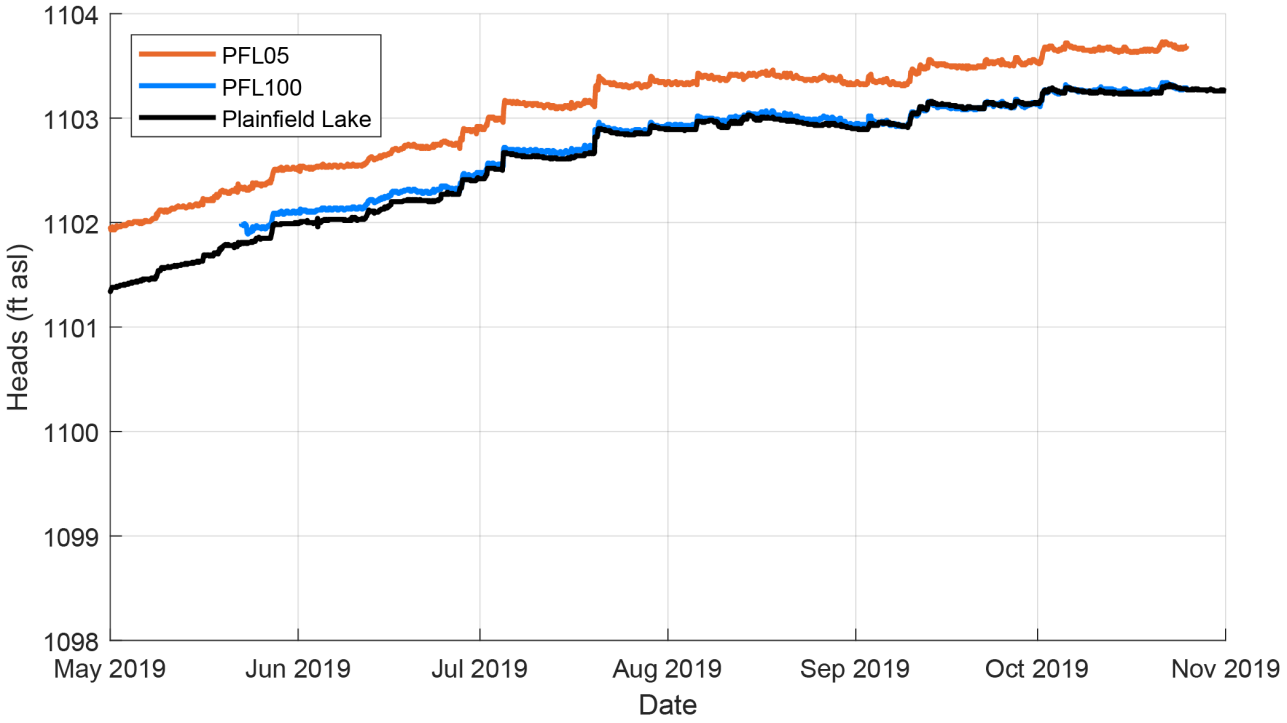

Figure 45. Hydraulic heads in monitoring well PFL05 and piezometer PFL100 as measured from spring to fall 2019. Lake-level elevation is shown in black, water table monitoring well is shown in orange, and deep piezometer is shown in blue.

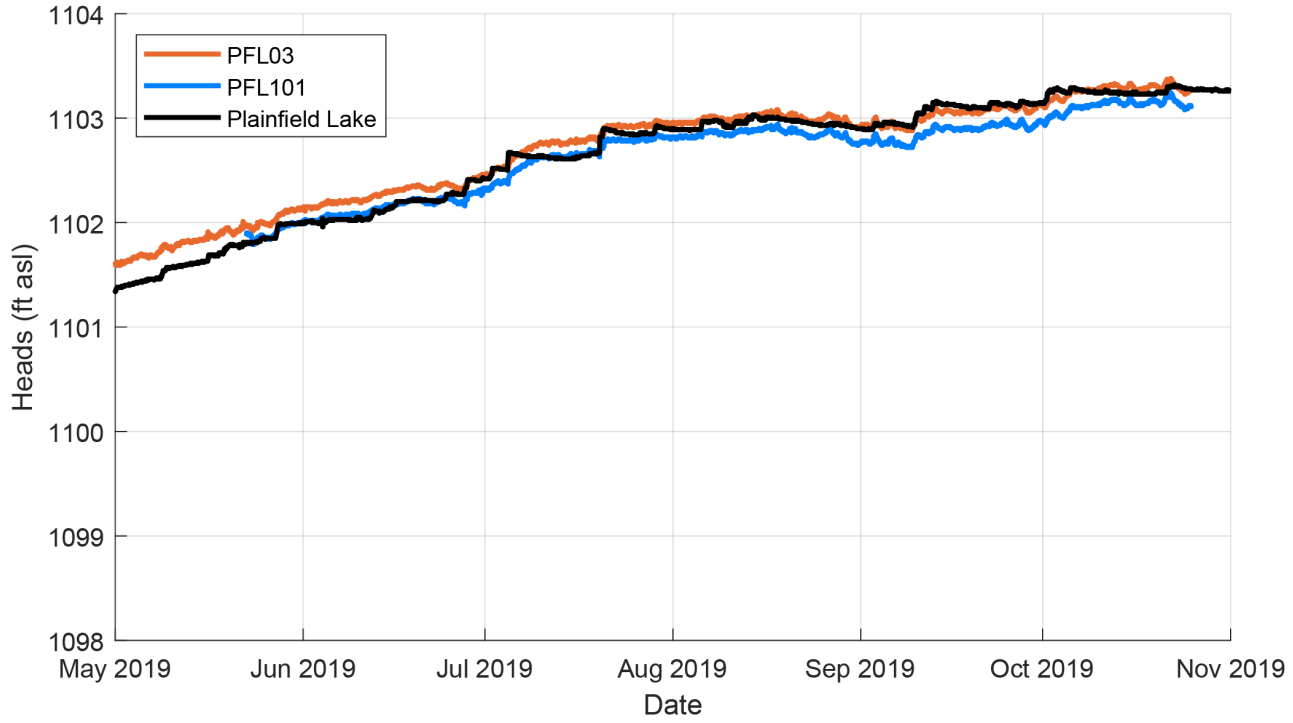

Figure 46. Hydraulic heads in monitoring well PFL03 and piezometer PFL101 as measured from spring to fall 2019. Lake-level elevation is shown in black, water table monitoring well is shown in orange, and deep piezometer is shown in blue.

Following installation of piezometer nests PFL100 and PFL101 in May 2019, the general groundwater flow direction in the area was towards Plainfield Lake in response to an exceptionally wet spring. The only observed downgradient outlet for Plainfield Lake at this time was to the southwest, towards well PFL14 (Figure 38). During this period, piezometer nest PFL05/PFL100 was upgradient of Plainfield Lake with a downward vertical gradient of approximately 0.4 ft. From spring until late October 2019, the vertical gradient between PFL05 and PFL100 remained steady, with levels dropping only slightly (0.1 ft) relative to Plainfield Lake. By mid-September, the level of PFL100 first dropped slightly below the level of Plainfield Lake and tracked the lake level throughout October 2019.

Starting in mid-May 2019, piezometer nest PFL03/PFL101 exhibited a downward vertical head difference of approximately 0.2 ft. At this time, monitoring well PFL03 was upgradient of Plainfield Lake while PFL101 closely tracked the level of Plainfield Lake. Beginning in late June, the levels of PFL03/PFL101 started to drop relative to Plainfield Lake but maintained a steady downward vertical head difference of 0.2 ft. This trend continued over summer and into fall 2019, with the level of PFL101 first consistently dropping below lake level in late June followed by PFL03 falling below lake level in September. Although the gradients between PFL05/PFL100 and PFL03/PFL101 varied slightly, the overall trends for each piezometer nest generally tracked those for Plainfield Lake throughout the entire data collection period, with a steady increase in levels through mid-summer, followed by more stabilized levels from late summer into fall 2019.

While the vertical gradient trends for piezometer nests at Plainfield Lake behave rather consistently, they serve as an important point of comparison with trends observed at nearby Long Lake. Although piezometers were not yet installed around Plainfield Lake, the period from January to mid-March 2019 may best illustrate the different water-level responses for Plainfield and Long Lakes (Figures 34 and 35). As presented above, piezometers LL01B, LL02B, and LL09B were the only monitoring points around Long Lake to record falling water levels during this period of frozen-ground conditions. As levels in the piezometers fell, Long Lake continued its upward rise and shallow monitoring wells also rose but at a more modest rate. By contrast, at Plainfield Lake, the rise in all observed water levels slowed markedly in January and peaked in February, followed by a distinct decline through mid-March 2019. While these trends did reverse, following the spring thaw in mid-March, they stand in contrast to the trend observed at Long Lake and the surrounding shallow groundwater (above the fine-grained sediments). .

This interpretation does not suggest that Long Lake is disconnected, or separated from the regional groundwater system, but rather that underlying fine-grained sediments delay and attenuate groundwater stresses, leading to slightly different responses for Long Lake and shallow groundwater compared to deeper groundwater (below fine-grained sediment layers). By contrast, observed water-level trends for Plainfield Lake and surrounding groundwater (wells and piezometers), in the absence of a fine-grained sediment layer, do not exhibit delayed or attenuated responses to regional groundwater trends.

Lakebed Hydrology

Lakebed hydraulic properties and groundwater fluxes are important factors in defining a lake's hydrology and predicting their responses to stressors. WGNHS and WDNR conducted field work in the nearshore parts of the three study lakes in June and September of 2018 to estimate patterns of groundwater movement and lakebed characteristics. Shallow lakebed piezometers and seepage meters were installed to allow calculation of groundwater gradients, fluxes, and lakebed hydraulic conductivity. A photo of lakebed piezometer and flux meter installation is shown in Figure 47. A canoe survey of nearshore water quality was used to assess groundwater inflow and outflow zones.

Figure 47. Lakebed piezometer and seepage meter installation

METHODS:

Lakebed Piezometers

Personnel from WDNR and WGNHS measured groundwater gradients into and out of the study lakes using shallow lakebed piezometers (mini piezometers). During the first round of sampling in June of 2018, 12-13 lakebed piezometers were placed around each of the study lakes; a smaller number of piezometers were also installed in September of 2018. The piezometers were installed near the shore in water up to 2.5 ft deep. A mesh fabric well screen was secured to the end of a length of clear plastic tubing. The tube was manually driven to a depth of 1.6-3.3 ft (0.5-1 m) into the lake bed and allowed to equilibrate for 12 hours or more. The water level inside the tubing was then measured relative to the lake level. During the September round of measurements, a stilling well was used to increase the accuracy of the head measurements.

When reading piezometer heads, the water level in the tubing represents the hydraulic head at the well screen, 1.6-3.6 ft (0.5-1.1 m) below the lake bed. If the water level in the piezometer is above the lake level, groundwater movement is into the lake, while a water level in the lakebed that is lower than the lake level indicates flow out of the lake. A conceptual diagram of a lakebed piezometer is included in Figure 48.

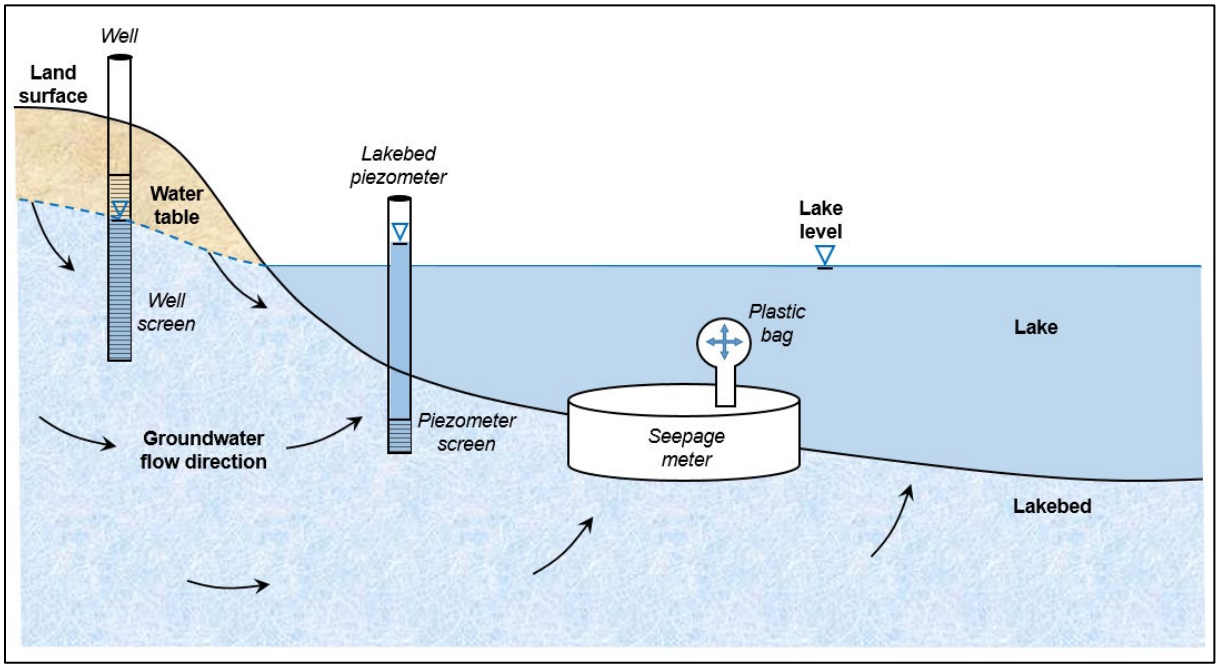

Figure 48. Illustration of a monitoring well, lakebed piezometer, and seepage meter deployed at a lake. Groundwater is shown moving towards, and discharging to, the lake. In this example, where groundwater discharges to the lake, the water level in the lakebed piezometer rises above the lake level and the plastic bag on the seepage meter inflates. If water were seeping out of the lake into the groundwater system, the water level in the lakebed piezometer would drop below lake level and the plastic bag would deflate. (Figure created by WGNHS for Description of Fieldwork Methods, Appendix D)

Seepage Meters

Seepage meters were used to directly measure fluxes between groundwater and surface water. The measurements were used to qualitatively identify areas of inflow and outflow and to quantitatively calculate groundwater/lake fluxes. In conjunction with lakebed piezometer readings, fluxes were also used to estimate lakebed hydraulic conductivity.

In June, 2018, WGNHS, WDNR, and Dr. Sue Swanson with students from Beloit College installed seepage meters at 7 locations spaced around each of the study lakes. The seepage meters consist of an open-bottomed cylindrical drum with a nozzle on the top. The meters were installed near the lakeshore in water 1-2 feet deep. Substrate type was noted, the drum was pushed into the lake sediment, and a plastic bag with a known volume of water (200-250 ml) was placed over the nozzle on the top of the drum. Where groundwater flows from the subsurface into the lake, the amount of water in the bag increases over time. Where water flows out of the lake into the groundwater system, the amount of water in the bag decreases. A conceptual illustration of a seepage meter installation is shown in Figure 48. After a known length of time, several hours to overnight, the amount of water in the bag was measured. The change in volume over time was used to determine of the rate of groundwater flow.

Seepage meters allow direct measurement of groundwater fluxes, but also have a large associated measurement error. Heterogeneity in the lake bed can cause flux measurements a short distance apart

from one another to vary significantly. Seepage meter setup can also introduce errors (Rosenberry and LeBaugh, 2008). For example, it may also be difficult to obtain a good seal between the drum and the lakebed. Disturbances such as walking on the lakebed near the installation can also affect results. During the first round of sampling, a single seepage meter was placed at each measurement location. While reasonable results were derived using this method, the accuracy of the readings were difficult to determine. During a second round of sampling in September, 2018, WDNR and WGNHS installed three seepage meters at each seepage meter location (3-5 locations per lake) so that an average flux value could be used and obvious outliers neglected.

RESULTS:

Lakebed Piezometers and Seepage Meters

Results from lakebed measurements are used in concert with the groundwater monitoring network (described below) to define groundwater movement patterns into and out of the study lakes. Results obtained from the in-lake measurements agree well with gradients derived from monitoring wells and existing water table mapping (Lippelt, 1981).

Heads in the lakebed piezometers and seepage meter readings at Pleasant Lake generally indicate that groundwater enters the lake on the west and north sides and flows out of the lake on the east and southeast (Figure 49). Pleasant Lake had the largest vertical gradients of the three study lakes; Pleasant Lake gradients were an order of magnitude greater than those at Long or Plainfield Lake. The largest gradient into Pleasant Lake was 0.25 feet/foot on the western shoreline, while the largest gradient out of the lake was -0.22 feet/foot on the northeast side of the lake. Seepage meter readings during the second round of sampling (3 seepage meters at each site) also indicate flux into the lake on the west. Low levels of flux out of the lake were observed at measurement points on the southwest, southeast, and northeast sides of the lake.

Long and Plainfield Lakes are situated near the groundwater divide and both have relatively small vertical gradients. At Plainfield Lake, water levels in lakebed piezometers show that groundwater generally enters the lake on the north side and flows out of the lake to the south. Vertical gradients range from -0.048 to 0.025, but most of the observed gradients were close to zero, especially on the south side of the lake. June 2018 seepage meter readings (single meter per site) showed water entering the lake at all measurement points. Readings in September 2018 (3 meters per site) show water entering the lake on the northwest and exiting to the southwest, with very small gradients into the lake on the eastern edge. Flux measurements at Plainfield Lake ranged from -0.0034 to 0.33 ft/d Seepage meter readings for September 2018 are shown in Figure 50, remaining meter readings are available in Appendix B.

At Long Lake, lakebed piezometer heads indicate that water enters the north side of the lake and exits to the south. This agrees with measurements taken in shallow groundwater monitoring wells around the lake during the same time period. Relatively low vertical gradients were recorded by the lakebed

piezometers; between -0.01 and 0.01. All seepage meters installed at Long Lake on both the June and September measurement dates indicated small amounts flux into the lake (0.0018 to 0.15 ft/d).

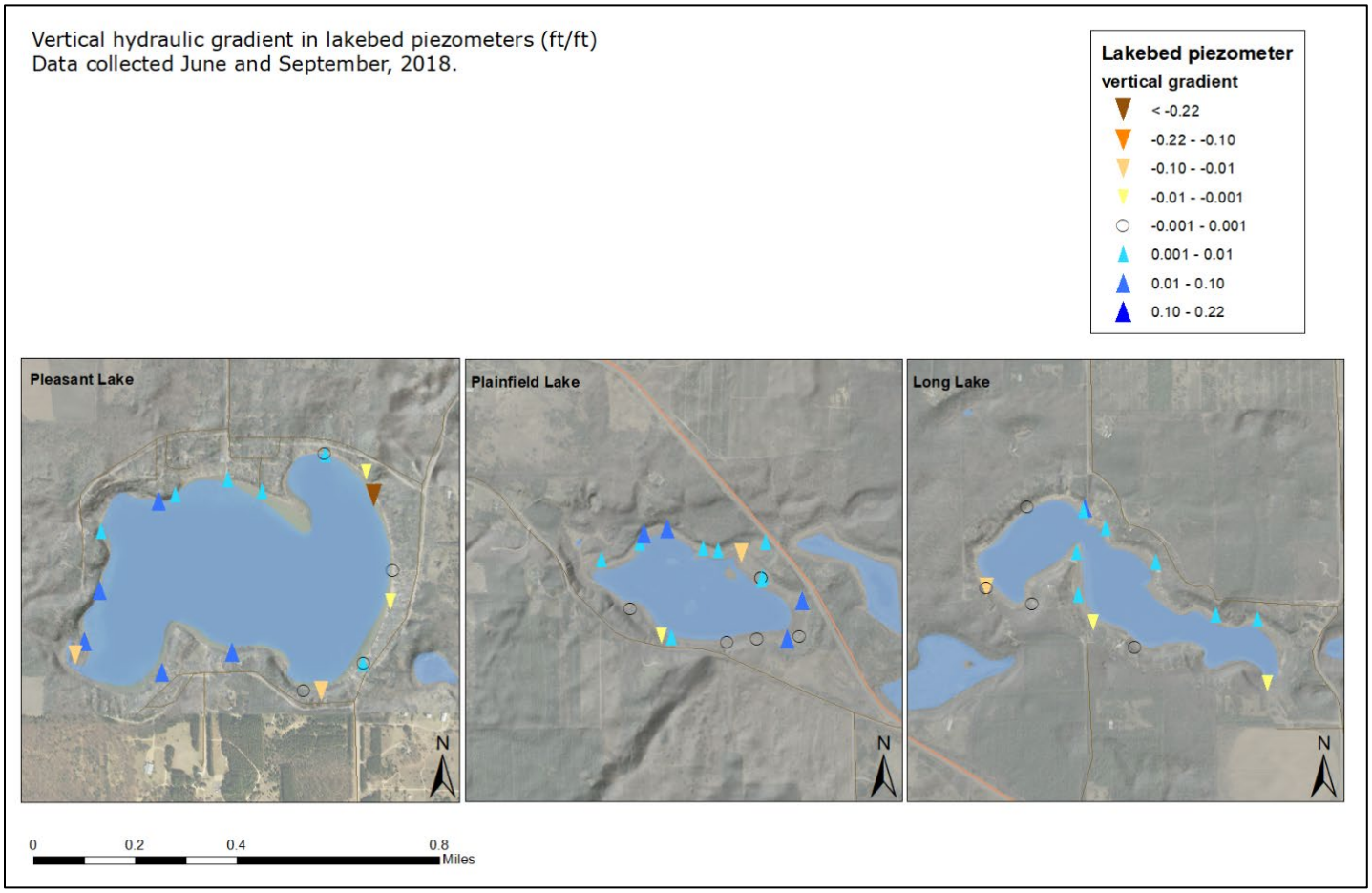

Figure 49. Vertical gradients measured in lakebed mini-piezometers in June and September, 2018. Positive gradients (upward arrows) indicate groundwater entering the lake from the aquifer. Negative gradients (downward arrows) indicate water moving downward out of the lake.

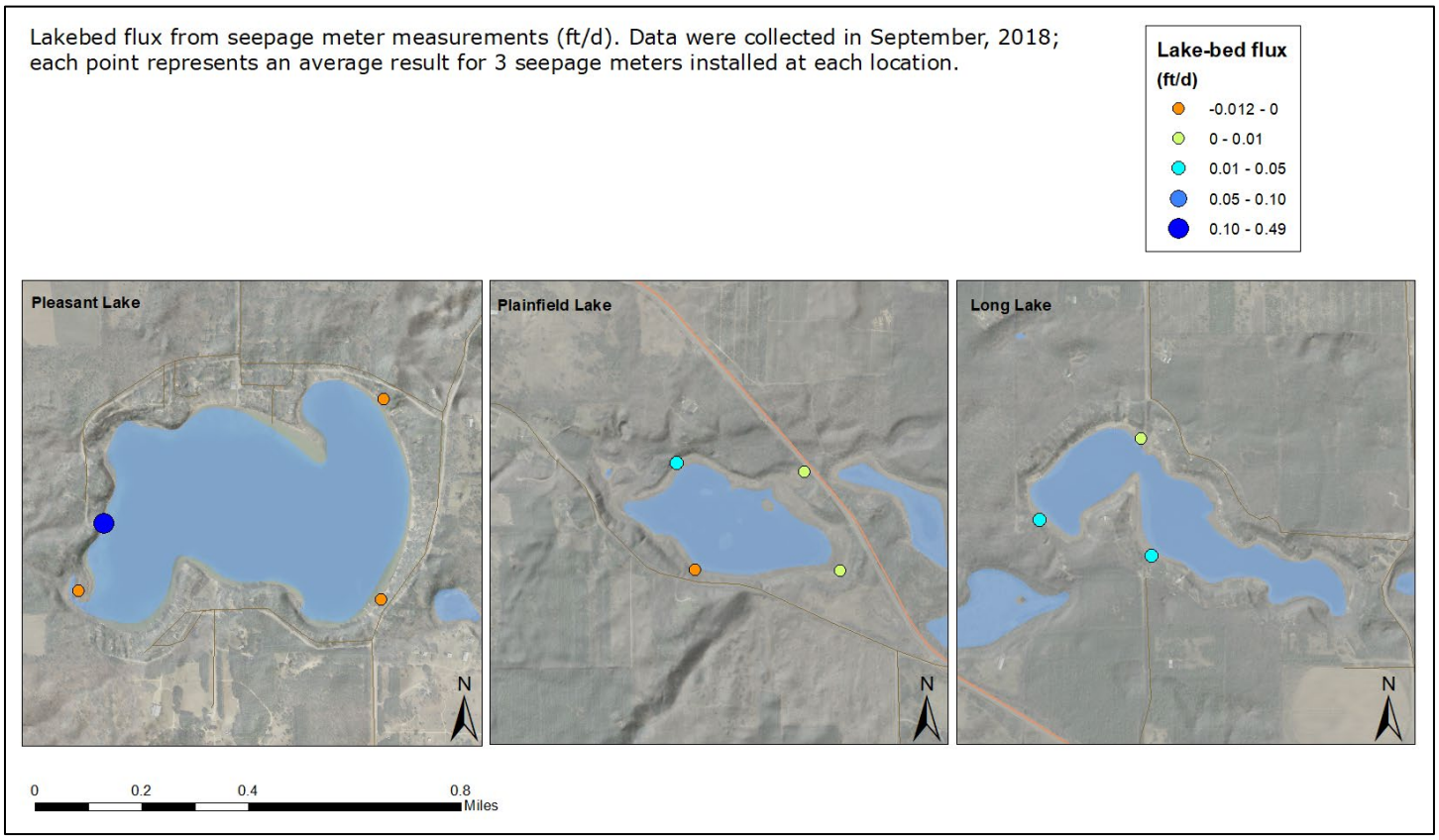

Figure 50. Seepage meter measurements collected in September 2018. Positive gradients (blue and green dots) indicate groundwater entering the lake from the aquifer. Negative gradients (orange dots) indicate water moving downward out of the lake.

Paired lakebed piezometer hydraulic gradients and seepage meter fluxes were used to estimate lakebed hydraulic conductivity. Hydraulic conductivity was calculated using Darcy's Law:

$$K = (Q/A)/(\Delta h/\Delta l) \qquad \text{Equation 2}$$

where K is hydraulic conductivity (ft/d), Q is the measured flow rate (ft^3/d), A is the area of the seepage meter, Δh is the head change between the lake and mini-piezometer, and Δl is the depth of the mini-piezometer screen situated 0.5-1 m below the lakebed (unitless).

Figure 51 shows the results of the lakebed conductivity analysis. Several sites were excluded from the calculation: at three sites, the hydraulic gradient measured in the mini-piezometer was zero, and at five sites there was mismatch in gradient and flux direction that would result in a negative estimate of hydraulic conductivity. WGNHS calculated lakebed hydraulic conductivity and conducted a simple error analysis for the remaining 23 sites. The sources of potential error included in the analysis were the accuracy of water-levels readings (±1 cm), depth of installation (±10 cm) in the mini-piezometers, and seepage meter errors.

The seepage meter error was estimated using the coefficient of variation of fluxes at the 12 sites where three seepage measurements were collected. The coefficient of variation is defined as the standard

deviation divided by the mean. Calculated error varied from ±8% to ±560% with an average of ±130%. It must be noted that a coefficient greater than 100% suggests that the flow direction could be opposite of what was measured, resulting in a negative estimate of hydraulic conductivity.

The seepage error estimate was combined with the mini-piezometer error estimate. For those locations where only one seepage flux measurement was made, the average coefficient of variation was assumed to represent the seepage meter error. The error estimates are shown as the error bars in Figure 51. Note that only five of the 23 lake bed conductivity estimates have total error less than 100 percent as indicated by the error bars of those five not going below the x-axis.

Calculated lakebed hydraulic conductivity values range from about 0.1 to 5 ft/d for Long and Plainfield Lakes and from 0.001 to 2.6 ft/d at Pleasant Lake. These hydraulic conductivity estimates, although associated with large error, still provide useful information for the modeling effort. Apart from the two lowest estimates, the conductivity values vary between 0.1 and 6 ft/d with a median estimate of 0.8 ft/day. The upper bound from the error estimates is less than 10 ft/d. This suggests that reasonable estimates of lakebed hydraulic conductivity fall in the range of 0.1 ft/d to 10 ft/d.; these values are about an order of magnitude less than what is expected for the surrounding aquifers. It also seems that the three lakes all have similar vertical lakebed conductivities.

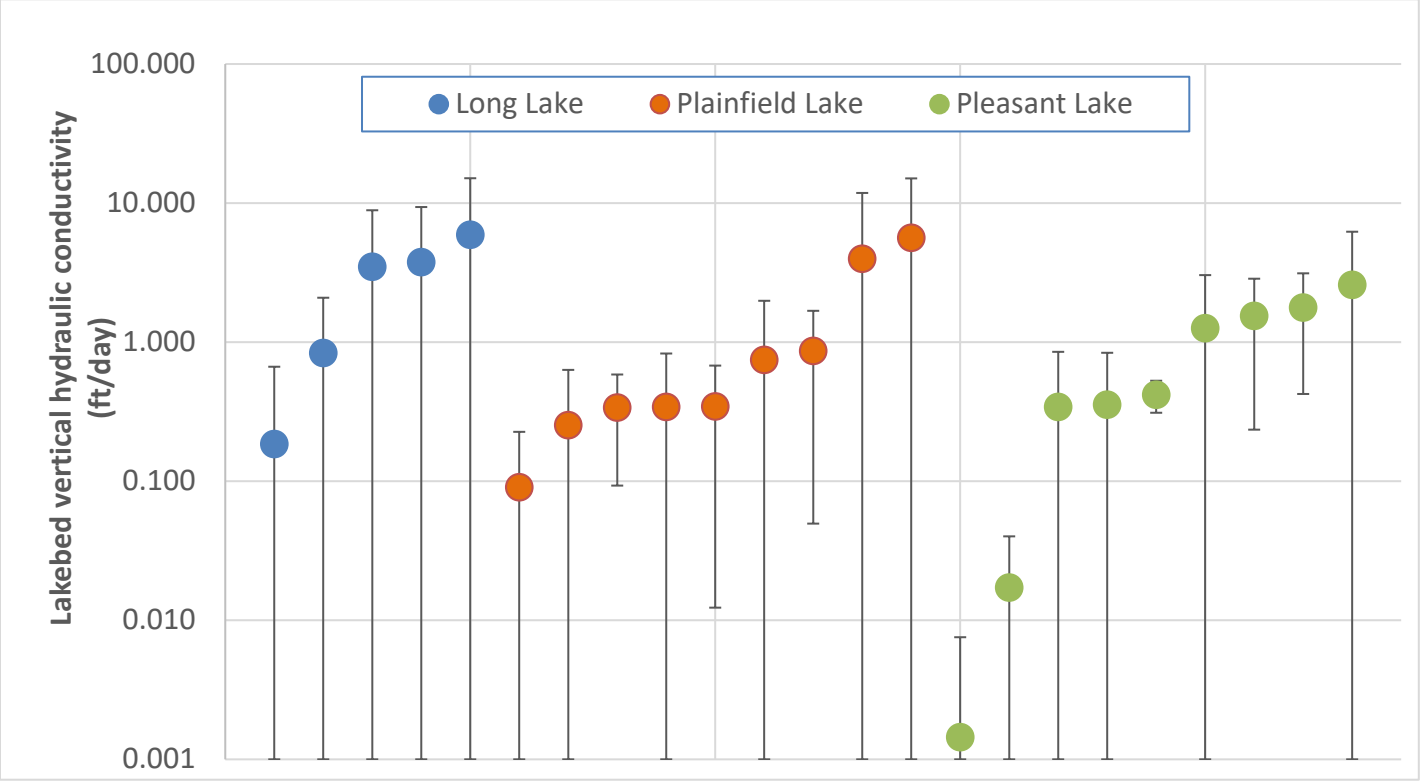

Figure 51. Lakebed vertical conductivity estimates determined from mini-piezometer and seepage meter data. Each lake is plotted in a different color; each dot represents the lakebed conductivity estimate at a location around the lakes. Error bars represent the combined error of seepage meter and piezometer measurements. Error bars terminate at K=0 as calculated hydraulic conductivities less than zero were not allowed.

Canoe Surveys

METHODS:

WGNHS conducted instrumented canoe surveys in the three lakes. The canoe was instrumented with an EM-31 electromagnetic conductivity meter to measure water and sediment conductivity, a depth finder, a GoPro video camera, and water quality instrumentation that recorded water temperature, conductivity, pH, dissolved oxygen, chloride, and nitrate concentrations. Data points were geolocated using GPS. These surveys were part of a larger effort to develop this method of rapidly characterizing smaller streams and lakes. Complete results and discussion are available in Christenson (2019). Figure 52 shows the instrumented canoe on Plainfield Lake. The data was collected by first circling the lake counter-clockwise until reaching the start point and then turning around and circling the lake clockwise back to the start. This tested for repeatability.

Figure 52. Canoe instrumented with EM-31 conductivity meter, depth finder, water temperature and quality instruments, and Go Pro video cameras.

RESULTS:

Examples of water quality data for Plainfield Lake are shown in Figures 53, A-D. The path of the canoe and data are shown as colored dots. Figure 53A shows the dissolved oxygen (blue) is lowest on the western edge of the lake and highest (red) on the eastern edge. The reason for the variation is possibly a combination of wind and vegetation. The pH was measured at the same time as the dissolved oxygen and has a similar distribution, with the western edge being more neutral and the eastern edge being most basic. The similarity between the two water quality parameters might be due to biological activity,

perhaps decaying vegetation lowering both the pH and dissolved oxygen on the western edge. The fluid conductivity was also measured during this canoe survey, Figure 53C. The conductivity is highest along the northwest shore and lowest along the southeast shore. These values are approximately in line with the groundwater flow direction with water flowing into the lake from the northwest and discharging to the southeast. A potential explanation might be that as groundwater discharges to the lake, carbonate precipitates out of solution, lowering the concentration of ions in the water. This is likely an oversimplification since the pH appears to be controlled by other factors. Dissolved oxygen percentages for Long and Pleasant Lakes are also shown for comparison in Figures 53E and F. Both of these lakes have higher dissolved oxygen levels than Plainfield Lake. However, like Plainfield Lake, the oxygen levels vary with higher levels at one side of the lakes compared to the other side. In Long Lake, the oxygen is highest to the west and lowest to the east while in Pleasant Lake, the oxygen levels are highest to the east and lowest to the west. Many factors could create this variation including wind, groundwater inflows, and biological activity. The quality of the data for the other measurements for these two lakes was insufficient for them to be reported. The survey method was still in development at the time of the surveys and so not all measurements in the surveys were always successful.

One of the goals of the effort by Christenson (2019) was to estimate the sediment electrical conductivity using the water depth and conductivity and the EM-31 data. The EM-31 instrument electrical conductivity incorporates both water and sediment conductivities. If the water conductivity and depths are known, then it is possible to estimate the sediment conductivity (McNeill, 1980). Figure 53D shows the results of that calculation for the perimeter of Plainfield Lake. The lowest sediment electrical conductivity (blue) values are found on the northeast side of the lake while the highest sediment electrical conductivity (red) are found on the western edge of the lake. The sediment electrical conductivities are correlated to sediment type and hydraulic conductivity. In general, sediments with low electrical conductivities have less clay or organic material than sediments with higher electrical conductivities. Sediments with less clay and organic materials usually have higher hydraulic conductivities than those with more. This then implies that the areas shown in blue have higher hydraulic conductivities than those in red with the other areas having intermediate hydraulic conductivities.

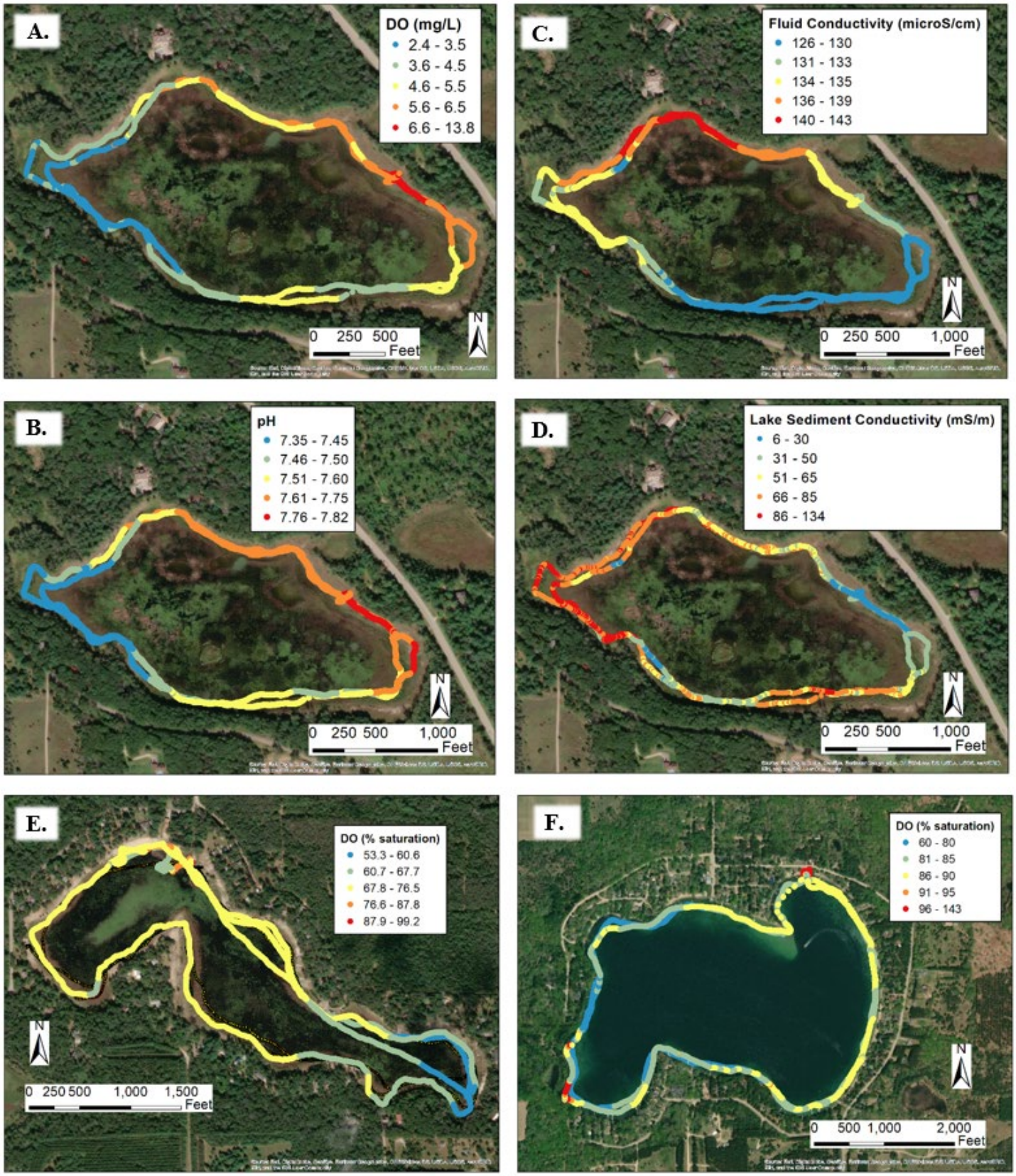

Figure 53. Canoe survey results. Dissolved oxygen (DO), pH, and fluid conductivity were directly measured. Sediment conductivity was calculated from EM-31 data using water depth and fluid conductivity.

WGNHS: PRODUCTS

Hydrostratigraphy – Conceptualization and Layer Creation

The main goal of geologic data collection efforts for the Central Sands Lakes Study was to develop a conceptual model of hydrostratigraphy and to convert the conceptual model to a set of layer surfaces for use in the groundwater flow model. The following section presents methods WGNHS used to create the areal extent and layering for the hydrostratigraphic model.

Hydrostratigraphy provides the basic framework for the conceptualization of flow systems by dividing the different sediments and rock units into distinct mappable domains and layers based on their hydrogeologic properties. Hydrostratigraphic units in the Central Sands study area include both unconsolidated glacial sediments and bedrock units. Bedrock in the Central Sands study area is divided into three potential hydrostratigraphic units:

1. Paleozoic sandstones
2. Paleozoic dolomites
3. Precambrian crystalline bedrock

The Paleozoic units were grouped into one hydrostratigraphic unit, while Precambrian crystalline bedrock is assumed to be impermeable and forms the base of the groundwater model.

Using glacial history as a guide, WGNHS divided the glacial deposits into five hydrostratigraphic domains (areas):

1. Glacial Lake Wisconsin lake plain sediment
2. Outwash plain sediment between the Hancock moraine and the lake plain sediments
3. Intermorainal sediment between the Hancock and Almond moraines
4. Stagnant ice sediment extending east from the Almond moraine to glacial Lake Oshkosh
5. Glacial Lake Oshkosh sediment

In some instances, these glacial sediments are relatively laterally continuous and can be divided into mappable layers. In other instances, they are heterogeneous, without clear mappable units for layering. Where the geology is heterogeneous such as east of the Hancock moraine, length scales of different lithologies vary, or data are sparse, there are several options for defining hydrostratigraphy. The geology could be treated as homogeneous so that little variation is recognized. Alternately, small-scale heterogeneities could be created throughout the domain based on extrapolation from the presence of bodies identified where high-density data are available. A third option, which was chosen for use in the parts of the study area east of the Hancock moraine, was to create a probability-based distribution of coarse and fine-grained sediments in the subsurface based on available boring data. This approach honors the available data in areas where heterogeneity is observed in boring logs without imposing an artificial distribution of fine-grained zones in no-data areas.

Conceptualization and Layer Creation – Paleozoic and Precambrian Bedrock Elevation

WGNHS created bedrock surfaces for the top of bedrock and for the crystalline Precambrian bedrock surface. The upper bedrock aquifer includes sandstone throughout most of the model domain, Precambrian rock in some areas to the north, and some dolomite in the east. Dolomite occurs mainly in the glacial Lake Oshkosh basin, outside the Central Sands area. The total calculated thickness of the Paleozoic sandstone and dolomite is shown in Figure 54. The bedrock elevation surface (Figure 55), and the Precambrian bedrock elevation surface (Figure 56), were produced by integrating available point and polygon data relating to bedrock elevation. Sources for point data for bedrock elevations and Paleozoic/Precambrian contact elevations include well construction reports, geophysical logs of boreholes, drill core, and passive seismic surveys. Polygon data were used for bedrock elevations in areas where shallow bedrock was previously mapped at or near the land surface. Data steps used in ArcGIS to create the bedrock surfaces are detailed in Appendix J.

Point data were compiled from geolocated WCRs and geologic logs that intersect bedrock (including the two rotosonic holes drilled for this study), from bedrock depths reported in literature, and from geophysics work conducted for this and other studies within the CSLS model domain. As a first step in layer creation, WGNHS interpolated the bedrock surface from point data (borehole data, wells construction data, passive seismic data, direct push coring, bedrock coring, etc.) using the "Topo to Raster" tool in ArcGIS.

GIS personnel compiled a geodatabase of shallow bedrock areas mapped in previous WGNHS projects and shallow bedrock data identified in USDA/NRCS soils maps. The sources for that data are as follows:

- Data Accompanying Information Circular 56: Pleistocene Geology of Portage County, Wisconsin
- Data Accompanying Information Circular 59: Pleistocene Geology of Adams County, Wisconsin
- Data Accompanying WOFR2015-01: Preliminary Quaternary Geology of Columbia, Green Lake, and Marquette Counties, Wisconsin
- Data Accompanying WOFR2004-04 : Preliminary Quaternary Geologic Map of the Central Fox River Lowland, Wisconsin
- Data Accompanying WOFR2015-01 : Preliminary Quaternary Geology of Columbia, Green Lake, and Marquette Counties, Wisconsin
- NRCS Bedrock Minimum Depth DATCP - downloaded by DATCP from NRCS on 2/18/2014 and joined to the statewide map unit layer.

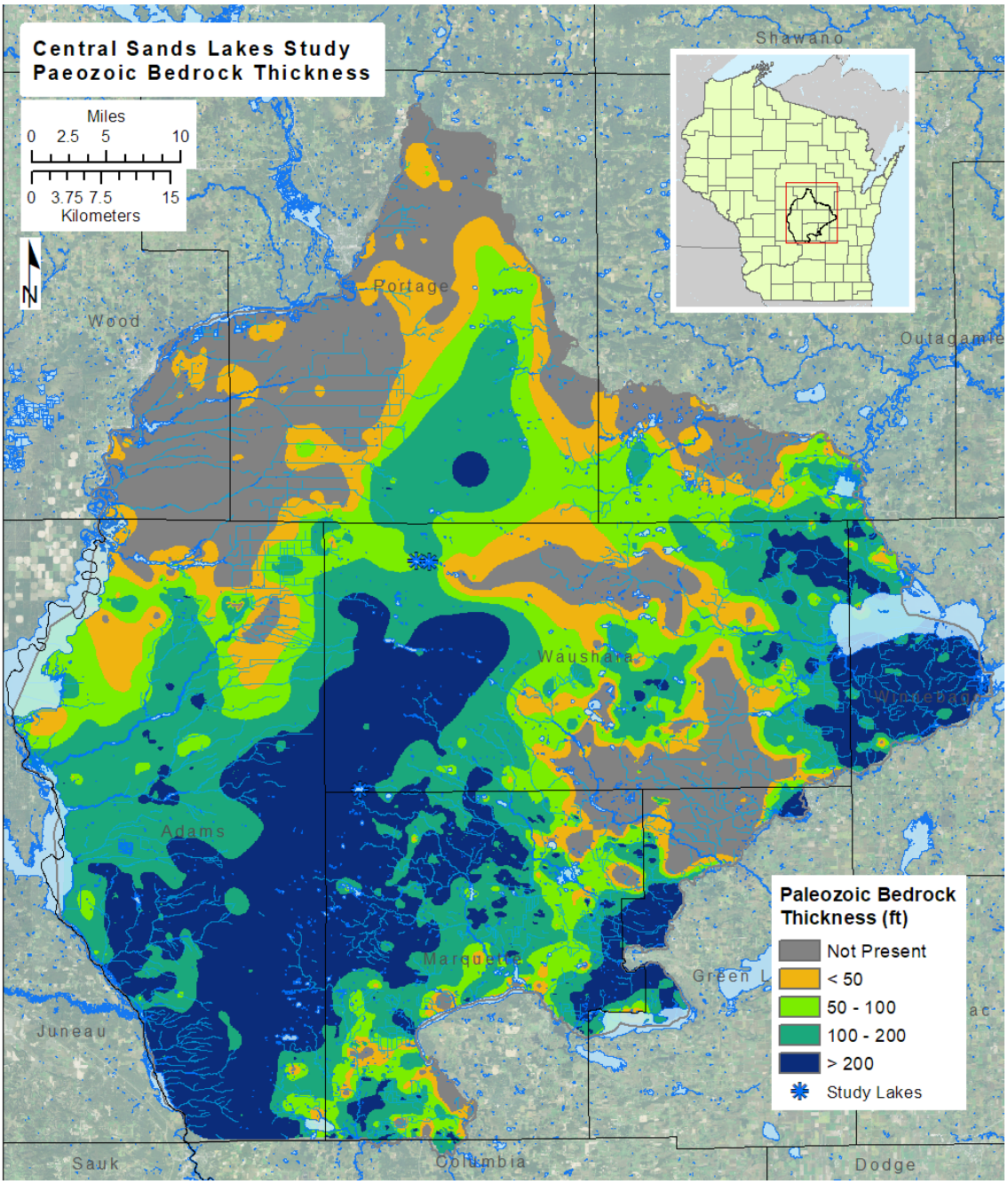

Figure 54. Thickness of Paleozoic bedrock, typically Cambrian sandstone except in the far eastern part of the CSLS model domain, where dolomite is present.

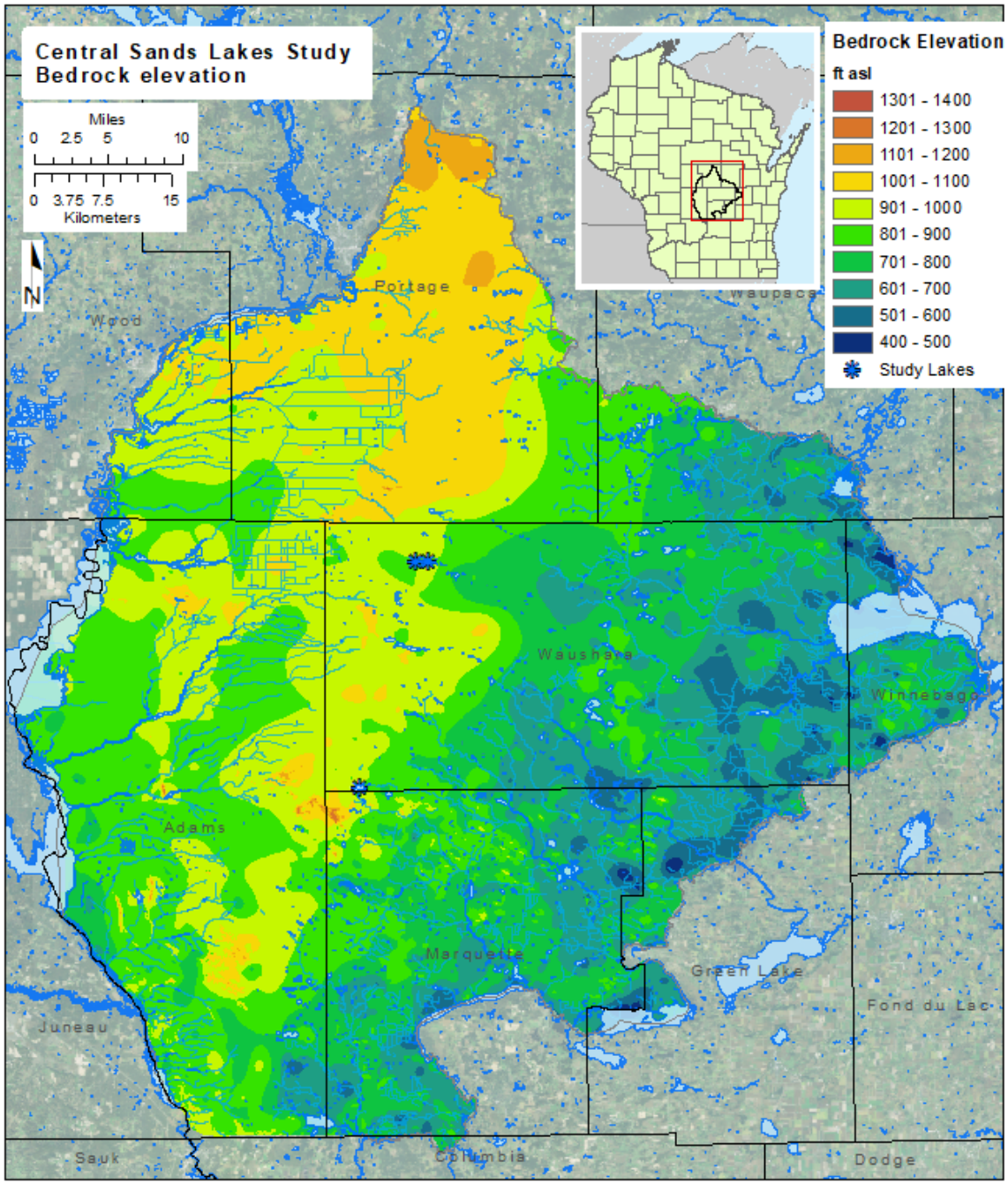

Figure 55. Bedrock surface elevation. Upper bedrock units include crystalline bedrock to the north, dolomite to the east, and sandstone over the majority of the model domain. Bedrock data points near the study lakes are shown in Figure 11.

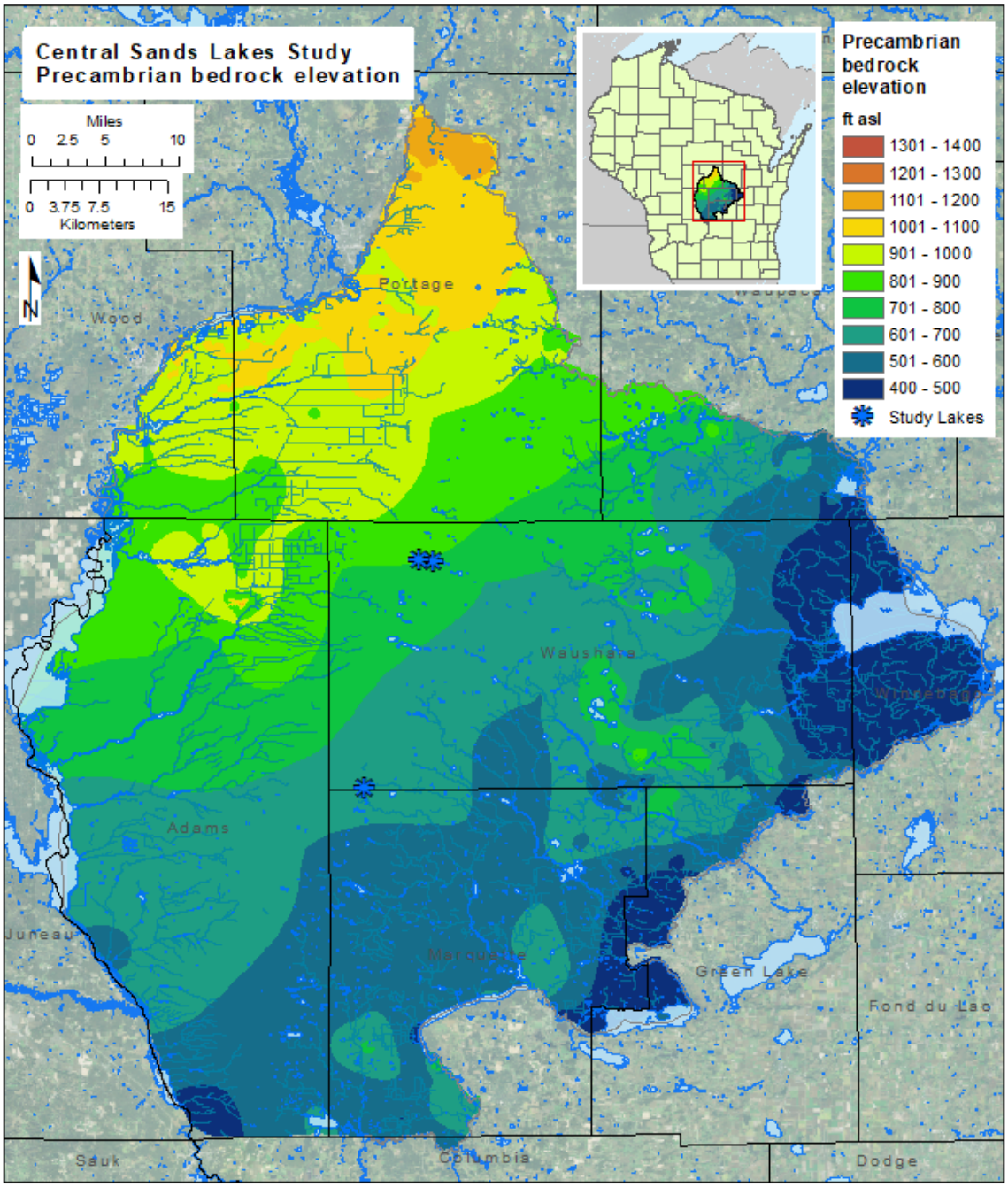

Figure 56. Precambrian bedrock surface elevation

All the shallow bedrock polygons were aggregated and loaded into a single feature class. Polygon boundaries were edited based on inspection of DEMs, DEM hillshade rasters, and borehole data. Near-surface bedrock areas were given elevations ten feet below the DEM land surface and bedrock elevations were contoured. Subsurface bedrock elevations around the shallow bedrock areas were then buffered at 10-meter increments extending beyond the shallow bedrock polygons. Depth values were calculated for these buffers based on a 40-degree slope, chosen to simulate the observed angle of repose for the eroded

sandstone bedrock. Buffer depths were converted to elevations, and buffer contours were combined with shallow bedrock contours to create a bedrock elevation raster for these areas.
Shallow bedrock areas were combined with point data to create final bedrock surfaces. The buffered shallow bedrock polygons were clipped include to only areas where they were at higher elevation than the bedrock surface interpolated from point data only. Point data and the clipped shallow bedrock contours were then combined using the Topo to Raster ArcGIS tool. Both the upper bedrock surface and Precambrian surface were interpolated in this way (Precambrian bedrock crops out in northern Adams County and at some points along the Wisconsin River).

Several lines of passive seismic data points extending north-south across the Plainfield Tunnel channel indicate the presence of a bedrock valley beneath the tunnel channel. A set of artificial bedrock points was included in the bedrock surface interpolation to prevent the bedrock surface from becoming artificially shallow between existing data points. Because of the highly productive sand and gravel aquifer and relatively thick sediment package, few depth-to-bedrock data points are available in the intermoraine area. The same set of dummy points was used to lower the surface of the sandstone bedrock in the vicinity of the eastern rotosonic boring, as the upper bedrock observed in the core was Precambrian granite. Following interpolation, any bedrock surfaces that exceeded land surface were altered to be a minimum of 1m (3 ft) below land surface (2m for Precambrian bedrock).

Conceptualization and Layer Creation – New Rome Member

The Glacial Lake Wisconsin Basin, located in the western part of the model domain, includes a thin and generally continuous layer of clay and silt, mapped as the New Rome Member of the Big Flats Formation (Figure 3, Figure 5). The New Rome is underlain and overlain by sand and gravel outwash sediments. It slopes to the south and west, away from sediment sources at the glacial margins, and becomes thicker to the south, farther out into the former lake basin. To the north and east, in Wood County and eastern Adams County, the layer becomes thin and discontinuous. The sandstone bluffs and pinnacles that outcrop in the former Lake Wisconsin basin would have formed islands in the lake that caused disruption to sediment movement and discontinuity in the deposition of the fine-grained sediments. In places, especially near the Wisconsin River, modern stream channels have down-cut through the New Rome layer so that it is absent in those areas. The New Rome terminates to the west at the terraces of the Wisconsin River.

Work by Hart (2015) suggests that the New Rome has a hydraulic conductivity orders of magnitude lower than the surrounding sand and gravel aquifer and, where it is continuous, it creates a local aquitard, affecting groundwater gradients and movement.

Most well logs in the lake plain identify a clay layer (or multiple clay layers). Geologic logs from well construction reports and lithologic logs examined by WGNHS were used to define the extent of the New Rome layer. For the purposes of layer creation, areas in the lake plain with consistent clays with a thickness greater than 2 feet were considered to have the New Rome layer present.

The upper and lower elevations of units from well logs with “clay” as a primary or secondary descriptor were used to create the top and bottom surfaces of the New Rome model layer.

As noted by Brownell (1986) and Clayton (1987), multiple clay layers are present in some parts of southern Adams County, for example near the towns of Adams/Friendship. WGNHS examined the available geologic data in ArcScene to determine whether these secondary layers were hydrostratigraphically important or mappable. Because clay layers below the New Rome appear to be spatially limited and data are discontinuous, WGNHS determined that the additional clay units would not be included as layers in the groundwater model. It was noted that some driller logs appear to ignore multiple units or to lump multiple layers into a single clay interval. Where multiple clay layers were identified in a log, WGNHS used the top and bottom of the upper clay to define the New Rome surfaces.

Driller descriptions in well construction logs were inspected, and data points that did not sufficiently describe the actual vertical extent of the clay layer were removed. Some examples of excluded data include log intervals with descriptions such as “clay, sand, and gravel” over long intervals or “sand with clay streaks.” In wells where both “clay and sand” and “clay” were noted in a log, the finer unit was used to define the New Rome surfaces. Following initial interpolation, data points with geologic descriptions substantially in disagreement with multiple nearby logs were also removed.

Upper and lower New Rome surfaces were interpolated using inverse distance weighting and smoothed using focal statistics with a focal distance of approximately 0.5 miles. The calculated New Rome surfaces were compared to LiDAR-derived land surface elevations and bedrock elevations. The New Rome intersected these surfaces at logical locations. It typically intersects the land surface in stream channels and near the Wisconsin River and intersects bedrock where bedrock is shallow or forms bluffs. The interpolated New Rome dips to the south and west and thickens to the south (Figure 57). This configuration agrees with the conceptual model of the formation of the New Rome, with fine-grained sediments sourced from the north and east being deposited in the more distal parts of the glacial Lake Wisconsin basin.

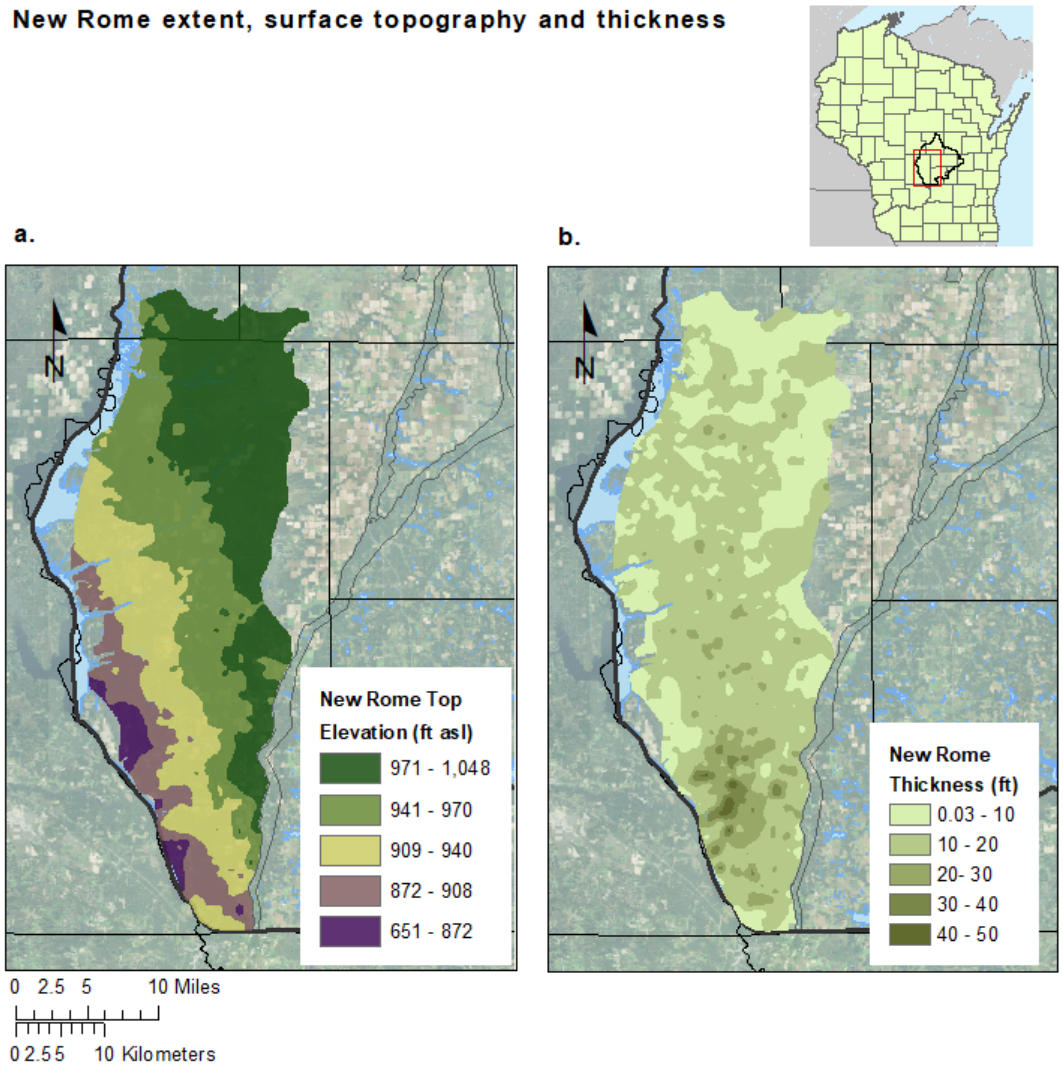

Figure 57. Configuration of the New Rome Member within the model domain interpolated from well construction and geologic log data. (a) Upper surface of the New Rome. The unit slopes to the southwest. (b) Thickness of the New Rome increases to the south. The unit becomes thin and discontinuous to the north and may be intermittently present north of the extent mapped.

Conceptualization and Layer Creation – Heterogeneity east of the terminal moraine

The glacial sediments to the east of the Hancock/Johnstown moraine are heterogeneous and not as easily mappable as those to the west. Heterogeneity in the area between the Hancock and Almost moraines is shown in the transect of well logs in Figure 5 and the oblique view of the well logs in Figure 58. In addition to the observed heterogeneity, few wells penetrate all the way to bedrock in this area. This creates an issue of how to incorporate heterogeneity into the groundwater flow model and to fill in regions with little data. The method chosen was to identify coarse and fine materials in existing logs and interpolate these data spatially within the 3-layer structure of sediments in the groundwater model. This allows aquifer properties in the model to be varied based on the observed distribution of fine-grained materials.

WGNHS used sediment types reported in well logs, direct-push and rotosonic cores, and geophysical data to evaluate heterogeneity. No widespread fine-grained layers were identified based on boring log data. Reported sediment types from driller descriptions and geologic logs were categorized as coarse (sand, gravel), fine (clay, silt), or mixed (clayey sand, clay and gravel, etc.). The "mixed" category was given a weight of 50% coarse, 50% fine. The sediment column was divided into three zones, corresponding to layering in the groundwater model, with thicknesses determined as described below. The percent coarse material in each layer was calculated for each data point in each layer. Data were then interpolated using ArcGIS to create a distribution of coarse and fine materials.

The eastern part of the model domain was divided into two areas for the purpose of creating layer thicknesses to incorporate into the groundwater model with coarse-fine distribution: 1) the intermoraine area where the upper surface is dominated by relatively flat-lying glacial outwash, and 2) a zone of mixed glacial sediments further east which includes collapsed till surfaces and the Glacial Lake Oshkosh basin (Figure 3). The intermoraine and eastern areas were treated slightly differently with respect to the creation of layer thicknesses.

In the intermoraine, the upper layer was identified as mainly outwash from the last glacial retreat and is therefore made up of mostly coarse materials (sands and gravels). The lower two layers incorporate a mix of coarse and fine-grained sediments associated with stagnant ice, basal tills, and outwash from prior glacial retreat(s). In the intermoraine, the elevation of the bottom of layer 1 was interpolated between the upper occurrence of fine-grained sediments in boring logs. The elevation of the bottom of layer 2/top of layer 3 was obtained by dividing the remaining sediment thickness in half. Figure 57 shows the well data in the area between the Hancock and Almond moraines, looking from above towards the northeast. Fine-grained materials (clays and silts) are shown in red. Coarse-grained materials include: sand (light blue), sand and gravel, and gravel (dark blue). Mixtures of fine and coarse-grained materials are shown in orange. Light yellow lithology, visible to the south, indicates sedimentary bedrock. A cluster of fine-grained material underlies Long Lake, visible as the red and orange lithologies on the west-central margin of the intermorainal area. Two other finer grained zones are also indicated, one underlying Huron Lake and one located to the south and east of the other two zones.

In the eastern zone, the three layers were created by evenly dividing the thickness of unconsolidated sediment into thirds. No consistent geologic layers comparable to the outwash seen in the intermoraine were identified in this zone, with the exception of the Glacial Lake Oshkosh clays, which are distal to the area of interest. Heterogeneity was therefore assessed for three layers of equal thickness.

The interpolated distribution of coarse materials is shown in Figure 59. Fine-grained sediments observed in the vicinity of Long Lake appear in layers 2 and 3, as does the fine-grained zone near the Almond Moraine shown in Figure 57. Few areas outside the Glacial Lake Oshkosh basin have more than 50% fine

materials. The distribution of coarse materials was used in the creation of the hydraulic conductivity distribution in the modeling effort.

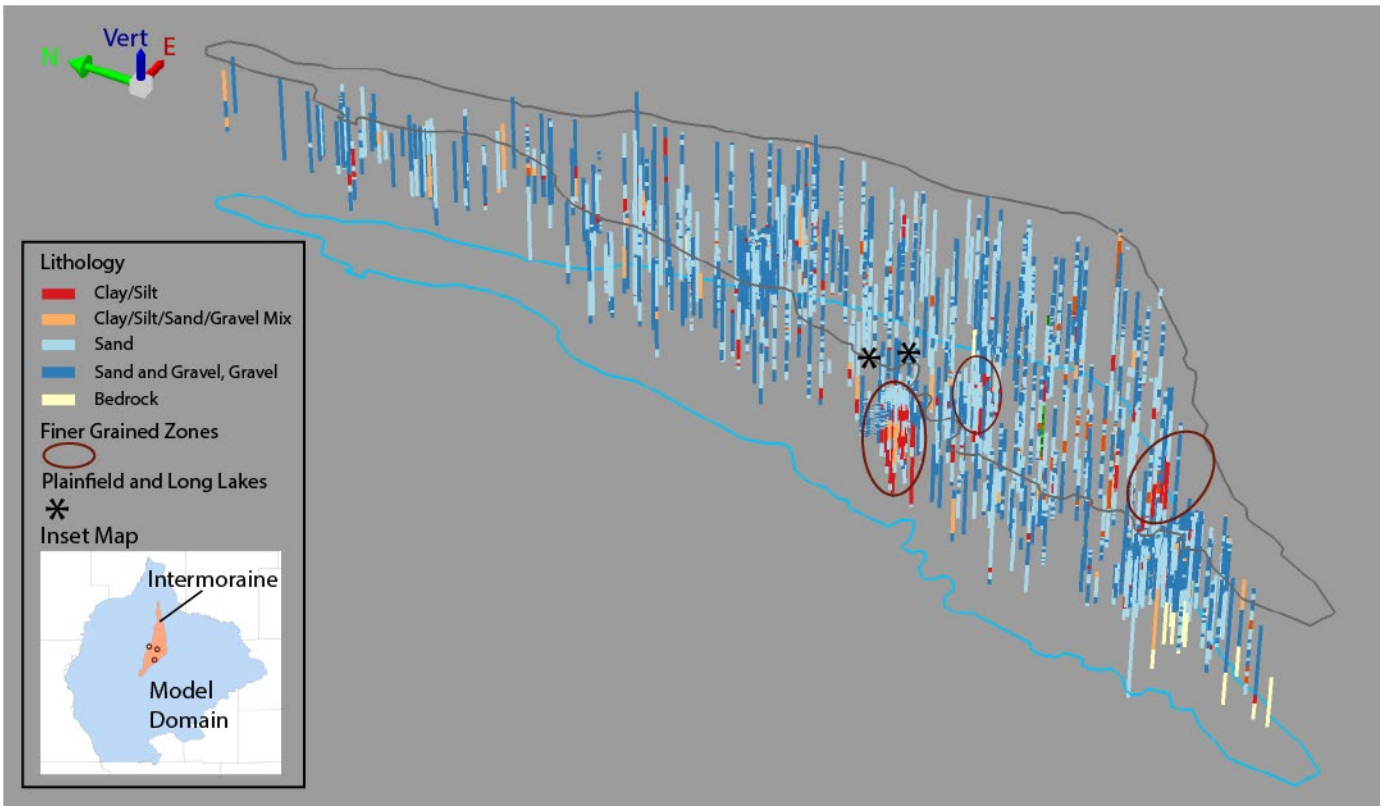

Figure 58. Northwest looking view of the well log lithologies in the intermorainal area. Area shown corresponds to the Intermoraine area in the inset map. In contrast to the outwash plain to the west, fine-grained sediments are fairly common at depth. The two fine-grained zones noted to the north are in the Plainfield Tunnel Channel around Long Lake and Huron Lake. The more southerly fine-grained zone may represent a former pro-glacial lake or backwater area.

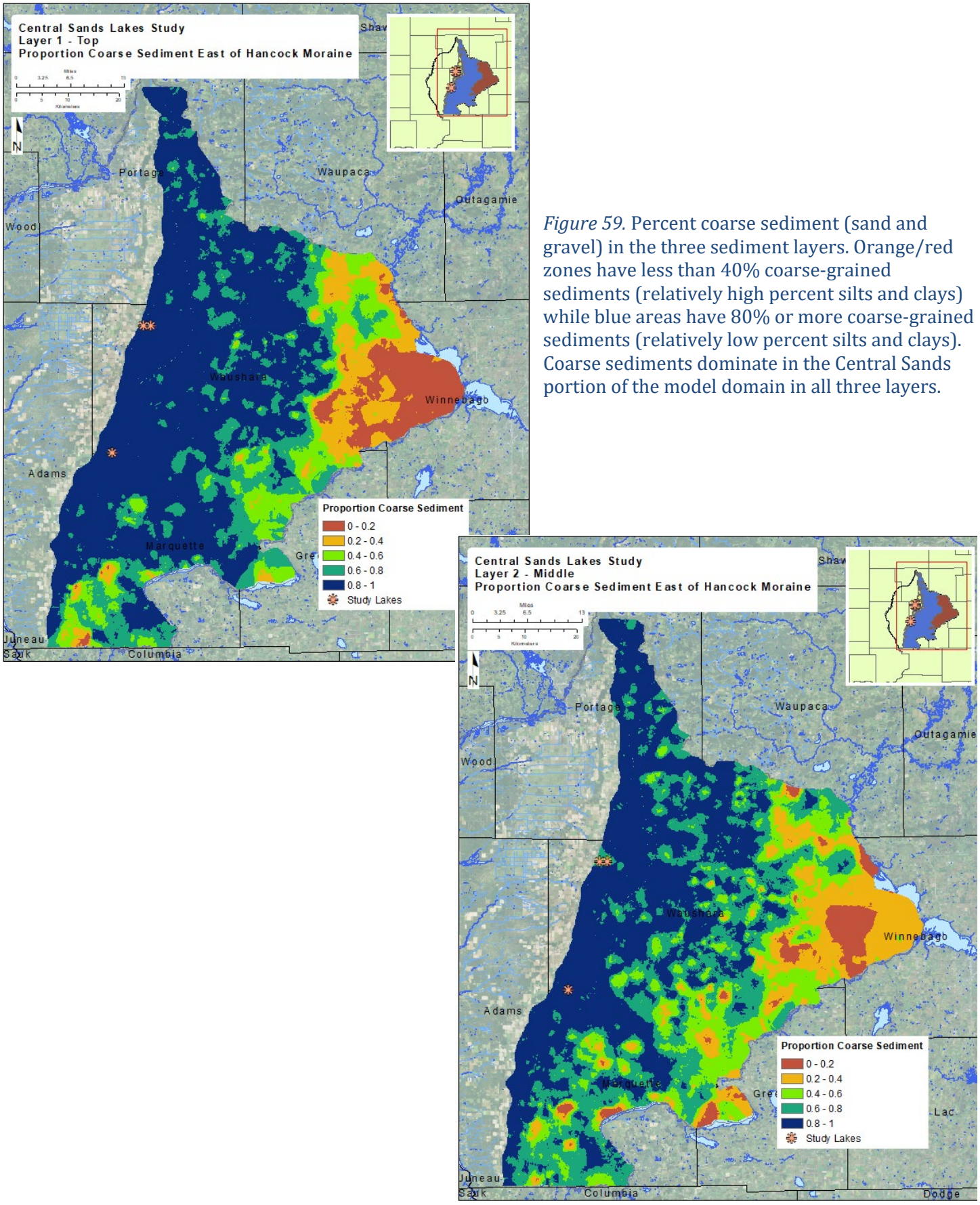

Figure 59. Percent coarse sediment (sand and gravel) in the three sediment layers. Orange/red zones have less than 40% coarse-grained sediments (relatively high percent silts and clays) while blue areas have 80% or more coarse-grained sediments (relatively low percent silts and clays). Coarse sediments dominate in the Central Sands portion of the model domain in all three layers.

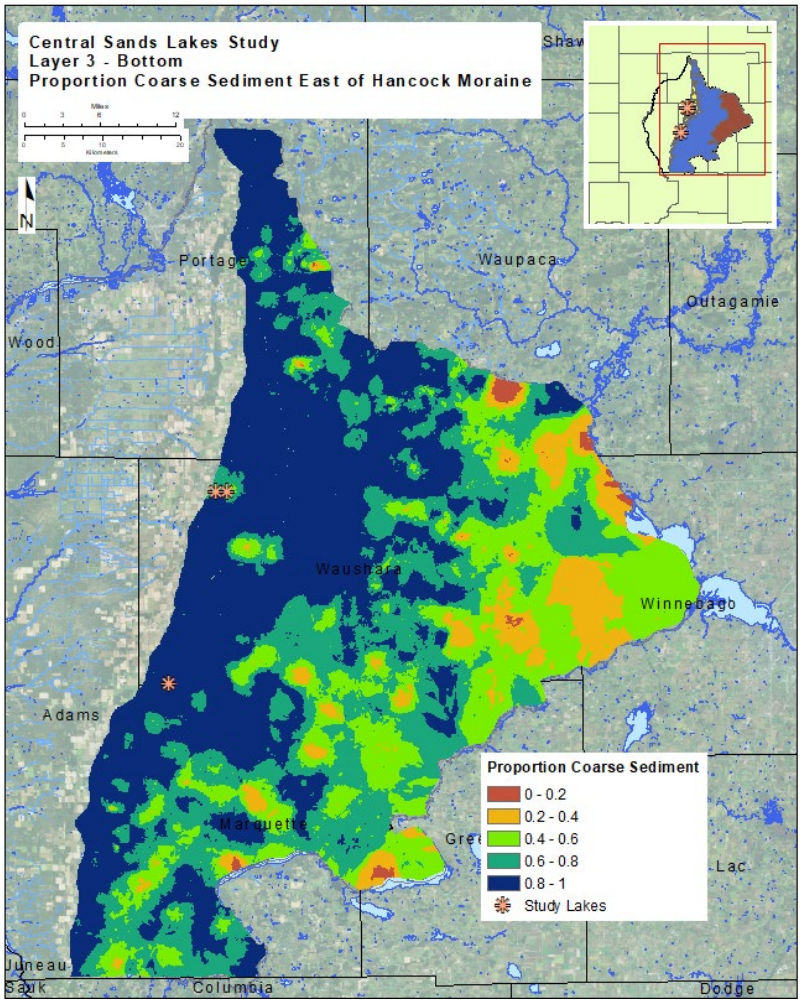

...Figure 59, continued

Conceptualization and Layer Creation – Cross Sections

WGNHS synthesized data from WCRs, geologic borings, and geophysical investigations to visualize the stratigraphy near the study lakes and in the Plainfield Tunnel channel. Cross-sections were created along six transects within the study area (Figure 60-65): Long Lake, Plainfield Lake, along the axis of the Plainfield Tunnel channel, in the intermoraine perpendicular to the Plainfield Tunnel channel, and at Pleasant Lake (two cross-sections). All cross-sections are shown at about sixteen times vertical exaggeration. These conceptual cross-sections depict the approximate distribution of coarse and fine-grained sediments in the subsurface, generalized groundwater elevation and gradients, and bedrock features that were incorporated into the groundwater flow model. The cross-sections represent the current conceptualization of stratigraphy in the areas of interest. Conceptualizations are based on likely depositional environments and available data. However, it is important to recognize that data gaps do exist in some areas, especially at depth, and that the primary sources of existing data (WCRs) are suitable for generalized regional analysis rather than detailed stratigraphy. Sands and gravels are the dominant sediment type in all areas that were examined, with the largest fine-grained fraction at Long Lake and the smallest percentage of fines only a few miles away at Plainfield Lake.

Cross-section Data Sources

Data sources of varying quality were used for cross-section creation. The highest-quality data are the rotosonic and direct-push borings conducted as part of this study. Data collection and analysis for those borings are described in the quaternary sediment data collection section. The rotosonic borings especially offer insight into deep stratigraphy not available from other logs, including depth to bedrock. Direct-push borings around the lake provide detailed view of sediment types from ground surface to tens of feet below the lake elevations. Driller-reported geology from well construction reports provide the largest available dataset, but also have the most uncertainty. These logs give a general picture of sediment types encountered during drilling. However, specific logs may be inaccurate for several reasons: cuttings obtained from typical drilling methods may not be conducive to identifying small-scale changes in lithology, highly accurate description of sediment type is not the primary concern of typical well-drilling, and the location/elevation of wells may not be known precisely.

In addition to the geologic boring data, depth to bedrock and the orientation of fine-grained materials were informed by geophysical data (passive seismic, active seismic, and ground-penetrating radar). Geophysical data were used to fill data gaps and to conceptualize stratigraphy patterns. Geophysical data collection methods and results are discussed above.

Long Lake (A-A')

The Long Lake cross-section (Figure 60) line runs north to south, approximately perpendicular to the Plainfield Tunnel Channel axis. Fine-grained sediments (fine sands to clays) are found in the majority of WCR and geologic logs near Long Lake. The fine-grained sediments are located within the Plainfield Tunnel Channel; logs outside the tunnel channel show few or no fine-grained sediments. The Long Lake rotosonic boring, near the southern edge of the tunnel channel, records a thin zone of silty sand that may represent the edge of fine-grained sediment layers seen in other logs nearer the lake. Most fine-grained sediments described in WCR logs occur below the lake-bed elevation. The degree of connectivity between the fine-grained sediments cannot be definitively determined from the WCR data; the cross-section depicts one reasonable sediment configuration based on available data. Sediments within the tunnel channel are collapsed by about 30 feet, consistent with tunnel channel formation as shown in Figure 7. The upper surface of the fine-grained sediments can be observed in some of the direct-push boring logs and in GPR data (Figure 16).

The water table at Long Lake has very little gradient. This is a result of Long Lake's proximity to the regional groundwater divide, the relatively flat surface topography, and the absence of nearby streams to control groundwater levels. Groundwater and lake levels at Long Lake generally rise and fall together, with some degree of delay or attenuation between signals seen in deeper groundwater and those in shallow groundwater and the lake (see water level discussion). This is expected because the water table lies above the top of the fine grained sediments providing a direct connection between the water table and lake levels. The water table elevation shown on the cross-section is interpolated from well-

construction data reported over several decades and does not represent the high water levels observed during the study period.

The upper bedrock at Long Lake is sandstone, as seen in rotosonic boring LL101. Passive seismic data indicate that the tunnel channel follows a bedrock valley. It is not known whether this was an existing preglacial valley or whether it was formed at the same time as the tunnel channel. No borings go all the way through the sandstone, so sandstone thickness is interpolated based on Precambrian elevations relatively far away from the study lakes. Because bedrock is relatively deep here and has a much lower hydraulic conductivity than the overlying sediments, the configuration of the bedrock surface will have little influence on groundwater flow relative to surface waters.

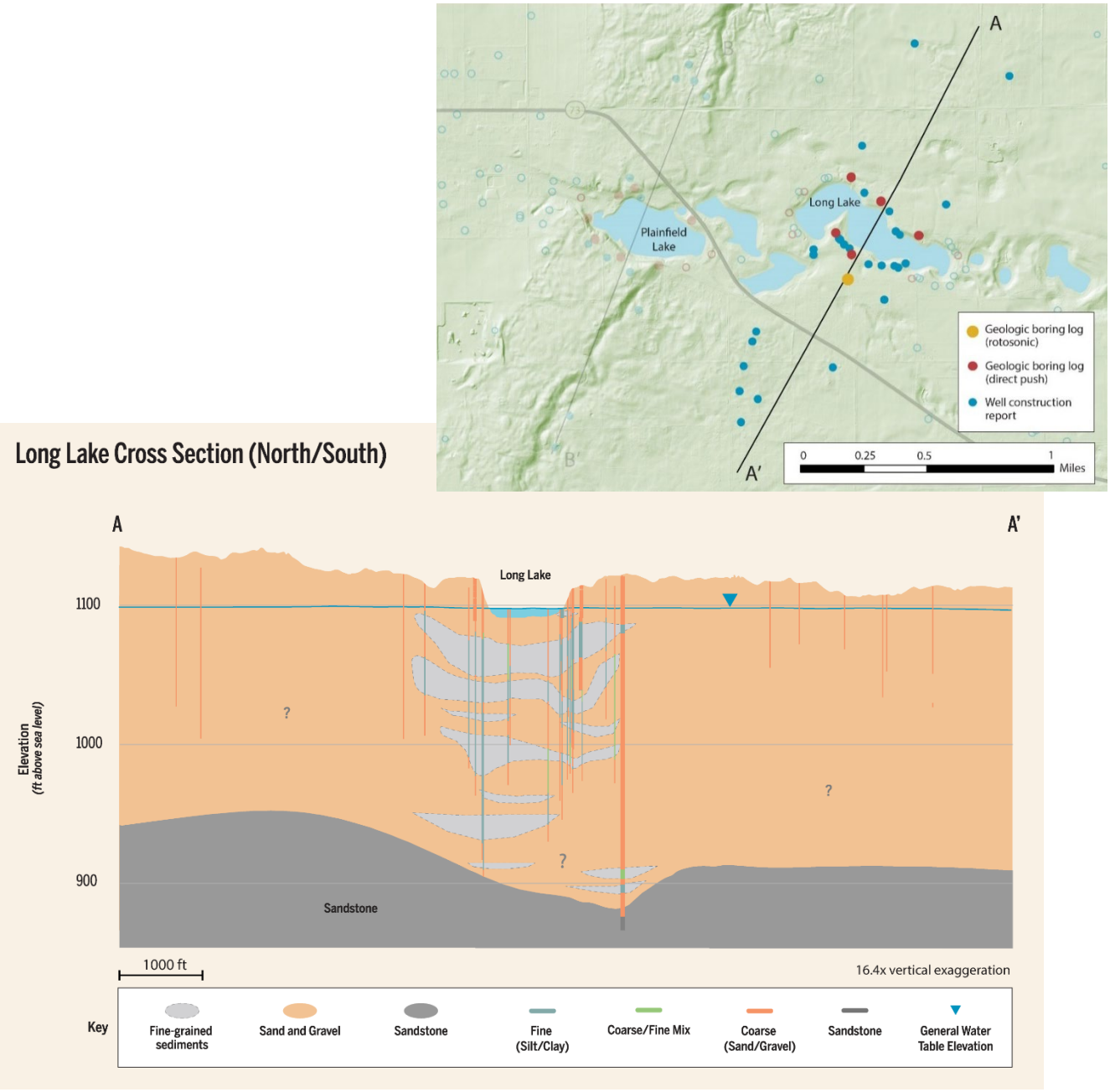

Figure 60. Conceptual cross section through Long Lake, approximately perpendicular to the Plainfield Tunnel Channel.

Plainfield Lake (B-B')

The Plainfield Lake cross-section (Figure 61) line runs north to south, approximately perpendicular to the Plainfield Tunnel Channel axis. Sediments around Plainfield Lake are almost entirely sand and gravel, with a few occurrences of fine or silty sand. Plainfield Lake is situated within the Hancock Moraine at the west end of the Plainfield Tunnel Channel. A few zones of mixed fine and coarse sediments are noted in some WCR logs in the moraine north and south of the lake. As at Long Lake and for similar reasons, the

water table has a very flat gradient. Plainfield Lake is located on or very close to the regional groundwater divide and there are no nearby streams to control groundwater levels. The bedrock valley seen in passive seismic data at Long Lake is also seen to the west of Plainfield Lake. It is assumed that the upper bedrock is sandstone, as was seen in the rotosonic boring at nearby Long Lake.

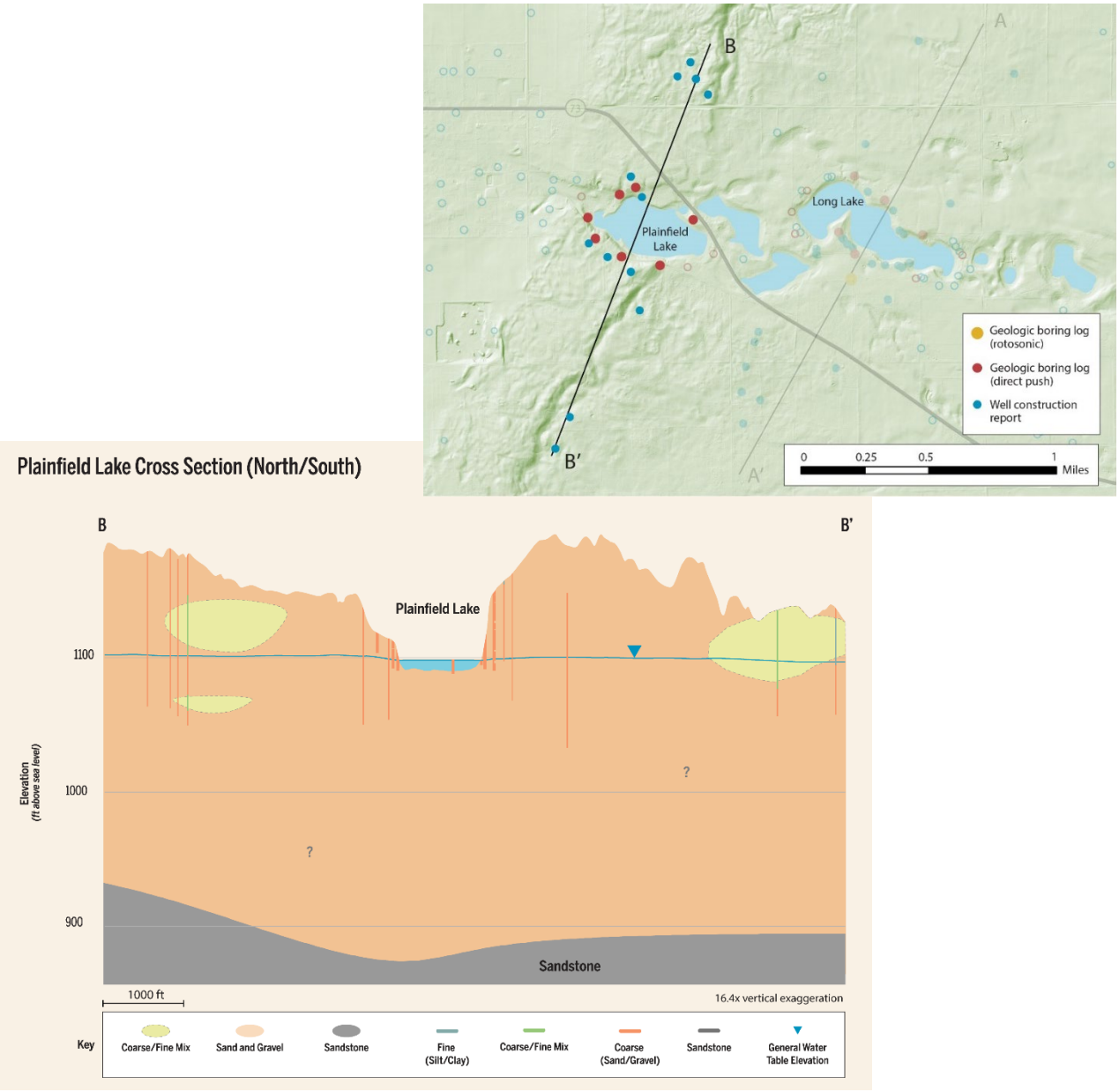

Figure 61. Conceptual cross section through Plainfield Lake, approximately perpendicular to the Plainfield Tunnel Channel.

Intermoraine North-South (C-C')

The Intermoraine cross-section (Figure 62) shows a north-south view of the area lying between the Hancock and Almond Moraines. The cross-section line intersects the eastern rotosonic boring and is perpendicular to the Plainfield Tunnel Channel. Topography in the intermoraine is a flat-lying outwash

plain except for collapsed tunnel channels. The bulk of sediments in the intermoraine are sands and gravels, but fine-grained sediments are noted in many logs, indicating a complex depositional history. Coarse-fine analysis of boring data indicates that the fine-grained sediments do not form a continuous layer through the intermoraine but consist of disconnected fine-grained bodies. The Plainfield Tunnel channel sediments are collapsed, as shown in active seismic data. The water table has little gradient, reflecting surface topography and the high-conductivity sand and gravel aquifer. The buried bedrock valley, indicated by passive seismic data, associated with the tunnel channel is also shown. The upper bedrock at the rotosonic boring in the center of the figure is Precambrian granite. Upper bedrock elsewhere in the intermoraine is mapped as sandstone; this is based on interpolation of data from borings outside the cross-section transect. The sandstone is thin to the north, thickening to the south. Bedrock depth is 200 feet or more, and bedrock will have little influence on shallower groundwater flow patterns.

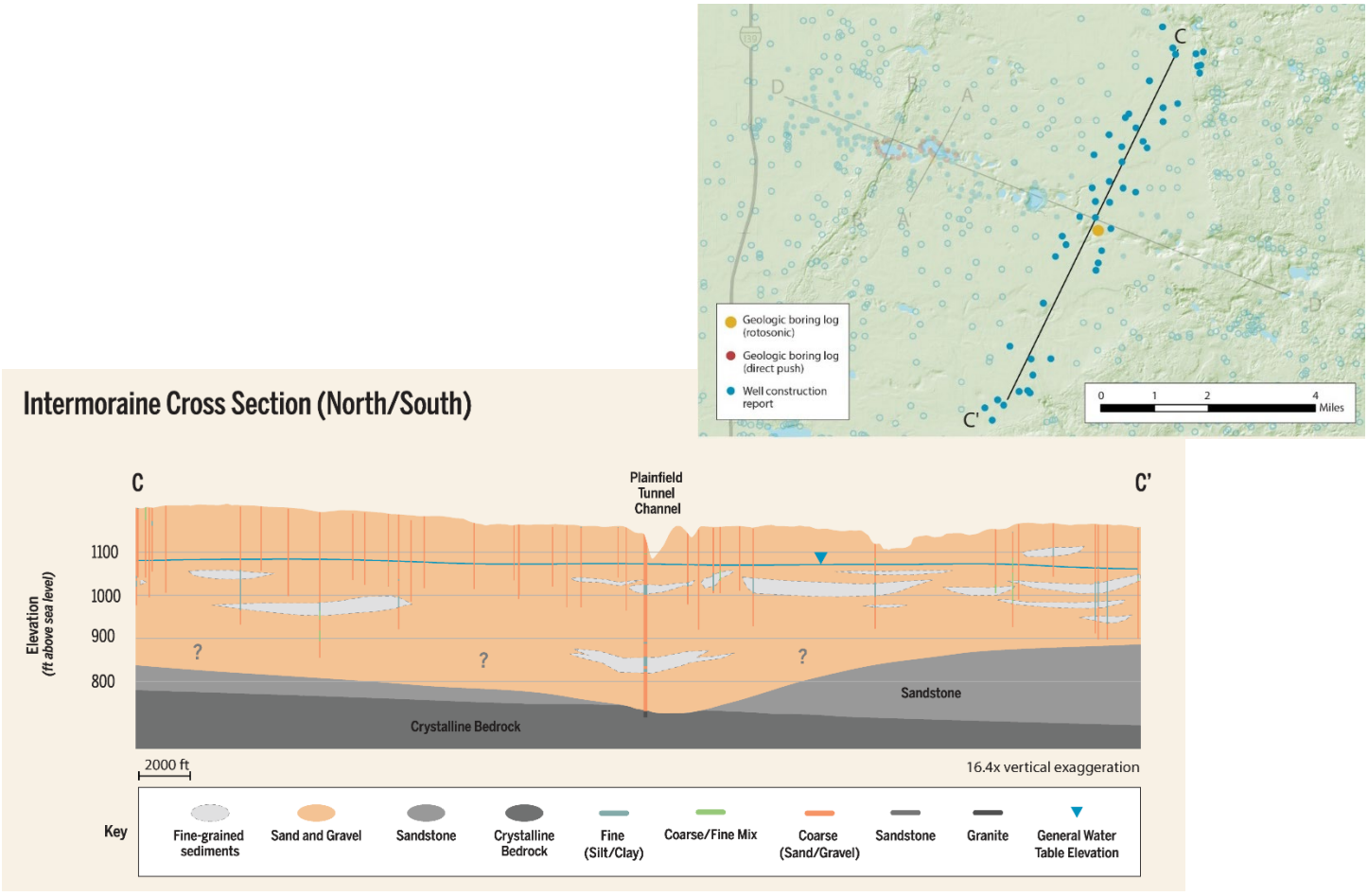

Figure 62. Conceptual cross-section perpendicular to the Plainfield Tunnel Channel at the eastern rotosonic site.

Plainfield Tunnel Channel Longitudinal (D-D')

The Plainfield Tunnel Channel cross-section (Figure 63) roughly follows the tunnel channel axis and includes the Hancock Moraine and outwash plain to the west and Almond Moraine to the east. The

outwash plain west of the Hancock Moraine has few fine-grained sediments. Fine grained sediments are more common east of the moraine, reflecting a different set of depositional environments. While fine-grained sediment is present in many logs along the Plainfield Tunnel Channel, there does not appear to be a consistent fine-grained unit that could provide regional confinement. The greatest concentration of fine-grained sediments is in logs near Long Lake. Fine-grained sediments were seen to a lesser degree in well logs near Huron Lake. It should be noted that the highest concentration of boring logs is around these lakes: fine-grained sediments are only shown in the cross-section where supported by data but could also be present in other areas. As seen in the center of Figure 61, almost all sediments near Plainfield Lake are coarse sands and gravels. Plainfield Lake is within the moraine at what was probably a high-energy outlet for meltwater during glacial recession and so fine grained sediment was not deposited but carried away by the meltwater. The Almond Moraine, on the east end of the transect, also contains some finer-grained sediments. These are typically described as a mix of fine and coarse materials (e.g. clay and gravel) rather than as clays or silts. The land surface in the intermoraine area rises gradually toward the Almond Moraine to the east. The water table falls gradually from the regional groundwater divide, which is located near Long and Plainfield Lakes. (The regional groundwater divide in this area is 6 miles west of the regional surface water divide.) There is little data constraining bedrock surface elevation in the intermoraine. Bedrock surfaces were estimated based on interpolation from the rotosonic borings (shown in orange on the transect map) and from calibrated passive seismic points. The upper bedrock unit at the western rotosonic boring near Long Lake is sandstone. To the east, the bedrock surface elevation is almost 200 feet lower, and upper bedrock is Precambrian granite.

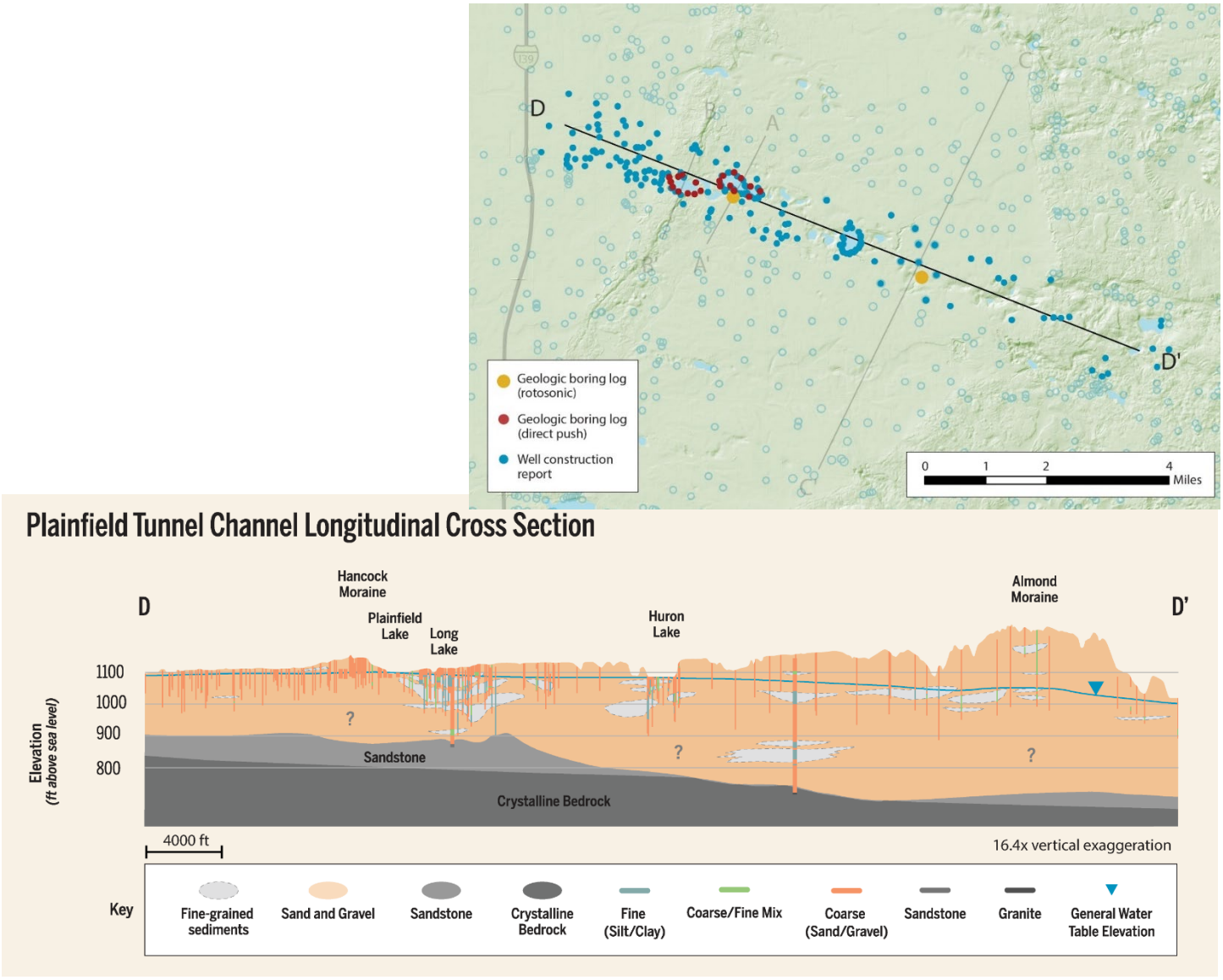

Figure 63. Conceptual cross-section through the intermoraine parallel to the Plainfield Tunnel Channel axis

Pleasant Lake East-West (E-E') and North-South (F-F')

At Pleasant Lake, west-to-east (Figure 64) and north-to-south (Figure 65) cross sections were created to show groundwater discharge points, bedrock features, and sediment distribution. The coarse fraction (sand and gravel) dominates near Pleasant Lake, as it does throughout the Central Sands. Finer horizons are typically a mix of coarse and fine sediments (tills, fine sediments associated with stagnant ice features) and are not laterally extensive. It is likely that a there is a similar distribution of mixed sediments in the no-data areas shown with question marks on the cross-sections. Pleasant Lake is in the collapsed zone east of the Hancock moraine and has more nearby surface topography than the Plainfield Tunnel Channel Lakes. The water table has pronounced slope to the east and south, and water levels are controlled by the elevations of discharge points at Chaffee and Tagatz creeks. Sandstone bedrock was

encountered in multiple wells logs near Pleasant Lake. Because of this, the bedrock surface is better understood at Pleasant Lake than in the intermoraine area. The bedrock surface rises from the east to the west. The water generalized water table is shown above the bedrock surface, but at times the water table may drop to within the bedrock aquifer. Pleasant Lake is situated in and east-west trending bedrock valley (Figure 65), seen in boring logs and passive seismic data points.

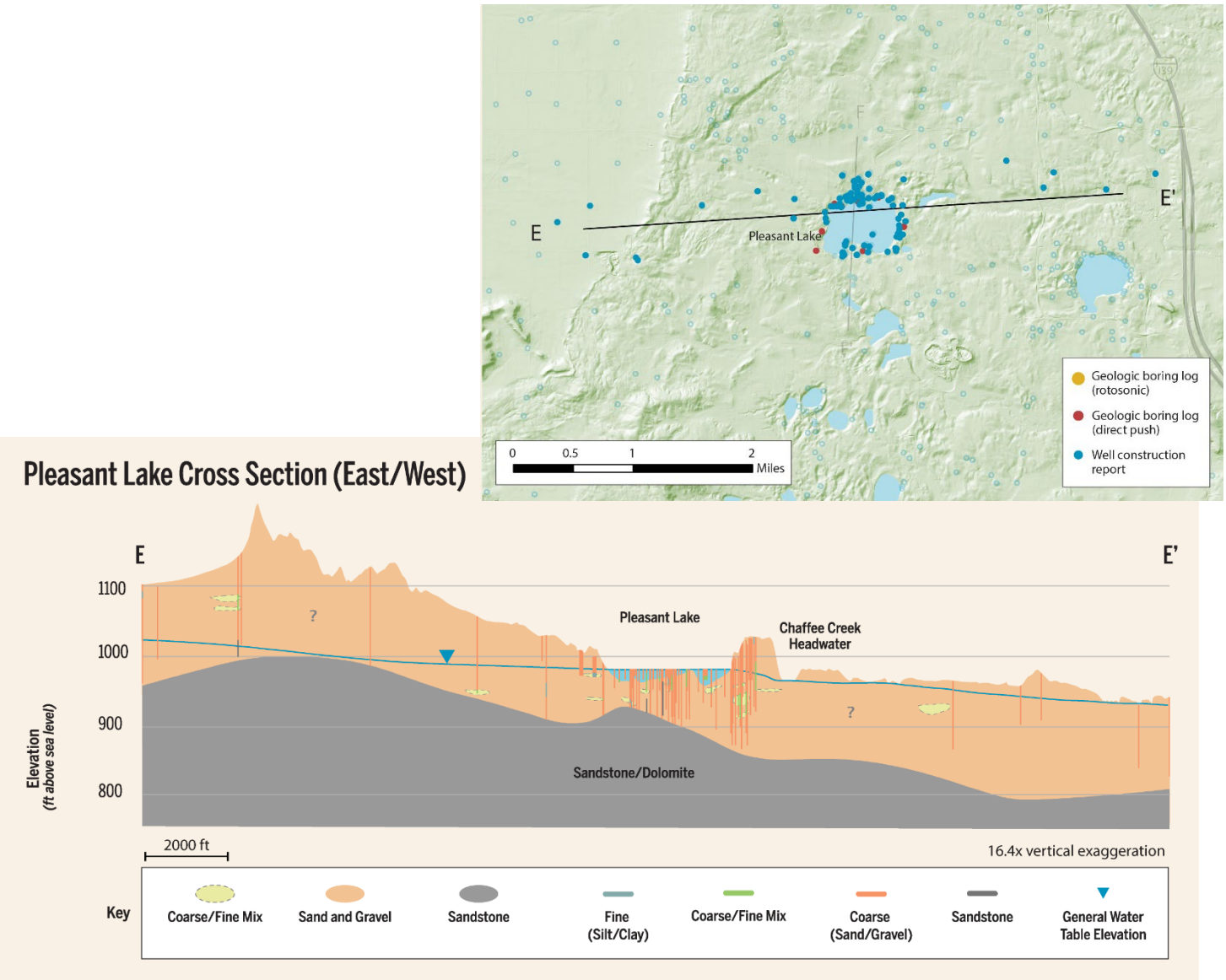

Figure 64. Conceptual cross section from west to east through the Almond Moraine and Pleasant Lake.

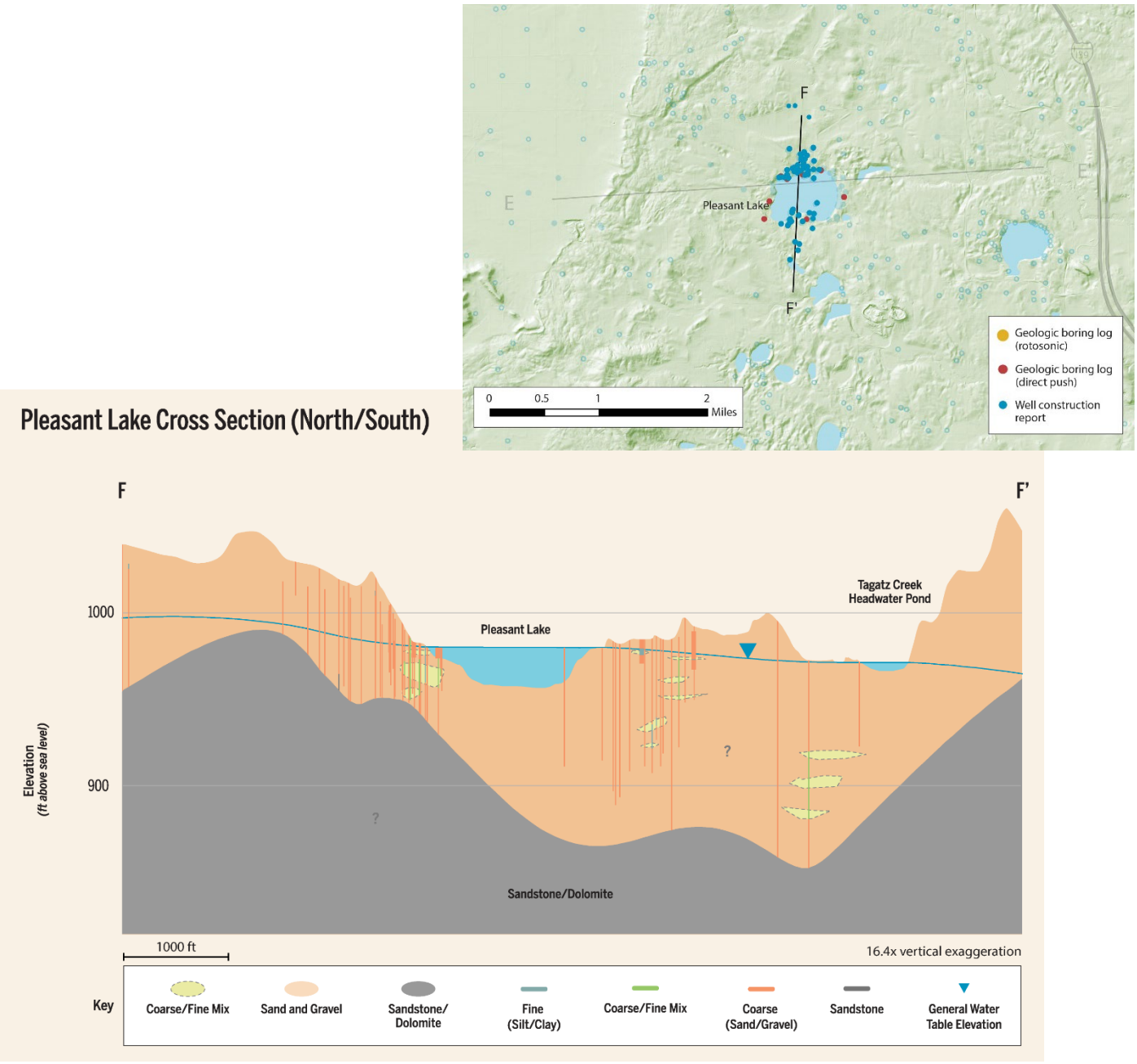

Figure 65. Conceptual cross section from north to south through Pleasant Lake.

Discussion

These cross-sections were created to clarify the hydrostratigraphic conceptualization of the study lakes and their vicinity that was used to inform the groundwater model. Because of the available data quality and spatial distribution of data, the cross-sections are intended to convey general sediment distribution rather than precise configuration. Important points of the hydrostratigraphic conceptualization include: 1) a dominant coarse fraction with zones of heterogeneity, 2) a water table that is fairly flat and unconstrained near Long and Plainfield Lakes and controlled by surface water features near Pleasant Lake, and 3) a bedrock surface that is relatively deep in the intermoraine and shallower with significant topography near Pleasant Lake. Zones of fine-grained sediments shown in the cross-sections are

represented in the groundwater flow model by varying hydraulic conductivity using the coarse-fine analysis discussed above.

Hydrostratigraphy – Aquifer Properties

Aquifer properties in the CSLS model domain, especially hydraulic conductivity, were calculated using a range of methods. The resulting values were provided to the modeling team to inform the hydraulic conductivity distribution of the model and to confirm that modeled conductivity values fall within a reasonable range based on observed data. Table 4 summarizes the types of data compiled to evaluate aquifer properties for the study. Results of the aquifer property analyses are detailed in the Aquifer Properties and Geophysical Investigations sections and in Appendices F and I.

Table 4. Summary of data types use for aquifer characterization, the appropriate use of the data (Data Quality), aquifer parameters derived from each data type, and the number of data points in each category (*n*).

Data Source	Method/Test	Data Quality	Aquifer Parameters	*n*
Historic Aquifer Tests	Slug Tests, Multi-well Pumping Tests	site specific	hydraulic conductivity, aquifer storage, anisotropy	70
Well Construction Reports/TGUESS	Specific Capacity Tests	regional estimation	Transmissivity → hydraulic conductivity, regional groundwater flow	36,220
CSLS monitoring well aquifer tests	Pumping Tests, Injection Tests	site specific, study area	hydraulic conductivity, groundwater flow and gradients	36
Investigative Borings - geophysical	Direct-Push Permeameter	site specific	bulk hydraulic conductivity, vertical conductivity distribution	4
Rotosonic core (east)	Grain-size Analysis	qualitative estimates	vertical conductivity distribution	1
Geologic logs, well construction logs	Sediment type classification: Coarse-fine analysis	qualitative regional estimation	spatial distribution of high- and low-conductivity sediment types, potential anisotropy distribution	12,938

Hydraulic conductivity values were determined using the results of pumping tests, slug tests, and specific capacity tests. As shown in Tables 1 to 3, hydraulic conductivity values in sandy aquifer materials of the Central Sands are typically on the order of 10^2 ft/d. Somewhat higher hydraulic conductivity values occur in the glacial outwash of the western model domain and the intermoraine, while conductivity is lower in the clay-rich Glacial Lake Oshkosh basin. Typical hydraulic conductivity values for bedrock wells were an order of magnitude lower than those finished in the sand and gravel aquifer.

Specific yield values from multi-well pumping tests in the sand and gravel aquifer averaged 0.17, with all but one of the test values falling within the range typical of sands and gravels (0.1-0.35, Freeze and Cherry, 1979).

Geophysical work (DPP) at the Wallendal site in Adams County showed that the hydraulic conductivity of the fine-grained New Rome member was more than two orders of magnitude lower than the conductivity of the overlying and underlying sandy aquifer materials. The New Rome member is assumed to provide some local confinement. This layer is widespread in the southwestern part of the model domain but is not present within several miles of the study lakes (Figure 3). A similar DPP analysis of the conductivity distribution with depth at two borings at Plainfield Lake did not encounter any comparable low-conductivity layers.

Rotosonic boring PFD24 within the Plainfield Tunnel channel encountered two zones of fine-grained sediments at 113-132 and 275-318 ft bgs. Estimates of hydraulic conductivity based on grain-size analysis indicate that these fine-grained zones could have conductivities as low as 10^{-2} to 10^{-4} ft/d (Figure 21). The intermoraine area specifically, and the eastern part of the model domain as a whole were investigated for potential heterogeneity that could act as a regional confining unit. No widespread fine-grained layer similar to the New Rome member was identified near the three study lakes or anywhere east of the Hancock Moraine in the Central Sands region. Localized areas of fine-grained sediments were identified, including the Plainfield Tunnel channel near Long Lake (Figure 59). The spatial distribution of coarse and fine-grained sediments was provided to the modeling team to inform calibration of the hydraulic conductivity distribution.

The degree of variability in sediment type with depth indicates that vertical anisotropy is likely to influence groundwater movement in many parts of the model domain. Anisotropy values from five pumping tests in the fairly homogeneous outwash sands west of the Hancock moraine average 7:1. Aquifer anisotropy is very likely higher in the more heterogeneous sediments east of the glacial moraines.

In the nearfield, pumping or injection tests were conducted at 36 CSLS monitoring wells adjacent to the study lakes. Results provide a more detailed set of hydraulic conductivity values around the lakes (distribution shown on Figures 32 and 33). Hydraulic conductivity values reflect observed sediment types. Plainfield Lake has the coarsest sediments and also the highest hydraulic conductivity range (73-637 ft/d). Hydraulic conductivity values at Pleasant Lake are slightly lower than at Plainfield Lake (24-130 ft/d). Pleasant Lake's sediments are generally sandy but include some more poorly sorted zones with a mix of coarse and fine-grained sediments. Boring logs in the vicinity of Long Lake commonly report finer-grained sediments in addition to outwash sands (Figures 21, 60). The presence of finer-grained sediments is reflected in the measured conductivity value range of 7-69 ft/d.

Conclusions

The following conclusions are based on observations and data collected during this study and previous studies. Incorporation of these data and observations into the groundwater flow model will improve our understanding of the study lakes and provide guidance on additional data needs.

- Central Sands Region sediments are dominated by sand, but also have areas of significant heterogeneity.
    - Results from mini-piezometers and seepage meters indicate that lakebed hydraulic conductivity from all three study lakes is 1-2 orders of magnitude lower than surrounding sediments.

    - While coarse sediments predominate, significant thickness of fine-grained sediment is common in well logs and study borings in the area between the Hancock and Almond moraines. Fine-grained sediments are especially common in borings in the Plainfield tunnel channel (well logs, rotosonic boring PFD24, direct push borings), but not in other tunnel channels like the Hancock tunnel channel. Well boring data indicate that the fine-grained sediments in the intermoraine zone are not laterally continuous. Zones where fine-grained sediment are present are likely tied to glacial collapse features, proglacial lakes, and backwater areas of the outwash plain.

    - The New Rome forms a consistent clay layer in Adams County that is typically more than 10 feet thick, has a several foot head drop across it where measured, and is likely to affect groundwater flow where it is present. The eastern edge of this formation is 5-8 miles west of the 3 study lakes. The unit has been shown to cause local confinement in some areas where it is present. In wells cased below the clay, this could result in more rapid propagation of impacts, but with more moderate effects distributed among relatively distant surface water bodies.

    - East of the Almond moraine is a zone of collapsed glacial till. Coarse sediments continue to dominate in this area, but materials are more heterogeneous than in the outwash areas west of the moraines. This includes areas such as Westfield, where confining layers within unconsolidated sediments lead to artesian conditions in some wells. Analysis of coarse and fine-grained sediments reported in well logs indicates that anisotropy is likely be a factor in determining groundwater flow patterns.

- Hydraulic conductivity values and water levels derived from WCRs offer insights into groundwater movement and aquifer properties at a regional scale. Hydraulic conductivities derived using specific capacity tests and TGUESS match well with other aquifer test data. Hydraulic conductivity values reflect the more transmissive parts of the aquifer where wells are completed. In the Central Sands, where most of the aquifer has high hydraulic conductivity, these tests are fairly representative of the aquifer as a whole. Based on aquifer tests and specific capacity tests, typical hydraulic conductivity for wells in the Central Sands is on the order of 10^1 to 10^2 ft/d.

- The lakes and groundwater are well-connected and rise and fall together, driven by climate variation.

- Water levels in all three study lakes are closely tied to surrounding groundwater levels. As climate or other variables cause the water table to rise and fall, lake levels respond.

- Water level variability is more muted at Pleasant Lake due to nearby surface water features and more pronounced at Plainfield Lake and Long Lake, located high on the landscape with no nearby surface water features.

- The observed groundwater flow patterns and groundwater-surface water interactions at Plainfield Lake and Long Lake showed significant variability during the 1-year observation period.

    - At the beginning and end of the observation period, the lakes were flow-through lakes, with groundwater entering to the north and exiting to the south. Following an extended period of above-average precipitation and rapidly increasing groundwater levels, the lakes were temporarily converted to discharge points with little or no groundwater outflow. This condition persisted for several months.
    - Patterns of water-level rise and fall in Long Lake show that it is well connected to groundwater and follows regional rises and falls in the water table. In some cases, responses for the lake and shallow groundwater (monitoring wells) were observed to be delayed or attenuated compared to deeper groundwater (piezometers). This appears to be related to changes in groundwater flow patterns caused by fine-grained sediments occurring near the lake.

- Pleasant Lake did not experience changes in flow patterns like those observed in the Plainfield Tunnel Channel lakes. Although lake levels rose due to increased precipitation, groundwater continued to enter the lake on the north and west and exit to the south and east. Pleasant Lake is adjacent to the headwater springs of both Chaffee and Tagatz Creeks, two points of groundwater discharge that are expected to continue to hold the flow pattern steady.

Acronym List

asl	above mean sea level
BGS	below ground surface
CSLS	Central Sands Lakes Study
DATCP	Department of Agriculture, Trade and Consumer Protection
DEM	Digital Elevation Model
DO	Dissolved Oxygen
DPP	Direct Push Permeameter
ft/d	Feet per day
ft asl	Feet above Mean Sea Level
ft bgs	feet below ground surface
GIS	Geographic Information System
GPS	Global Positioning System
GP	Geoprobe®
HVSR	Horizontal-to-Vertical Spectral Ratio Passive Seismic Method
K	Hydraulic Conductivity (*l/t*)
LiDAR	Light Detection and Ranging: remote sensing technique
LPR	Little Plover River
MHRCEC	Mt. Horeb Research Collection and Education Center (core lab)
NMR	Nuclear Magnetic Resonance
NRCS	National Resources Conservation Service
NWIS	National Water Information System (USGS)
PLSS	Public Land Survey System (township/range/section)
PVC	Polyvinyl chloride
RTK GPS	Real-time kinetic GPS
TC	Tunnel Channel
TOS	Top of Well Screen
USDA	U.S. Department of Agriculture
USGS	U.S. Geological Survey
WCR	Well Construction Report
WDNR	Wisconsin Department of Natural Resources
WGNHS	Wisconsin Geological and Natural History Survey
WisDOT	Wisconsin Department of Transportation
WOFR	Wisconsin Open-File Report

Bibliography

Batchelor C.L., Dowdeswell J.A., Ottesen D., 2018, Submarine glacial landforms. In: Micallef A., Krastel S., Savini A. (eds) Submarine Geomorphology. Springer Geology. Springer, Cham, p. 207-234.

Bradbury, K.R. and Muldoon, M.A., 1990, Hydraulic conductivity determinations in unlithified glacial and fluvial materials, in Nielsen, D.M., and Johnson, A.I., eds., Ground water and vadose zone monitoring: Philadelphia, American Society for Testing and Materials, ASTM STP 1053, p. 138–151.

Bradbury, K.R., and Rothschild, E.R., 1985, A computerized technique for estimating the hydraulic conductivity of aquifers from specific capacity data: Ground Water, v. 23, no. 2, p. 240–246.

Bradbury, K.R., Fienen, M.N., Kniffin, M.L., Krause, J.J., Westenbroek, S.M., Leaf, A.T., and Barlow, P.M., 2017, A Groundwater flow model for the Little Plover River basin in Wisconsin's Central Sands: Wisconsin Geological and Natural History Survey Bulletin 111, 82 p.

Brownell, J.R., 1986, Stratigraphy of unlithified deposits in the central sand plain of Wisconsin: University of Wisconsin, Madison, M.S. thesis, 172 p.

Butler, J.J., Dietrich, P., Wittig, V., and Christy, T., 2007, Characterizing hydraulic conductivity with the direct-push permeameter: Ground Water, v. 45, no. 4, p. 409-419.

Carson, E.C., Attig, J.W., and Rawling J.R., III, 2017, New stratigraphic and chronologic controls on the formation and drainage of glacial Lake Wisconsin. Geological Society of America Abstracts with Programs. v. 49, no. 6

Ceperley, E.G., Marcott, S.A., Rawling, J.R., III, Zoet, L.K., Zimmerman, S.R.H., 2019, The role of permafrost on the morphology of an MIS 3 moraine from the southern Laurentide Ice Sheet: Geology, v. 47, no. 5, p. 440-444.

Christenson, C.A., 2019, Big Data for Small Streams: Establishing a method for collection of spatially and temporally dense water-quality and geophysical datasets via canoe: University of Wisconsin, Madison, M.S. thesis, 72 p.

Clayton, L. 1987, Pleistocene geology of Adams County, Wisconsin: Wisconsin Geological and Natural History Survey Information Circular 59, 14 p., includes map, cross sections, GIS files, https://wgnhs.uwex.edu/pubs/000309/.

Clayton, L. and Attig, J.W., 1989, Glacial Lake Wisconsin: Geological Society of America Memoir 173, 80 p.

Clayton, L., Attig, J.W., and Mickelson, D.M., 1999, Tunnel channels formed in Wisconsin during the last glaciation, in Mickelson, D.M. and Attig, J.W., eds., Glacial processes past and present: Boulder, Colorado, Geological Society of America Special Paper 337, p. 69–82.

Clayton, L., Attig, J.W., Mickelson, D.M., 2001. Effects of late Pleistocene permafrost in the landscape of Wisconsin, USA. Boreas 30, p. 173–188.

Clayton, J.A. and Knox, J.C., 2008, Catastrophic flooding from Glacial Lake Wisconsin: Geomorphology, v. 93, p. 384-397.

Freeze, R. A. and Cherry, J.A., 1979, Groundwater. Prentice-Hall Inc., Englewood Cliffs, v. 7632, 604 p.

Greve, R.M., Hart, D.J., Central Sands Lakes Study: Annotated Bibliography: Wisconsin Geological and Natural History Survey Open File Report 2018-04, 44 p.

Hart, D.J. 2015, Using the New Rome Formation as a geologic weighing lysimeter for water management in Wisconsin's sand plain: Final Report for WDNR Project Number 14-HDG-03, 18 p.

Holt, C.L.R., 1965, Geology and water resources of Portage County, Wisconsin: U.S. Geological Survey Water Supply Paper 1796, 77 p., 2 plates.

Ibs-von Seht, M. and Wohlenberg, J., 1999, Microtremor measurements used to map thickness of soft sediments. Bulletin of the Seismological Society of America, v. 89, iss. 1, p. 250-259.

Kniffin, M.L., 2018, Investigations of groundwater-surface water interactions and stakeholder engagement in the Central Sands region of Wisconsin: University of Wisconsin-Madison, PhD thesis, 171 p.

Konert, M. and Vandenberghe, J.E.F., 1997, Comparison of laser grain size analysis with pipette and sieve analysis: a solution for the underestimation of the clay fraction: Sedimentology, v. 44, p. 523-535.

Lippelt, I.D., Hennings, R.G. 1981, Irrigable Lands Inventory – Phase I Groundwater and Related Information: Wisconsin Geological and Natural History Survey.

McNeill, J.D., 1980, Electromagnetic terrain conductivity measurement at low induction numbers: Geonics Limited, Technical Note TN-6, 15 p.

Miller, B.A., Schaetzl, R.J., 2012, Precision of soil particle size analysis using laser diffractometry: Soil Science Society of America Journal, v. 76, p. 1719-1727.

Rawling, J.E. III, Hanson, P.R., Young, A.R., Attig, J.W., 2008, Late Pleistocene dune construction in the Central Sand Plain of Wisconsin, USA: Geomorphology, v. 100, 494–505.

Reynolds, J.M., 1997, An introduction to applied and environmental geophysics: Wiley, Michigan, 806 p.

Rosenberry, D.O., and LaBaugh, J.W., 2008, Field techniques for estimating water fluxes between surface water and ground water: U.S. Geological Survey Techniques and Methods 4–D2, 128 p.

Syverson, K.M., and Colgan, P.M., 2011, The Quaternary of Wisconsin: an updated review of stratigraphy, glacial history and landforms, *in* Ehlers, J., Gibbard, P.L., and Hughes, P.D. (eds.) Quaternary Glaciations – Extent and Chronology: a closer look: Developments in Quaternary Sciences series, v. 15, p. 537-552.

Weeks, E.P. and Stangland, H.G., 1971, Effects of irrigation on streamflow in the Central Sand Plain of Wisconsin: U.S. Geological Survey Open-File Report 70-362, 113 p.

Wen, B., Aydin, A. and Aydin-Duzgoren, N. S., 2002, A comparative study of particle size analysis by sieve-hydrometer and laser diffraction methods: Geotechnical Testing Journal, Vol. 25, No. 4, pp. 434–442.

Zoet, L.K., Muto, A., Rawling, J.E. III, Attig, J.W., 2019, The effects of tunnel channel formation on the Green Bay Lobe, Wisconsin, USA: Geomorphology, v. 324, no. 1, p. 36-47.